EXPLORING THE VARIABILITY IN MECHANICAL PROPERTY TESTING OF DENTAL RESIN COMPOSITES

By

NARESH KUMAR

A thesis submitted to the
University of Birmingham
for the degree of
DOCTOR OF PHILOSOPHY

Biomaterials Unit
School of Dentistry
St. Chad's Queensway
Birmingham B4 6NN

January 2011

SYNOPSIS

The invention of dental resin based-composites (RBCs) has provided a broad range of materials for the restoration of load-bearing posterior teeth with excellent clinical results and adequate longevity. Currently, a lack of consensus exists among researchers regarding classification of RBCs as a result of slight variations in filler size and associated interchangeable mechanical properties of "microhybrid", "nanohybrid" and "nanofilled" RBCs. Also, the inconsistency in mechanical property testing of RBCs is evident amongst researchers. This research explored the variability in experimental and statistical testing methodologies of RBCs.

The current study identified a wide variation in the bi-axial flexure strength (BFS) of commercial and experimental RBCs with respect to deformation rate with a complex relationship between resin constituents and filler morphology. Experimental unfilled resins revealed deformation rate dependence in BFS following 1 week dry, 1 and 13 weeks wet storage regimes, whereas the addition of fillers modified the deformation rate dependence following 13 weeks wet storage and resulted in the BFS of filled resin composites being independent of testing speed. These findings suggested the need for the development of RBCs with appropriate formulations for clinical situations where variable strain rates may occur, for example, patients with parafunctional habits.

To date, the alignment of specimens during storage regimes prior to mechanical property testing has rarely been reported. The effect of specimen alignment on the BFS and surface hardness of RBCs was evaluated and a greater decrease in the both properties were found following wet upright compared with stacked and upper surface exposed alignments. These observations were attributed to a variation in diffusion of

water as the result of difference in exposed surface areas of specimens, which may lead to different findings and associated interpretation between investigators.

Weibull statistics are used for the analysis of strength data of RBCs, however their applicability to RBCs might be questioned due to some viscous deformation prior to brittle failure. The findings of current study supported the applicability of Weibull statistics for the microhybrid and nanofilled RBCs but not a flowable RBC, which suggested that Weibull statistics may not necessarily be applicable for all RBC types.

It was demonstrated that variability and irrelevance in testing methods may cause incorrect interpretation of data among researchers and consequently affect the future research and development of RBCs. Therefore, further standardisation of testing methods is required.

ACKNOWLEDGEMENNTS

Firstly, I would like to express my sincere gratitude to my supervisors, Dr Will Palin and Dr Owen Addison, for their valuable guidance, constant support and scholarly feedback throughout the course of my research and thesis writing. This research work would not have been completed without their help and support. I am also extremely grateful to Dr Adrian Shortall and Professor Peter Marquis for their supervision.

I am thankful to Liaquat University of Medical and Health Sciences, Jamshoro, Pakistan for funding this PhD.

I would like to extent my thanks to Mrs Sue Fisher for her technical assistance and all the PG students in Biomaterials for their friendship and support.

I would also like to thank Dr Julian Leprince, Dr Yusuke Takahashi and Dr Kevin Carter for their friendship and help.

I would like to express my gratitude to my parents, uncle, Mr Shafi M Korai, sister, brothers and friend, Dr Muhammad Farooq for their enduring support.

Finally, I would like to thank my wife, Sapna and our daughter, Suhana for their love, understanding and encouragement.

DEDICATED TO AMA, MUM, DAD, SAPNA & SUHANA

TABLE OF CONTENTS

LIST OF FIGURES

LIST OF TABLES

LIST OF ABBREVIATIONS

BFS	Bi-axial flexure strength
BHT	Butylated hydroxytoluene
BisEMA	Bisphenol A hexaethoxylated dimeyhacrylate
BisGMA	Bisphenol A diglycidyl ether dimethacrylate
BOR	Ball-on-ring
C=C	Carbon-to-carbon double bonds
CQ	Camphoroquinone
DMAEMA	Dimethylaminoethyl methacrylate
E	Elastic modulus
FEA	Finite element analysis
FSB	Filtek™ Supreme XT 'body shade'
FST	Filtek™ Supreme XT 'translucent shade'
FSF	Filtek™ Supreme XT Flowable Restorative
PMMA	Polymethyl methacrylate
RBCs	Resin-based composites
ROR	Ring-on-ring
TEGDMA	Triethylene glycol dimethacrylate
UDMA	Urethane dimethacrylate
Z100	Z100 MP Restorative™
Z250	Filtek™ Z250

Chapter 1 Development of Resin-Based Composites

1.1 Historical perspectives

In 1937, Dr Walter Wright introduced a methyl methacrylate resin, which was considered as a major development since methyl methacrylate resin exhibited improved properties compared with conventional denture base materials, such as "Vulcanite". Subsequently, Vulcanite was removed from general use in dental practice and the first polymethyl methacrylate (PMMA) heat-cured denture material namely, Vernonite (Rohm and Hass, Philadelphia, Pennsylvania) was marketed and in addition it was also used for the fabrication of inlays, crowns and fixed partial dentures (Peyton, 1943).

After World War II, chemical or self-curing acrylics were introduced in dentistry, which polymerised at room temperature. This alteration in polymerisation mode led to the application of these materials as a direct filling material and in 1940s PMMA was used as a direct filling material in restorative dentistry (Philips, 1982). These chemically cured materials consisted of a PMMA powder, methyl methacrylate monomer and benzoyl peroxide and dimethylparatoluidine initiators. They were categorised as composites as the set structure consisted of a dispersed phase by the polymer powder and a continuous three dimensional phase of polymerised resins following polymerisation at room temperature. These materials exhibited reasonable aesthetic characteristics but a variety of problems were observed; for example, poor colour stability, high polymerisation shrinkage, poor bonding to tooth structure, and a mismatch of coefficient of thermal expansion between tooth structure and material (Bowen, 1956). To overcome the problems associated with the PMMA based material, further efforts were taken by Rafael L. Bowen in the late 1950s and early

1960s who started research on the use of high molecular weight epoxy and methacrylate derivatives (Bowen, 1958). This later resulted in the introduction of a high molecular weight, difunctional monomer known as BisGMA or Bowen's resin prepared by the combination of bisphenol-A and glycidyl methacrylate. This innovation by Bowen significantly assisted the industrial development of a composite resin restorative material containing inorganic fillers. Bowen (1958) patented a novel resin-based composite (RBC) composed of 25 weight% resin and 75 weight% quartz or aluminosilicate glass filler. Consequently, Adaptic RBC (Johnson and Johnson, New Brunswick, N.J, USA), a chemically cured two-paste composition was marketed after the work of Robert Chang and Henry Lee in 1969 and 1970, respectively (Chang, 1969; Lee, 1970). Initially, adequate filler loadings in resin matrices were not achieved due to the highly viscous nature of BisGMA. Consequently, Bowen (1962) suggested the need for the admixture of a low molecular weight monomer, triethylene glycol dimethacrylate (TEGDMA) to achieve a suitable viscosity and to allow for the incorporation of a sufficient quantity of filler particles required for a successful RBC (Peutzfeldt, 1997). Moreover, the degree of conversion of the polymeric network was reduced due to the presence of high molecular weight BisGMA (Ferracane and Greener, 1986) which resulted in decreased mechanical properties. Consequently, a less viscous resin than BisGMA, namely urethane dimethacrylate (UDMA) was added and an improvement in mechanical properties was observed (Asmussen and Peutzfeldt, 1998). A silane coupling agent γ-methacyloxypropyltrimethoxysilane (γ-MPTS) was used to coat the surface of the filler particles in order to achieve a strong bond between the inorganic fillers and the resin matrix (Bowen, 1962).

In 1970, the photo-activated resin formulation, namely Prisma-Fil (Caulk Dentsply, Milford, DE, US) was introduced (Leinfelder, 1995). The RBC possessed a

photoinitiator i.e. benzoin methyl ether and required ultra-violet (UV) light to initiate the polymerisation. An increased wear resistance and colour stability of light-cured RBCs compared with chemically-cured RBCs was reported (Powers et al., 1978, 1980). The increased wear resistance of light-cured RBCs was ascribed to a decrease in the incorporation of oxygen, which is likely to be greater in chemically-cured RBCs during mixing of base and catalyst pastes. Furthermore, a light-curing method provided an increased working time for the more accurate handling of material in contrast to chemically-cured RBCs. Despite the improved properties of such RBCs, concerns over harmful effects of UV light i.e. damage to mucosa or eyes, arose. Subsequently, low energy radiation, visible light cured (VLC) RBCs were introduced. Dart et al. (1978) patented the first VLC RBC composition containing diketone initiator such as camphoroquinone (CQ) and co-initiator, namely dimethylaminoethyl methacrylate (DMAEMA), which are still utilised in RBC technology. The photoinitiator chemistry of VLC RBCs absorbed intense visible (blue) light at a wavelength of 470 nm for polymerization of the resin matrix. The wavelength of visible light was penetrated efficiently in RBCs compared with UV light and led to an increased depth of polymerization (Watts et al., 1984).

Fillers were incorporated in RBCs to provide

- Increased compressive strength (Li et al., 1985; Germain et al., 1985)
- Increased diametral tensile strength (Chung, 1990)
- Increased flexural strength (Braem et al., 1989)
- Increased fracture toughness (Ferracane et al., 1987)
- Increased elastic modulus (Braem et al., 1989; Kim et al., 1994; Li et al., 1985)
- Reduced polymerisation shrinkage (Labella et al., 1999)
- Radiopacity (Van Dijken et al., 1989)
- Enhanced aesthetic quality
- Improved handling (Pallav et al., 1989; Ikejima et al., 2003)

The carbon-to-carbon double bonds (C=C) of the methacrylate monomer convert into C-C single bonds following irradiation and form a polymer network with an associated closer packing of the molecules, which causes shrinkage (Davidson and Feilzer, 1997). Increased filler loading reduces the amount of monomer and related C=C double bonds in RBCs and hence reduces polymerisation shrinkage. The mechanical behaviour of composites is based on the theory of load sharing between the matrix and fillers. The stronger and stiffer fillers and their higher volume fraction in composites bear greater external load compared with resin matrices that contain lower filler content which can result in higher strength and elastic modulus (Hull and Clyne, 1996).

1.2 The typical constituents of modern light-cured resin-based composites

RBCs generally comprise of organic resin matrix, inorganic filler particles, coupling agent, photoinitiator system, inhibitors and optical modifiers (Table).

Constituents	Examples	Function
Resin matrix	Bisphenol A diglycidyl ether dimethacrylate (BisGMA), Triethyleneglycol dimethacrylate (TEGDMA), Bisphenol-A hexaethoxylated dimethacrylate ($BisEMA_6$), Urethane dimethacrylate (UDMA)	Creates a rigid and heavily cross-linked polymer network surrounding the filler particles and leads to hardening of a RBC.
Inorganic filler particles	Silica, quartz, barium glasses	Improve the mechanical and physical properties of RBCs.
Coupling agent	3-methacryloxypropyl-trimethoxysilane (MPTS)	Facilitates the bond between resin matrix and fillers.
Photoinitiator system	Camphoroquinone (CQ), Dimethylaminoethyl methacrylate (DMAEMA)	Initiates the process of polymerisation when light is applied.
Inhibitors	Butylated hydroxytouline (BHT)	Prevent the RBC restorative from premature polymerisation and provide improved shelf life.
Optical modifiers	Titanium dioxide, magnesium oxide, iron oxide	Improve aesthetics

1.3 Traditional resin-based composites (macrofilled)

In 1960s, grinding of larger pieces of quartz, glass, borosilicate or other ceramics was carried out for the manufacture of RBC fillers and resulted in splintered and irregular shaped particles of size 1 to 100 μm (Figure 1.1). The examples of traditional RBCs included Concise (3M, St. Paul, MN, US) and Adaptic (Johnson & Johnson, Windsor, NJ, US), which contained a particle size range of 1-40 μm (Willems et al., 1992; Sabbagh et al., 2004). The major disadvantage of traditional RBCs included insufficient wear resistance as a consequence of differential wear, which led to rapid loss of resin compared with the filler. This resulted in the large wear facets and dislodgment of filler particles from the surrounding matrix (Willems et al., 1992; Sabbagh et al., 2004). Moreover, conventional RBC restorations exhibited increased surface roughness and were more susceptible to stain and plaque deposition (Lutz and Phillips, 1983). The rough surface and dull appearance of restorations was likely due to the greater particle size of fillers in contrast to wavelength of light which render them visible from resin. Moreover, the large filler particles increased the diffuse reflection compared with specular reflection, as a result of increased surface roughness (Nanbu and Tani, 1979). Therefore, researchers developed smaller and rounded fillers with a suitable particle size distribution, which attempted to avoid the aforementioned problems (Lutz and Phillips, 1983).

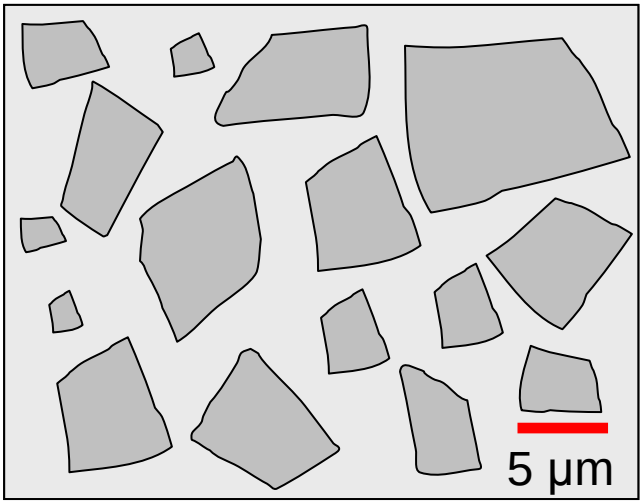

Figure 1.1. Schematic representation of traditional RBCs illustrating filler particles of approximately 1-30 µm size.

1. 4 Microfilled resin-based composites

Between 1970 and the early 1980s, RBCs with an average filler size less than 1 µm diameter were developed to improve the inferior properties of traditional types, for instance, poor wear resistance and poor aesthetic quality. In 1974, Ivoclar Vivadent were awarded a patent for "Isoplast" (Tetric EvoCeram/Tetric EvoFlow, Scientific documentation, Ivoclar-Vivadent, 2006), containing a homogenous distribution of microfillers of fumed or pyrogenic filler particles with a size of 0.05 to 0.1 µm diameters. These materials exhibited substantially improved polishing characteristics, compared with traditional RBCs, which were most likely due to the filler particle being smaller than the wavelength of visible light (Leinfelder, 1995). Theoretically, microfilled RBCs may have been classed as nanocomposites since the average size of the fumed silica was approximately 40 nm (Figure 1.2). However, due to lack of the "nano" perception during that period, these materials were categorised as microfilled.

Despite the high polishability and aesthetic appearance of homogenous microfilled RBCs, the reduction in particle size of microfilled RBCs and resulting

increase in the surface area to volume ratio of the filler particles compared with traditional macrofillers caused difficulty in loading of a comparable weight percentage of fillers particles within the resin matrix. Moreover, uncontrollable viscosity and thixotropic mixtures occurred in highly filled microfilled resins (Leinfelder, 1995; Lutz and Phillips, 1983), Therefore, the only way to avoid an increase in viscosity was to decrease the filler content, but that unavoidably compromised the strength, wear and polymerisation shrinkage characteristics of RBCs. Consequently, in order to increase the loading of smaller filler particles without affecting the handling properties, other mixing options were required for the incorporation of microfillers into resin matrix. Filler particles were produced from a prepolymerised homogeneous microfill RBC after grinding into particles of about 25 μm diameter. These filler particles were then added within a low viscosity resin matrix having a decreased volume fraction of pyrogenic silica and resulted in a heterogeneous microfilled RBC (Figure 1.2). The microfilled RBCs offered adequate polishability and colour stability, however, reduction in filler loading (45-50 weight %) reduced the wear resistance in load bearing restorations and in addition elastic modulus and fracture strength were also lower in contrast to macrofilled RBCs (Lutz and Phillips, 1983). Examples of microfilled RBCs included, Durafill (Heraeus Kulzer, Armonk, New York), Renamel Microfill (Cosmedent, Chicago, Illinois), and Heliomolar (Ivoclar Vivadent).

Lu et al. (2006) identified lower diametral tensile strength, flexural strength and flexural modulus of microfilled RBCs (Heliomolar and Renamel) compared with nanofilled and microhybrid RBCs (Section 1.2.4, 1.2.5.2). Moreover, Heliomolar exhibited inferior wear resistance in contrast to other materials. The degradation of microfilled RBCs may be attributed to the lack of covalent bonding between

prepolymerised resin fillers and polymer matrix (Ferracane, 1995). In contrast, Leinfelder and Suzuki (1999) have reported better wear resistance of Heliomolar compared with microhybrid RBCs. This contradictory finding may be explained by "protection theory", which states that the dispersion of sub-micron size fillers in microfilled RBCs reduces the interparticle spacing, thus protecting the resin between fillers against the abrasive action of food bolus (Jørgensen et al., 1979). In addition, Bayne et al. (1992) suggested that theoretically, a small amount of uniformly distributed microfiller particles (1.5-6 volume%) is needed for micro-protection to reduce wear. Due to inferior mechanical characteristics compared with hybrid RBCs (Section 1.4), the applications of microfilled RBCs are mainly confined with class III, class V and small class I restorations (Tyas, 1990).

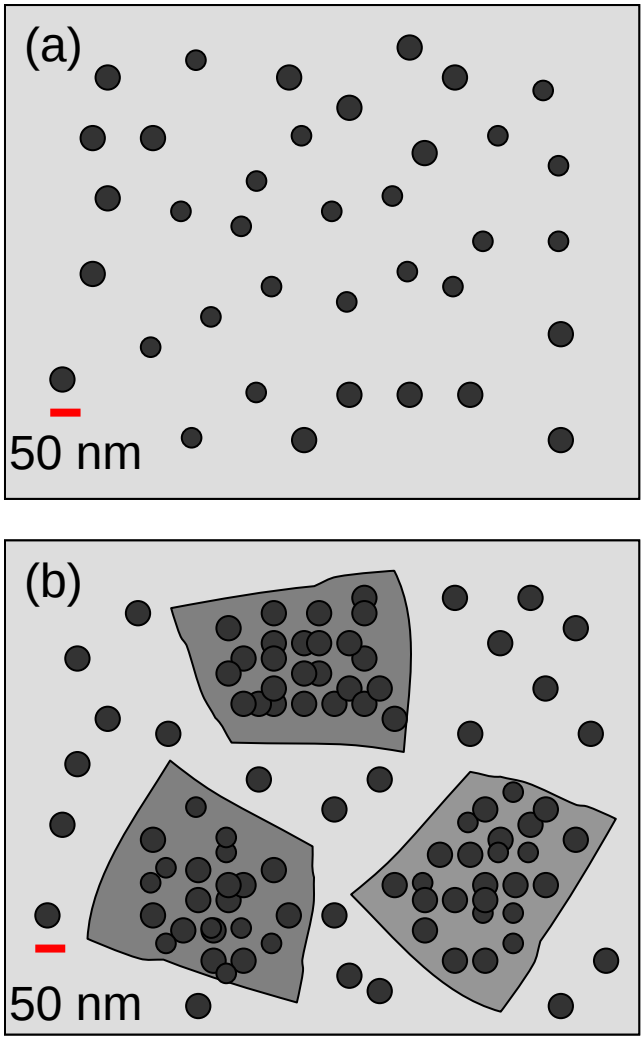

Figure 1.2. Schematic representation of (a) homogenous microfilled and (b) heterogeneous microfilled RBCs. Heterogeneous microfilled RBC shows prepolymerised filler particles of approximately 25 µm size in contrast to homogenous microfilled RBC.

1.5 Hybrid resin-based composites

Hybrid RBCs were developed to retain the advantages of both traditional macrofilled and microfilled RBCs by combining the fillers of different particle sizes and particle size distributions. Conventional hybrid RBCs possessed a bimodal filler particle distribution, i.e. larger filler particle sizes ranging from 1.0 to 5.0 μm and smaller fillers particles of 0.05 μm (Figure 1.3), which collectively resulted in an average size of about 1 μm (Willems et al., 1993). These materials showed a better wear resistance compared with traditional macrofilled RBCs (Mair et al., 1990; Leinfelder, 1987) but surface properties remained inferior because of the intrinsic wear pattern in a RBC that contains larger filler particles.

The further advancement in RBCs occurred with the development of the 'universal' hybrid material (Fig 1.3), which are indicated for all classes of cavities. These RBCs also comprised a bimodal filler distribution. Herculite XRV (Kerr Corporation, Orange, CA, USA) was introduced in 1984 as the first universal, also called a 'microhybrid', RBC which contained fine particles with an average diameter of 0.6 μm. It exhibited a flexural strength comparable with macrofilled RBCs (Peutzfeldt and Asmussen, 1992) and adequate surface smoothness for anterior restorations (Reusens et al., 1999). APH (All Purpose Hybrid) (L.D Caulk, Milford, DE, USA) RBC was introduced in late 1980s and was used for both anterior and posterior restorations and showed superior tooth-colour matching properties. Subsequently, TPH (Total Performance Hybrid) (L.D Caulk, Milford, DE, USA) emerged as product with greater wear resistance than APH in Class I and Class II restorations (Leinfelder, 1995). In general, the majority of modern microhybrid RBCs contain a filler load greater than 80 weight% and average particle size of less than 1 μm. The examples of microhybrid RBCs products include Herculite XRV (Kerr

Corporation, Orange, CA, USA), Charisma (Heraues Kulzer, Dormagen, Germany), Renew (Bisco, Schaumburg, IL, USA).

In 1992, a microhybrid RBC with monomodal filler distribution, namely Z100 (3M ESPE, St. Paul, MN, USA), was introduced. The fillers of Z100 are produced through a sol-gel process which results in rounded particles in wide distribution of 0.01 to 3.5 μm diameter, with an average of 0.6 μm. Consequently, the need of fumed silica to improve handling is eliminated in contrast to bimodal hybrid RBCs (Ferracane, 1995). Z100 exhibits good strength, abrasion resistance, polishability and handling comparable with bimodal hybrid RBCs, but, significantly greater marginal breakdown of Z100 in contrast to two hybrid RBCs (Fulfill, Caulk and Clearfil, Kuraray), has been reported in an in vitro study (Ferracane and Condon, 1999). The poor marginal behaviour of Z100 may be explained with its sensitivity to hydrolytic degradation due to the presence of a greater TEGDMA content. The increased structural heterogeneity of the TEGDMA polymeric network are likely to be higher than BisGMA, urethane dimethacrylate (UDMA) and hexaethoxylated bisphenol A glycol dimethacrylate (BisEMA) (Sideridou et al., 2003), which may allow an increase diffusion of water molecules and cause greater degradation of Z100. Filtek Z250 (3M ESPE, St. Paul, MN, USA), which comprises a similar filler type as Z100 but contains larger number of finer particles and less hydrophilic resins, was marketed. The main difference between Z100 and Z250 relates to their resin chemistries. In Z100, resin matrices comprise of BisGMA and TEGDMA, whereas in Filtek Z250, the majority of TEGDMA is replaced with urethane dimethacrylate (UDMA) and hexaethoxylated bisphenol A glycol dimeyhacrylate ($BisEMA_6$). Sideridou et al. (2003) and Palin et al. (2005) compared the water sorption of Z100

and Z250 and have reported greater sorption of former. The greater water sorption of Z100 was attributed to its greater TEGDMA content as described above.

The free radical polymerisation of dimethacrylate monomers results in polymerisation shrinkage and stress, which may deflect cusps and lead to micro-leakage, marginal staining and secondary caries. To examine this issue, Fleming at al. (2007) compared Z100 and Z250 and the authors observed a greater cuspal movement with Z100 and associated this with a greater amount of TEGDMA. The addition of TEGDMA in RBCs increases polymerisation shrinkage as the result of an increased concentration of C=C double bonds (Asmussen and Peutzfeldt, 1998) which may develop stresses and cause cuspal deflection. A useful property of Z100 is its greater flexural modulus compared with Z250 (Sideridou et al., 2003; Chung et al., 2005), which may be due to its high TEGDMA content and resultant high number of C=C double bonds which creates a high degree of crosslinking. Ideally, a greater elastic modulus of RBCs, at least equal to dentine is desirable in order to allow uniform stress distribution across restoration-tooth interface during mastication. Curtis et al. (2009) conducted the cyclic pre-loading of various RBCs including Z100 prior to bi-axial flexure strength testing at pre-loads of 20, 50 and 100 N and identified that approximately half of Z100 specimens failed to survive pre-loads of 100 N.

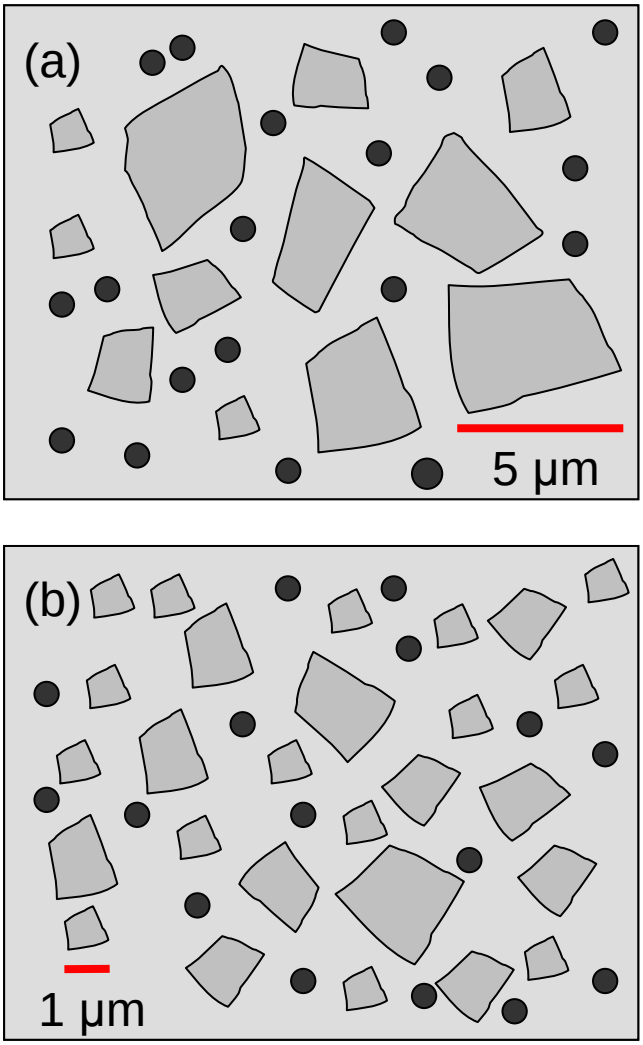

Figure 1.3. Schematic representation of (a) conventional hybrid and (B) microhybrid RBCs. Microhybrid RBC shows smaller filler particle size compared with conventional hybrid RBC.

1. 6 Classification of modern resin-based composite materials

RBCs have been classified according to filler size by different researchers (Section 1.2.2-1.2.4). However, a variety of RBCs, with bold claims of a technological advancement, have been marketed over last 15 years and complicated existing classifications. In reality, filler size and morphology have not been significantly modified compared with the existing classification of RBCs. Rheological properties of RBCs have been adjusted by changing filler particle distributions, resin monomer and resin/filler ratio. So called, "nanofilled" RBCs have been marketed in

last few years with a claim of advancement in technology, although the amorphous silica particles approximately 40 nm average size have already been used in microfilled and microhybrid RBCs. It is clear that there have only been incremental changes in filler size and morphology of currently available RBCs, thus existing classifications may remain valid. In last few years, resin chemistries of RBCs have been modified in an attempt to reduce the polymerisation shrinkage. However, until recently, RBCs were not classified according to resin monomer.

1.6.1 Rheological adjustments

The issues associated with the handling of RBCs in different clinical situations such as class II restorations and cavities with difficult access brought about demand for materials with improved handling characteristics. Consequently, a variety of RBCs, namely "flowable" and "packable", were developed and marketed.

Flowable RBCs were introduced in 1996 in an attempt to improve the handling characteristics of materials and in turn, increase flow towards inaccessible parts of the tooth and improve adaptation to the cavity walls (Bayne et al., 1998; Frankenberg et al., 1999). Flowable RBCs are usually comprised of conventional resins with a filler content of less than 50 volume% compared with 57 to 72 volume% of traditional hybrid RBCs and show substantial variation in flow properties (Combe et al., 1999). Some flowable RBCs have been produced by addition of large amount of a diluent monomer such as TEGDMA to high molecular weight monomer, for example BisGMA and UDMA in an attempt to reduce the viscosity (Al-Hiyasat et al., 2005; Baroudi et al., 2007).

Bayne et al. (1998) compared rheological properties of eight flowable RBCs (Aeliteflo, CrystalEssence, FloRestore, Flow-IT, Revolution, True-look, Ultraseal XT

Plus and Versaflo) and two hybrid RBCs (Prodigy and Z100) and identified five times greater flow of Ultraseal XT Plus than the Aeliteflo. In addition, a similar amount of fluidity was observed between Z100 and Aeliteflo but Prodigy exhibited the highest viscosity among all materials investigated. The broad discrepancies in the viscosities of flowable RBCs (Lee et al., 2003; Bayne et al., 1998) have led to considerable variation in polymerisation shrinkage, elastic modulus and other physical properties (Attar et al., 2003). Labella et al. (1999) found higher polymerisation shrinkage and lower elastic modulus of flowable RBCs compared with hybrid RBCs. However, RBCs with greater elastic modulus are required for posterior restorations in order to bear high masticatory load, which otherwise may deform and lead to interfacial disruption. The reduced amount of fillers and inferior physical properties have restricted the use of flowable RBCs in low stress bearing cavities, such as small class I restorations, class V restorations, amalgam repair, pit and fissure sealants and as a base for class I and II restorations (Combe et al., 1999).

The use of flowable RBCs as a liner in class II restorations has also been suggested. During early phase of polymerisation, a low modulus RBC may flow plastically and reduce the interfacial stresses and maintain the marginal seal of restoration. The microleakage in class II packable RBCs restorations with and without flowable liner was evaluated by researchers in vitro and they have reported reduction in microleakage with the application of a flowable liner (Leevailoj et al., 2001). However, Jain and Belcher (2000) found no significant difference between microleakage of class II restorations with and without flowable RBC liner. Braga et al. (2003) evaluated the contraction stress of flowable and nonflowable RBCs and influence of flowable RBC in stress reduction under nonflowable RBCs restorations in vitro. They observed similar levels of stresses in flowable and nonflowable RBCs

and no significant reduction of stresses with flowable when used as liner under nonflowable RBCs.

RBCs have remained deficient in terms of handling and establishing adequate contours with neighbouring teeth in contrast to amalgam. Hence, so-called “packable” RBCs were introduced with an objective of increasing material viscosity and improving subsequent handling properties (Leinfelder et al., 1999). Generally, alteration in the filler particle size distribution, resin matrix or addition of rheological control additives, namely fumed silica, have been carried out to make a packable RBC which exhibits higher viscosity and less tackiness compared with other RBCs (van Noort, 2002). The manufacturers claim improved handling properties and better adaptation of packable RBCs in the proximal box of a class II restoration. However, Peumans et al. (2001) disregarded such claims and suggested that the matrix system has a significant effect over interproximal contacts in class II restorations rather than RBCs. The packable RBCs have shown inferior physical and optical properties compared with universal hybrid RBCs but some dentists prefer the viscous nature of the material. Physical properties of five RBCs were evaluated by Cobb et al. (2000) which include, three packable RBCs, Alert Condensable RBC (Jeneric Pentron), SureFil High Density Posterior Restorative (Dentsply Caulk) and Solitaire (Heraeus Kulzer); one conventional hybrid RBC, TPH Spectrum (Dentsply Caulk); and one microfill RBC, Heliomolar Radiopaque (Ivoclar-Vivadent). The authors reported that packable RBCs possess better handling characteristics, however, physical properties remained inferior compared with conventional hybrid RBC. They further added that large particles in packable RBCs may decrease wear resistance and increase surface roughness. The dynamic elastic modulus of 12 packable RBCs was investigated by Lambrechts et al. (2001) and they have reported wide variation in elastic modulus

ranging from of 8.5 to 23.4 GPa which may create confusion in terms of material selection for posterior restorations. Manhart et al. (2000) determined the flexural strength, flexural modulus, fracture toughness and wear resistance of commercially available packable RBCs and all materials exhibited substantial differences in mechanical properties. The greater diversity in mechanical characteristics was attributed to filler type, filler volume fraction, and particle distribution. The polymerisation shrinkage stress of packable RBCs was compared with a conventional hybrid RBC and authors have reported that packable RBCs exhibit significantly higher contraction stress in contrast to hybrid RBCs. The difference between materials was attributed to different filler loading, elastic modulus and resin matrix (Chen et al., 2000).

It is clear that rheological adjustments have been mainly carried out by changing filler volume, size distribution and resin matrix type, therefore, a variation in associated mechanical properties is expected.

1.6.2 Nanofilled composite technology

Nanotechnology can be defined as the construction of materials and structures of size 100 nm or less with novel characteristics through manipulating, measuring and modelling of matter on a molecular scale (Harris and Ure, 2006). The manufacturing of nanoparticles for microfilled and nanofilled RBCs involves a bottom-up synthetic chemical sol-gel process in contrast to the traditional milling technique employed for macrofilled RBCs (Mitra et al., 2003).

A nanofilled RBC, Filtek Supreme Universal Restorative, was introduced by 3M ESPE, St. Paul, MN, USA in 2003, which comprised of two types of particles. First, individual nanosized particles or ‘nanomers’ of 20 nm size and second, ‘nanoclusters’ of 0.6-1.4 μm size formed by the aggregation of 75 nm nanosized

particles. The nanoparticles and nanoclusters were coated or penetrated with silane before mixing with the resin matrix. This material is considered a nanofilled composite by the manufacturer as it only contains nanoscale particles. However, this it could also be termed a nanohybrid or a microhybrid, which may be due to the nanoclusters of 0.6-1.4 μm size. The manufacturer has suggested that nanofilled RBCs possess high polish retention similar to that of microfilled and physical and mechanical properties comparable with hybrid RBCs (Mitra et al., 2003). Beun et al. (2007) and Rodrigues Junior et al. (2008ab) compared various mechanical and physical properties of the microhybrid and nanofilled RBCs and their findings are in agreement with Mitra et al. (2003). On the contrary, Shah et al. (2009) identified higher flexural strength of a microhybrid RBC compared with a nanofilled RBC. Curtis et al. (2008, 2009) have reported distinct mechanical properties of RBCs with nano-sized particles and 'nanoclusters' in connection with water uptake and cyclic loading. The greater bi-axial flexure strength degradation of nanofilled RBCs compared with microhybrid RBCs at various storage regimes in water was most likely due to their greater surface area to volume ratio and resulting availability of hydrophilic component of the silane. However, enhanced fracture resistance and reliability in flexural strength following cyclic pre-loading was observed in RBCs having nanoclusters, which may be ascribed to infiltration of silane in the interstices of nanoclusters and subsequent reinforcement with resin matrix. Shah et al. (2009) compared the fracture toughness of a microhybrid (Filtek Z250) and a nanofilled (Filtek Supreme Plus) RBCs (3M ESPE, St. Paul, MN, USA) using fracture fatigue methods following post-cured heat treatment and hydration. Both heat treated RBCs showed an increased toughness resulting from extrinsic toughening mechanisms such as crack deflection and crack bridging, which occurred due to interparticle/intercluster

crack growth. Crack deflection is a shielding mechanism that increases the fracture resistance by lowering the stress intensity factor at the crack tip. Crack deflection may form uncracked bridges behind the crack tip and sustain part of the applied load, which would otherwise be experienced at crack tip and therefore toughens the material. Following hydration, toughness of Filtek Supreme decreased significantly in contrast to Z250 and reduced toughness of Filtek Supreme was attributed to filler/ matrix debonding which was not evident in Z250 (Shah et al., 2009).

1.6.3 Nanofilled controversy

Since the introduction of so-called, "nanofilled" RBCs by 3M ESPE (St. Paul, MN, USA), some dental material manufacturers have modified the formulations of their microhybrid RBCs by adding more nanoparticles and pre-polymerised fillers, and have named this category "nanohybrid" RBCs. However, it is difficult to differentiate nanohybrid from microhybrid RBCs as the result of slight variation in their particle size and also their interchangeable properties such as flexural strength and modulus (Ilie and Hickel, 2009). Consequently, a controversy exists among researchers regarding the RBCs classification and until now "nano" is not considered as a well-established classification (Harris and Ure, 2006; Curtis et al., 2008).

The overall reduction in particle size and incorporation of filler particles of various sizes have been carried out since the invention of RBCs in order to optimise mechanical properties. The introduction of so-called nanofilled or nanohybrid RBCs also seems to be a furtherance of such a concept. But, due to availability of a variety of nanofilled, nanohybrid and microhybrid RBCs with different formulations, it is difficult to justify which RBC is superior. Many studies have compared mechanical and physical characteristics of commercially available RBCs and reported a wide

variation in results. Most studies reveal similarities between nanohybrid and microhybrid RBCs, which may be due to similar filler morphologies and volume fraction (Beun et al., 2007; Rodrigues Junior et al., 2008ab), whereas some researchers have reported superior (Musanje and Ferracane, 2004; Curtis et al., 2009) or inferior (Curtis et al., 2008; Shah et al., 2009) properties of nanofilled RBCs compared with microhybrid RBCs. These differences in results may be explained, in-part, with different testing methods between investigators. In the majority of studies, commercial nanofilled RBCs have been investigated, therefore, effect of confounding variables such as resin and photo-initiator chemistry on the material properties may be expected during comparison of materials. Hence, determination of experimental nanohybrid or nanofilled RBCs with controlled variables is desirable to understand novel aspects of future nanocomposite technology. A nanofilled RBCs classification may develop in future, when RBCs are loaded entirely with nanosized components and exhibit distinct characteristics compared with currently available RBCs.

References

Al-Hiyasat AS. Darmani H, Milhem MM. Cytotoxicity evaluation of dental resin composite and their flowable derivatives. Clinical Oral Investigation, 2005; 9: 21-25.

Asmussen E, Peutzfeldt. Influence of UEDMA, BisGMA and TEGDMA on selected mechanical properties of experimental resin composites. Dental Materials, 1998; 14: 51-56.

Attar N, Tam LE, McComb D. Flow,strength, stiffness and radiopacity of flowable resin composites. Journal of the Canadian Dental Association, 2003; 69:516-521.

Baroudi K, Saleh AM, Silikas N, Watts DC. Shrinkage behaviour of flowable-resin composites related to conversion and filler fraction. Journal of Dentistry, 2007; 651-655.

Bayne SC, Thompson JY, Swift EJ, Stamatiades P, Wilkerson M. A characterization of first-generation flowable composites. Journal of the American Dental Association, 1998; 129: 567-577.

Bayne SC, Taylor DF, Heymann HO. Protection hypothesis for composite wear. Dental Materials, 1992; 8: 305-309.

Beun S, Glorieux T, Jacques D, Vreven J, Leloup G. Characterisation of nanofilled compared to universal and microfilled composites. Dental Materials, 2007; 23:51-59.

Bowen RL. Use of epoxy resins in restorative materials. Journal of Dental Research, 1956; 35: 360-369.

Bowen RL. Synthesis of a silica-resin direct filling material: progress report. Journal of Dental Research, 1958; 37:90-91.

Bowen RL. Dental filling materials comprising of Vinyl-silane treated fused silica and binder consisting of the reaction product of Bisphenol and Glycidyl Methacrylate. 1962, US Patent 3,066, 112.

Braem M, Finger W, Van Doren VE, Lambrechts P, Vanherle G. Mechanical properties and filler fraction of dental composites. Dental Materials, 1989; 5: 346-349.

Braga RR, Hilton TJ, Ferracane JL. Contraction stress of flowable composites materials and their efficacy as stress relieving layers. Journal of the American Dental Association, 2003; 134: 721-728.

Chang RWH. Dental restorative material. 1969, US Patent 3,452,437.

Chen HY, Manhart J, Hickel R, Kunzelmann KH. Polymerisation contraction stress in light-cured packable composite resins. Dental Materials, 2001; 17:253-259.

Chung KH. The relationship between composition and properties of posterior resin composites. Journal of Dental Research, 1990; 68: 852-856.

Cobb DS, Macgregor KM, Vargas MA, Denehy GE. The physical properties of packable and conventional posterior resin-based composites: a comparison. Journal of the American Dental Association, 2000; 131: 1610-1615.

Curtis AR, Shortall AC, Marquis PM, Palin WM. Water uptake and strength charactersistics of nanofilled resin-based composites. Journal of Dentistry, 2008; 36:186-193.

Curtis AR, Palin WM, Fleming GJP, Shortall ACC, Marquis PM. The mechanical properties of nanofilled rein-based composites: The impact of dry and wet cyclic pre-loading on bi-axial flexure strength. Dental Materials, 2009; 25:188-197.

Dart EC. Cantwell JB, Traynor JR, Taworzyn JF, Nemeck J. Method of repairing teeth using a composition which is curable by irradiation by visible light, 1978: US Patent 4,089,763.

Davidson CL, Feilzer AJ. Polymerisation shrinkage and polymerisation shrinkage stress in polymer-based restoratives. Journal of Dentistry, 1997; 25:435-440.

Ferracane JL, Greener EH. The effect of resin formulation on the degree of conversion and mechanical properties of dental restorative resins. Journal of Biomedical Materials Research, 1986; 20: 121-131.

Ferracane JL, Antonio RC, Matsumoto H. Varibales affecting the fracture toughness of dental composites. Journal of Dental Research, 1987; 66:1140-1145.

Ferracane JL, Current trends in dental composites. Critical Review in Oral Biology and Medicine, 1995; 6:302-318.

Ferracane JL, Condon JR. In vitro evaluation of the marginal degradation of dental composites under simulated occlusal loading. Dental Materials, 1999; 12: 262-267.

Fleming GJP, Cara RR, Palin WM, Burke FJT. Cuspal movement and microleakage in premolar teeth restored with resin-based filling materials cured using a ‘soft strat’ polymerisation protocol. Dental Materials, 2007; 23: 637-643.

Frankenberger R, Krämer N, Pelka M. Internal adaptation and overhang formation of direct class II resin composite restorations. Clinical Oral Investigations, 1999; 3:208-215.

Germain HS, swartz ML, Philips RW, Moore BK, Roberts TA. Properties of microfilled composite resins as influenced by filler content. Journal of Dental Research, 1985; 64: 155-160.

Harris J, Ure D. Exploring whether ‘nano’ is always necessary. Nanotechnology Perceptions, 2006; 2: 1-15.

Hull D, Clyne TW. General introduction. In: Hull D, Clyne TW. An Introduction to Composite Materials (2nd Edition). Cambridge University Press, 1996; Chapter 1: 1-8.

Ikejima I, Nomoto R, McCabe JF. Shear punch strength and flexural strength of model composites with varying filler volume fraction, particle size and silanation. Dental Materials, 2003; 19: 206-211.

Ilie N, Hickel R. Investigations on mechanical behaviour of dental composites. Clinical Oral Investigations, 2009; 13: 427-438.

Jain P, Belcher M. Microleakage of class II resin-based composite restorations with flowable composites in proximal box. American Journal of Dentistry, 2000; 13:235-238.

Jørgensen KD, Horsted P, Janum O, Krogh J, Schulz J. Abrasion of class I restorative resins. Scandinavian Journal of Dental Research, 1979; 87: 140-145.

Kim KH, Park JH, Imai Y, Kishi T. Microfracture mechanisms of dental resin composites containing spherically-shaped fillers particles. Journal of Dental Research, 1994; 73: 499-504.

Kleverlaan CJ, Feilzer AJ. Polymerisation shrinkage and contraction stress of dental resin composites. Dental Materials, 2005; 21:1150-1157.

Labella R, Lambrechts P, Van Meerbeek B, Vanherle G. Polymerisation shrinkage and elasticity of flowable composite and filled adhesives. Dental Materials, 1999; 15: 128-137.

Lambrechts YAP, Inoue S, Braem MJA, Takeuchi M, Vanherle G, Meerbeek V. Dynamic elastic modulus of 'packable' composites. Dental Materials, 2001; 17:520-525.

Lee HL. Dental filling material. 1970, US Patent 3,539,533.

Lee IB, Son HH, Um CM. Rheological properties of flowable, conventional hybrid and condensable composite resins. Dental Materials, 2003; 19:298-307.

Leevailoj C, Cochran MA, Matis BA, Moore BK, Platt JA. Microleakage of posterior packable resin composites with and without flowable liners. Operative Dentistry, 2001; 26: 302-307.

Leinfelder KF. Wear patterns and rates of posterior composite resins. International Dental Journal. 1987; 37:152-157.

Leinfelder KF. Posterior composite resins: The materials and their clinical performance. Journal of the American Dental Association, 1995; 126:663-676.

Leinfelder KF, Bayne SC, Swift JR EJ. Packable composites: overview and technical consideration. Journal of Esthetic Dentistry, 1999; 11: 234-249.

Leinfelder KF, Suzuki S. In vitro wear device for determining posterior composite wear. Journal of American Dental Association, 1999; 130: 1347-1353.

Li Y, Swartz ML, Philips RW, Moore BK, Roberts TA. Material science effect of filler content and size on properties of composites. Journal of Dental Research, 1985; 64: 1396-1401.

Lu H, Lee YK, Oguri M, Powers JM. Properties of a dental resin composite with spherical inorganic filler. Operative Dentistry, 2006; 31: 734-740.

Lutz F, Phillips RW. A classification and evaluation of composite resin systems. Journal of Prosthetic Dentistry, 1983; 50:480-488.

Mair LH, Voules RW, Cunningham J. The clinical wear of three posterior composites. British Dental Journal, 1990; 169: 335-360.

Manhart J, Kunzelmann KH, Chen HY, Hickel R. Mechanical properties and wear behaviour of light-cured packable composite resins. Dental Materials, 2000; 16:33-40.

Mitra SB, Dong WU, Holmes BN. An application of nanotechnology in advanced dental materials. Journal of the American Dental Association, 2003; 134:1382-1390.

Musanje L, Ferracane JL. Effects of resin formulation and nanofiller surface treatment on the properties of experimental hybrid resin composite. Biomaterials, 2004; 25:4065-4071.

Nanbu T, Tani Y. Study of surface gloss of composite restorative materials. Dental Materials Journal, 1979; 35: 421-430.

Palin WM, Fleming GJP, Burke FJT, Marquis PM, Randall RC. The influence of short and medium-term immersion on hydrolytic stability of novel low-shrink dental composites. Dental Materials, 2005; 21:852-863.

Pallav P, De Gee AJ, Davidson CL, Erickson RL, Glasspoole EA. The influence of admixing microfiller to small-particle composite resin on wear, tensile strength, hardness, and surface roughness. Journal of Dental Research, 1989; 68: 489-490.

Peumans M, Meerbeek BV, Asscherickx K, Simon S, Abe Y, Lambrechts P, Vanherle G. Do condensable composites help to achieve better proximal contacts? Dental Materials, 2001; 17:533-541.

Peutzfeldt A, Asmussen E. Modulus of resilience as predictor for clinical wear of restorative resins. Dental Materials, 1992; 8: 146-148.

Peutzfeldt A. Resin composites in dentistry: the monomer systems. European Journal of Oral Sciences, 1997; 105:97-116.

Peyton FA. Physical and clinical characteristics of synthetic resins used in dentistry. Journal of the American Dental Association, 1943; 30: 1179-1189.

Philips RW. Restorative resins. In: Philips RW. Skinners's Science of Dental Materials. 8th Edition. W.B.Saunders Company, 1982; Chapter 14:216-247.

Powers JM, Dennison JB, Lepeak PJ. Parameters that affects the colour of direct restorative resins. Journal of Dental Research, 1978; 57: 876-880.

Powers JM, Fan PL, Raptis CN. Colour stability of new composite restorative materials under accelerated aging. Journal of Dental Research, 1980; 59: 2071-2074.

Reusens B, D'hoore W, Vreven J. In vivo comparison of a microfilled and a hybrid minifilled composite resin in class III restorations: 2-year follow-up. Clinical Oral Investigations, 1999; 3: 62-69.

Rodrigues Junior SA, Ferracane JL, Bona AD. Flexural strength and Weibull analysis of a microhybrid and nanofill composite evaluated by 3- and 4-point bending tests. Dental Materials, 2008a; 24:426-431.

Rodrigues Junior SA, Scherrer SS, Ferracane JL, Bona AV. Microstructural characterisation and fracture behaviour of a microhybrid and a nanofill composite. Dental Materials, 2008b; 24:1281-1288.

Sabbagh J, Ryelandt L, Bacherius L, Biebuyck JJ, Vreven J, Lambrechts P, Leloup G. Characterisation of the inorganic fraction of resin composites. Journal of Oral Rehabilitation, 2004; 31: 1090-1101.

Shah MB, Ferracane JL, Kruzic JJ. R-curve behaviour and toughening mechanism of resin-based dental composites: Effects of hydration and post-cure heat treatment. Dental Materials, 2009; 25:760-770.

Sideridou I, Tserki V, Papanastasiou G. Study of water sorption, solubility and modulus of elasticity of light-cured dimethacrylate-based dental resins. Biomaterials, 2003; 24:655-665.

Tetric EvoCeram/Tetric EvoFlow, Scientific documentation, Ivoclor Vivadent, 2006.

Tyas MJ. Correlation between fracture properties and clinical performance of resins in class IV cavities. Australian Dental Journal, 1990; 35:46-49.

Van Dijken JWV, Wing KR, Ruyter IE. An evaluation of the radiopacity of composite restorative materials used in class I and class II cavities. Acta Odontologica Scandinavica, 1989; 47: 401-407.

van Noort R. Resin composites and polyacid–modified resin composites. In: van Noort R. Introduction to Dental Materials. 2nd Edition. Mosby, 2002; Chapter 2.2: 96-123.

Watts DC, Amer O, Combe EC. Characteristics of visible light-activated composite systems. British Dental Journal, 1984; 156: 209-215.

Willems G, Lambrechts P, Braem M, Celis JP, Vanherle G. A classification of dental composites according to their morphological and mechanical characteristics. Dental Materials, 1992; 8: 310-319.

Chapter 2 Mechanical Properties of Resin-Based Composites

2.2 Theoretical strength characterisation

The theoretical strength of a brittle material is the stress required to separate it into two parts (Griffith, 1921) (Section 2.1.1) and is dependent upon critical flaws, which are capable of initiating fracture at an applied stress. The flaws vary widely in size, severity and orientation and therefore a scatter in strength data will inevitably exist.

2.1.1 Griffith's Law

The concept that microscopic flaws present in a brittle material control the strength property of that particular material is based on the experimental and theoretical work of Griffith (Griffith, 1921). These flaws, which are located on the surface or within the volume of the specimens act as nuclei, from where cracks can propagate and lead to failure of specimens (Baran et al., 2001).

During experimental as well as theoretical tests, a crack in a brittle material is subjected to an increase axial stress and grows spontaneously in relation to critical stress and eventually leads to failure of the specimen. A larger crack requires smaller stress to grow. This relationship can be expressed as in the following equation (Darvell, 2002):

$$\sigma_{crit}.\sqrt{c} = \sqrt{4E\gamma/\pi} \qquad \text{Equation 2.1}$$

This relates the critical stress (σ_{crit}) for a given crack length (c), Young's modulus (E) and the surface energy (γ) of that material. The surface energy is

included because the growth of a crack requires formation of two new surfaces. The growth of a crack can be simply described by the energy balance relationship which states that crack extension occurs when the stored elastic energy in specimens exceeds the energy required to create the new surfaces (Darvell, 2002).

Griffith's law provides reasonable agreement with experimental data for brittle materials. However, some brittle-like materials such as resin-based composites (RBCs) may exhibit some plastic deformation at the crack tip and are therefore able to consume a greater amount of energy in contrast to the energy required for the creation of a new surface. In simple terms, plastic deformation near the crack tip leads to dissipation of elastically stored energy and slows the crack growth. In terms of Griffith's law, any flaw or defect in the structure such as porosity, an unbonded interface between a filler particle and resin matrix, a weak inclusion in a structure or a weak grain boundary in metal can act as a crack (Darvell, 2002).

The organic matrix and filler content of RBCs are bonded through a silane-coupling agent. Inadequate silanisation of the filler may lead to structural defects at the filler-matrix interface, which act as a micro-cracks and initiate crack propagation along the interface, consequently resulting in failure (Yoshida et al., 2002). Curtis et al. (2008) correlated the water uptake and bi-axial flexural strength of two nanofilled and one microhybrid RBC. All RBCs exhibited significant strength degradation following 6 months immersion in water compared with control specimens. The reduction in the strength of all RBCs was the result of debonding of the filler at the interface due to water infiltration, confirmed by interfacial micro-cracks under a scanning electron microscope. Opdam et al. (1996, 2002) investigated the effect of RBC consistency and application technique on porosity. The authors identified a lesser porosity with injection technique in contrast to smearing and condensation

techniques. Furthermore, the thick-consistency RBC produced more voids compared with thin- and medium-consistency RBCs. Porosity in the RBCs may therefore act as cracks in terms of Griffith's law and therefore accelerate the crack propagation and reduce the strength of materials and ultimately may compromise the clinical performance of materials.

2.1.2 Weibull Modulus

Fracture of brittle materials such as ceramics or materials that exhibit brittle-like failure, usually originates from flaws distributed at the surface or within the material. The major flaw size, on which the strength of a material is based, varies from specimen to specimen and therefore a variation in strength values is expected. However, the strength data of RBCs has been mainly reported by only mean strength values and associated standard deviations and it is assumed that mean strength is a true value and signifies a normal strength distribution. In reality, the defect population lacks this level of homogeneity and as a result the failure of material may occur at lower stresses (McCabe and Carrick, 1986). Therefore, the strength of RBCs may only become meaningful when it is evaluated by a probability function such as Weibull statistics (Weibull, 1951; McCabe and Carrick, 1986).

The Weibull modulus of a group of specimens may consider the flaw population in a brittle material. A high Weibull modulus suggests a narrow distribution of defects and an increased reliability of strength data (Weibull, 1951). Other useful features of Weibull statistics include its ability to predict changes in distributions according to the physical size of individual test specimen. By this property of Weibull statistics, strength values of one sample may be scaled to predict the corresponding strengths values for different sample size, shape or stress distribution (Quinn, 2003).

Weibull statistics have been employed for strength data of RBCs in numerous studies (Chadwick et al., 1989; Drummond and Mlescke, 1991; Zhao et al., 1997; Baran et al., 1998; Brosh et al., 1999; Lohbauer et al., 2003; Palin et al., 2003ab, 2005ab; Rodrigues Junior et al., 2008ab; Bhamra and Fleming, 2008; Curtis et al., 2009b; Ilie and Hickel, 2009; Pick et al., 2010). Palin et al. (2003) compared the reliability of bi-axial flexure test of RBCs with three-point flexure test using Weibull modulus and have suggested that bi-axial flexure testing method provides a more reliable testing method than three-point flexure. The increased reliability of bi-axial flexure testing was attributed to decreased curing variability in disc shaped specimens in contrast to three-point flexure specimens. Rodrigues Junior et al. (2008b) compared the four-point flexure strength of a nanofilled and a microhybrid RBCs by Weibull modulus and no significant differences between flexural strength and associated Weibull modulus of both RBCs were observed. The authors suggested that similar behaviour of RBCs might be a consequence of comparable filler content and morphology of both RBCs. Chadwick et al. (1989) investigated the influence of placement technique on compressive strength of RBC using Weibull statistics. In one group RBC specimens were prepared with an amalgam plugger, while in the other group specimens were prepared by smearing with a plastic spatula. The specimens group prepared by condensation technique showed lower Weibull modulus, which is indicative of decreased reliability compared with specimens prepared by smearing technique. The lower Weibull modulus may be explained by greater porosity in specimens, which were manufactured by a condensation technique.

It is clear that there is a considerable interest in using Weibull statistics for the evaluation of RBC strength reliability. However, a wide range of RBCs with variable elastic moduli are available. Despite this fact, no one has considered the applicability

of Weibull statistics with less brittle RBCs. Since Weibull statistics are well-established for highly brittle materials, it might be that RBCs with greater resin content may not provide strength data that is applicable to the use of Weibull statistics. Moreover, many studies have submitted RBC strength data to Weibull statistics and found a wide variation in Weibull moduli of similar RBCs. For example, a Weibull modulus of Filtek Z250 ranging between 4.2-12.4 has been reported in the literature (Table 2.1). These differences in results may lead to incorrect interpretation of data between investigators. Therefore, research in terms of applicability of Weibull statistics to different RBCs is required, which may consequently aid in the accurate interpretation of data.

Table 2.1. Weibull modulus (m) of different RBCs identified in some studies.

Reference	Year	Test method	Materials	Weibull modulus (m)
Curtis et al.	2009	Bi-axial flexure	Heliomolar Filtek Z250 Z100 Filtek Supreme Body Filtek Supreme Translucent Grandio Grandio Flow	5.1-8.2 4.3-11.5 3.3-10.8 4.0-11.8 6.0-16.9 7.3-12.1 2.1-9.5
Ilie and Hickel	2009	Three-point flexure	Filtek Silorane EsthetX Tetric Tetric Ceram Tetric Ceram HB Tetric EvoCeram Filtek Supreme XT	9.0-11.4 6.5-10.1 8.5-10.1 5.3-14.9 3.5-15.4 13.5-17.8 3.6-9.4
Lahbauer et al.	2003	Four-point flexure	Charisma Definite Filtek Z250 Heliomolar Solitaire Solitaire II Surefil Tetric Ceram	9.2 9.1 10.8 8.1 5.6 9.6 8.4 12.3

Table 2.1 (continued). Weibull modulus (m) of different RBCs identified in some studies.

Reference	Year	Test method	Materials	Weibull modulus (m)
Palin et al.	2003a	Bi-axial flexure	Oxirane-based RBC Filtek Z250 Z100	16.2 11.9 10.2
Palin et al.	2003a	Three-point flexure	Oxirane-based RBC Filtek Z250 Z100	9.2 8.5 6.3
Palin et al.	2003b	Bi-axial flexure	Oxirane-based RBC Filtek Z250 Z100	4.7-16.2 7.5-11.9 6.6-10.2
Palin et al.	2005a	Three-point flexure	Z250	8.5-10.1
Palin et al.	2005a	Bi-axial flexure	Z250	11.9-12.4
Pick et al.	2010	Three-point flexure	Concept Advanced Filtek Z250 Heliomolar	3.9 4.2 3.3
Pick et al.	2010	Bi-axial flexure	Concept Advanced Filtek Z250 Heliomolar	8.6 6.6 7.2
Rodrigues Junior et al.	2008	Three-point flexure	Filtek Z250 Filtek Supreme	7.6 9.7

2.2 Experimental strength characterisation

The mechanical strength of RBCs is reliant upon the complex intra-oral forces such as compressive, tensile and shear introduced during mastication (Douglas, 1996) and it has a significant influence on the performance of dental restorations (Ban and Anusavice, 1990). The reproduction of such complex stresses in vitro is likely to be difficult in terms of cost and methodology. In addition, the dynamic tests may increase the probability of inertial effects and lead to misleading data. Consequently, various static-load-to-failure strength testing techniques i.e. compressive (Brosch et al., 1999; Jandt et al., 2000) diametral tensile (Penn et al., 1987; Asmussen and Peutzfeldt, 1998; Aguiar et al., 2005) and flexure (Ferracane et al., 1998; Manhart et al., 2000ab; Palin et al., 2005) have been employed for the determination of the mechanical strength of RBCs.

2.2.1 Diametral Tensile Testing

In the diametral tensile test, cylindrical or disc specimens (6 mm diameter, 3 mm thickness) are employed and loaded in compression across their diameter (Ban and Anusavice, 1990) and tensile stresses are generated at right angles to loaded diameter (Figure 2.1) which result in fracture. In addition to uniform tensile stresses across the diameter, the occurrence of shear forces at contact between specimens and platens of loading machine have been suggested (Figure 2.1) (Williams and Smith, 1970; Palin et al., 2003) which may result in complex stresses and lead to a significant variation in fracture pattern of specimens (Ban and Anusavice, 1990). Moreover, less brittle specimens are likely to be deformed significantly and produce shear stresses at the apex of the diametral plane before failure, which may lead to invalid data

(Darvell, 1990; Ban and Anusavice, 1990) and render the comparison of results difficult between different researchers.

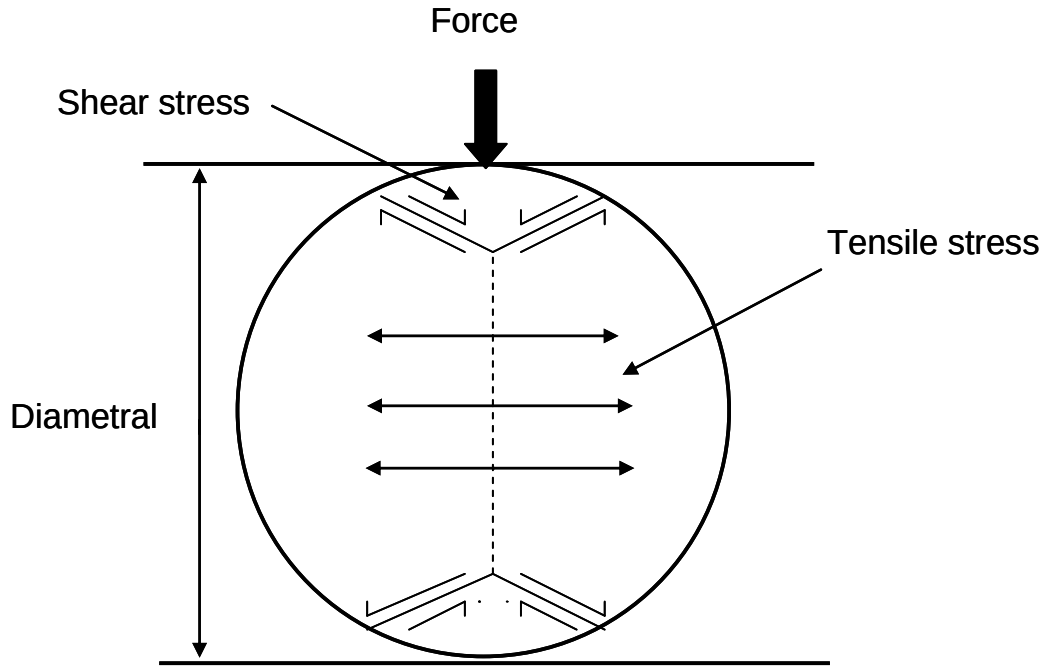

Figure 2.1. Schematic representation of diametral tensile testing adapted from (Darvell, 2002) illustrating tensile stresses in the centre and shear stresses at the point of contact of specimen.

2.2.2 Compressive Testing

For compressive strength, cylindrical specimens (4 mm diameter, 6 mm thickness) are used and loaded longitudinally in compression in contrast to diametral tensile testing. The failure of specimen in compressive testing is also believed to be the result of generation of tensile and shear stresses (Figure 2.2) (Berenbaum and Brodie, 1959). Consequently, a high correlation between diametral tensile and compressive strength has been suggested in literature (Ban and Anusavice, 1990).

The cylindrical specimens are not clinically relevant as their geometry does not mimic that of clinical restorations. Moreover, incomplete cure in the centre of light-activated RBC specimens (Palin et al., 2003) is expected despite the irradiation from both surfaces since most conventional RBCs exhibit a limited depth of cure of 2

mm (Tsai et al., 2004) or even less (Moore et al., 2008). However, in a previous study, Masouras et al. (2008a) irradiated the cylindrical specimens (5 mm diameter, 6 mm height) from upper and lower surface and subsequently an additional light cure was performed in a curing chamber. It is likely that additional curing may enhance the degree of conversion of polymer matrix as the result of greater heating effects in curing unit (Ferracane and Condon, 1992).

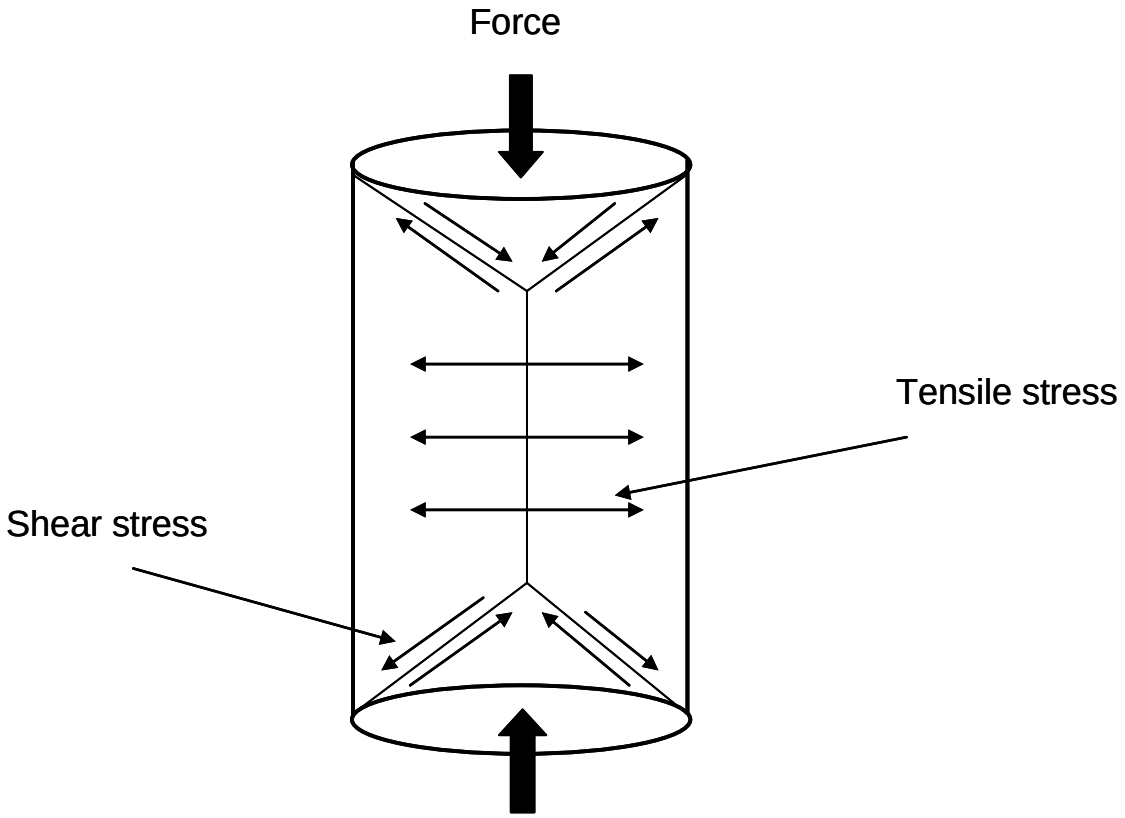

Figure 2.2. Schematic representation of compressive testing of a cylindrical specimen adapted from (Darvell, 2002) highlighting the shear stresses along the cone shaped area at either end of specimen and tensile stresses within the centre portion of cylinder. The stresses generated during compressive testing appear comparable with diametral tensile testing.

2.2.3 Three-Point Flexure Testing

The International Standards Organisation (ISO) recommends the three-point flexure test to determine the flexural strength of RBCs (ISO 4049) which is frequently employed for dental RBC research worldwide. The three-point flexure test utilizes bar-shaped specimens (25 mm length, 2 mm width, and 2 mm thickness) and specimens are centrally loaded using a knife-edge indenter with a support span of 20 mm at the crosshead speed of 0.75±0.25 mm/min. The three-point flexure test produces tensile stresses on the lower convex surface of specimen (Figure 2.3). A disadvantage of the three-point bending test is that undesirable edge failures of specimen may occur, which may lead to an error in strength measurements (Ban and Anusavice, 1990). Also, due to the greater length of specimens compared with the exit window diameter of all handheld curing-light tips, an overlapping light-curing procedure is employed for the polymerisation of specimens. This curing procedure may lead to an inhomogeneous curing as overlapped areas of specimens are likely to be polymerize greater than adjacent regions (Yap and Teoh, 2003; Palin et al., 2003) and decrease the reliability of flexure strength data (Palin et al., 2003, 2005). In order to eliminate inconsistent polymerisation of bar specimens, various alternative methods have been suggested.

Mehl at al. (1997) and Manhart et al. (2000ab) cured the bar-shaped specimens (25 mm length) with three light-units which were placed close to each other and operated simultaneously. Ferracane et al. (2003) has suggested the use of oven-light curing units for irradiation of bar-shaped specimens, which may allow efficient and simultaneous polymerisation of multiple specimens. Yap and Teoh (2003) employed a shorter bar-shaped specimen (12 mm length) in order to achieve uniform curing in a

single irradiation and authors have suggested a clinical relevance and easy fabrication of short bar-shaped specimens compared with long specimens.

Bhamra and Fleming (2008) evaluated the effect of light tip diameter (8, 11 and 13mm) on flexural strength of four commercial RBCs. The decreased tip diameter resulted in an increase number of overlapping irradiations. However, no significant differences were observed between Weibull modulus of each material with respect to light tip diameter. These results contradict the theory proposed by Palin et al. (2003, 2005a), who postulated that during overlapping curing procedure of bar-shaped specimens, the post-gel shrinkage stresses following irradiation of end regions place the central portion under tensile stress, which may decrease the homogeneity and consistency of polymerisation along the length of specimen and lead to reduction in the reliability of data. The gel point is the most important stage of polymerisation, where material begins to solidify. Following the post-gelation of resin, material can no longer flow sufficiently to absorb the contraction stresses (Stansbury et al., 2005). However, Bhamra and Fleming (2008) did not identify any significant differences in Weibull modulus in spite of using the increased number of overlapping irradiations. Despite the improved polymerisation of specimens, edge fracture of specimen and resultant variation in strength values remain a disadvantage of the three-point flexure test. Moreover, the large specimen geometry is not representative of the restorations placed clinically.

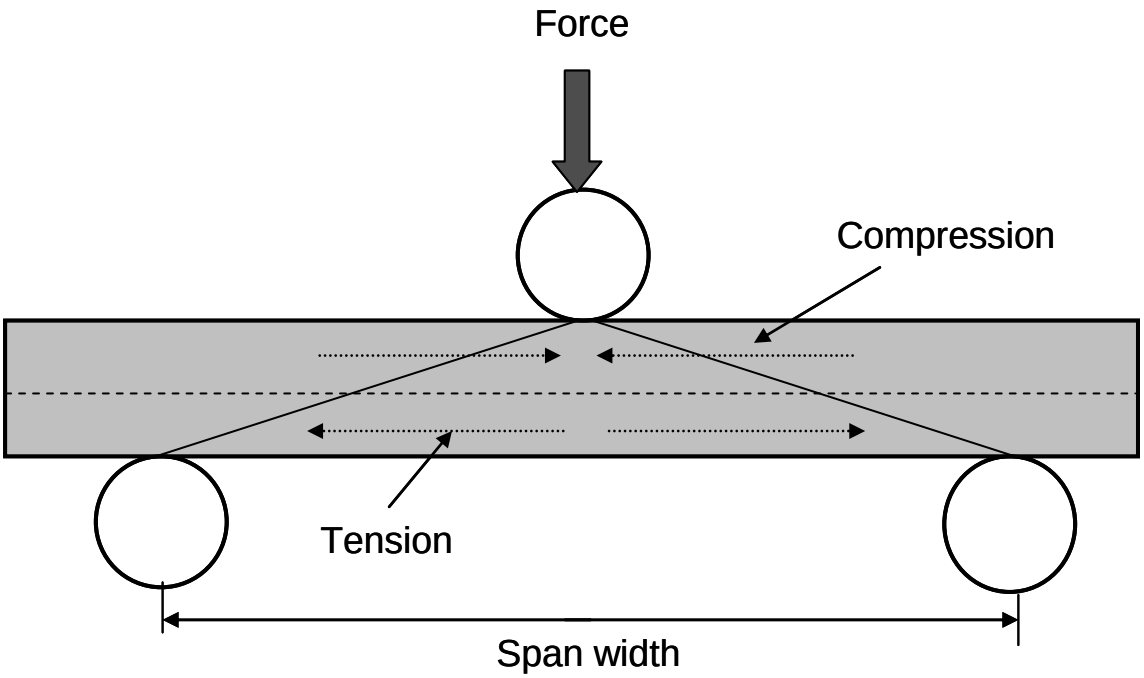

Figure 2.3. Schematic representation of three-point flexure test adapted from (Rodrigues Junior et al., 2008a) illustrating the compressive and tensile stresses in upper and lower half of specimen, respectively.

2.2.4 Four-Point Flexure Testing

The four-point flexure test also employs similar bar-shaped specimens as the three-point flexure test. The specimens are loaded symmetrically at two locations with loading rollers and the distance between loading points is usually one-third or one-fourth of the support span length (Figure 2.4). In four-point flexure test, maximum bending occurs between the loading points, whereas in three-point flexure test, the maximum bending occurs below the loading roller. Hammant (1971) stated that four-point flexure test generates uniform stress field along the surface and reduces the stress concentration near the loading points. Moreover, the results of four-point flexure tests are likely to be more representative of the bulk properties since a greater portion of specimen is stressed. Despite these advantages, four-point flexure test has not been used frequently due to experimental difficulties, which may include the complex test fixture in contrast to three-point flexure test (Kusy and Dilley, 1984).

Rodrigues Junior et al. (2008b) determined the flexural strength of a microhybrid and a nanofilled RBC by three-point and four-point flexure tests and the authors identified greater three-point flexure strength of both RBCs compared with four-point flexure strength. In the four-point flexure test a greater volume of specimen is subject to loading, therefore it is reasonable to expect that specimens will fail at lower stresses compared with three-point flexure test.

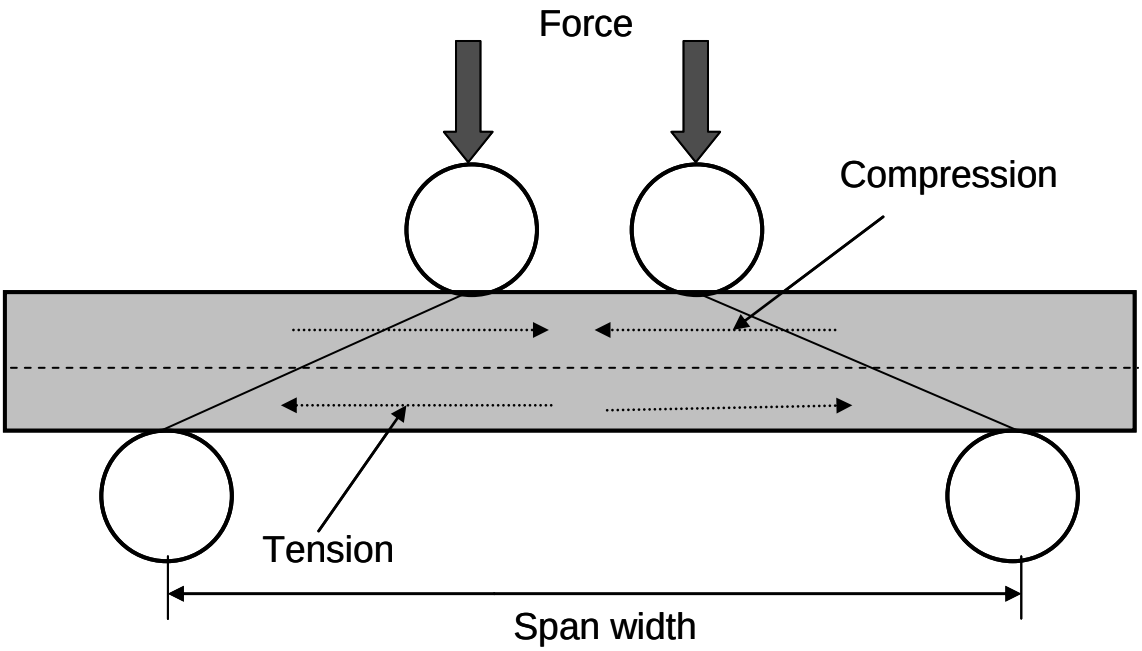

Figure 2.4. Schematic representation of four-point flexure test adapted from (Rodrigues Junior et al., 2008a) illustrating the compressive and tensile stresses in upper and lower half of specimen respectively. The effective volume is greater compared with three-point flexure test.

2.2.5 Bi-axial Flexure Testing

Bi-axial flexure testing is a commonly used technique for the evaluation of dental ceramics (Wagner and Chu, 1996; Cattell et al., 1997; Addison et al., 2007). The main advantage of the bi-axial flexure test is that the maximum tensile stresses occur within the central loading area and spurious edge failures are eliminated in contrast to three-point flexure testing. The bi-axial flexure test has also been employed for the assessment of RBCs (Palin et al., 2003, 2005ab; Curtis et al., 2008;

Pick et al., 2010). A disc-shaped specimen (12mm diameter, 1 mm thickness) is usually used for bi-axial flexure test, which represents the average width of molar teeth and also allows a clinically relevant single-shot irradiation protocol instead of an overlapping cure used for bar specimens in three-point flexure testing. Furthermore, the results achieved by bi-axial flexure testing are also independent of specimen geometry and flaw direction (Shetty, 1980; Piddock, 1987; Ban and Anusavice, 1990, 1992).

For bi-axial flexure test, various load and support configurations such as ring-on-ring, piston-on–three-ball and ball-on-ring (Figure 2.5) have been employed in ceramic-related studies. In a ring-on-ring bi-axial flexure test, a plate shaped specimen is supported by a coaxial ring and loaded at the centre with a smaller coaxial ring. Ritter et al. (1980) evaluated different bi-axial flexure test configurations, namely ring-on-ring, piston-on–three-ball and ball-on-ring, using finite element analysis and have reported a stress concentration under the loading ring in ring-on-ring configuration. Therefore, if the fracture initiates under the loading ring then the value of fracture stress is likely to be uncertain and in addition, the area and volume subjected to maximum stress are substantially less than theoretical assumptions. The piston-on-three-ball test employs plate shaped specimen supported on three symmetrically spaced ball-bearings and loaded centrally with a flat piston. The support utilized in the piston-on-three-ball configuration can accommodate slightly warped specimens, however, the stresses that occur below the flat piston are non-uniform and difficult to model and the calculation of flexure stress is uncertain, which may lead to inaccurate results. In a ball-on-ring configuration, the specimen is supported on a ring and centrally loaded with a spherical indenter. The useful feature of ball-on-ring test is that a minimal friction occurs between the test specimen and jig

during loading and it has been suggested as the most reliable bi-axial flexure strength test method (de With and Wagemans, 1989) which may also be the reason of its greater use in RBCs research (Palin et al., 2003, 2005ab; Curtis et al., 2009b) compared with other configurations.

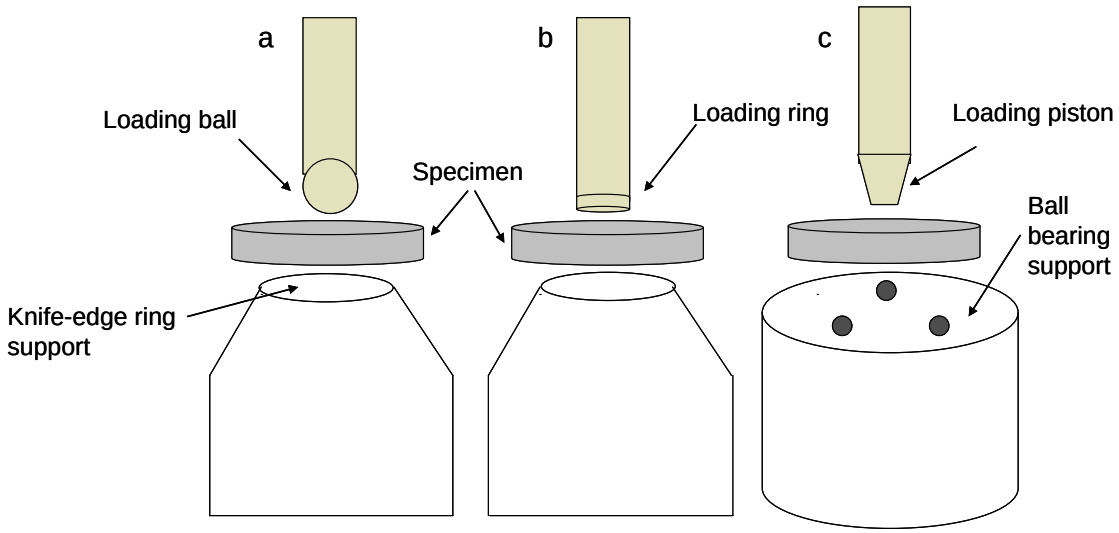

Figure 2.5. Schematic representations of (a) ball-on-ring (b) ring-on-ring (c) piston-on-three ball bi-axial flexure strength test configurations.

Curtis et al. (2009b) compared the bi-axial flexure strength data of microfilled, nanofilled, microhybrid and nanohybrid RBCs using Weibull statistics and identified an increased reliability of strength data of nanofilled RBCs in contrast to other RBCs. The increased reliability of nanofilled RBCs was attributed to silane infiltration within interstices of the nanoclusters and resulting modified response to pre-loading induced stress. The same authors have suggested in a previous study that that enhanced damage tolerance of nanofilled RBCs may be the result of crack bifurcation and capability of nanocluster to absorb and dissipate stresses by collapsing into the pre-existing cluster porosities or loss of fragments from the main cluster structure (Curtis et al., 2009a). Pick et al. (2010) evaluated the piston-on-three-ball bi-axial flexure strength and three-point bending strength of three commercial RBCs and identified a

greater data scattering for two of the materials tested by three-point bending compared with bi-axial flexure. The authors explained this by an increase in the probability of finding a critical size flaw in three-point bend specimen due to increased specimen's effective volume under tensile stresses. In addition, this may also be explained with the edge failure of some three-point bending test specimens.

The 12mm discs utilized in bi-axial flexure testing allow for "one-shot" curing and, as such are considered more clinically relevant. However, there is likely to be inhomogeneous curing in an axial direction due to Gaussian distribution of light intensity across the face of a curing-tip with bundled fibres. Consequently, inconsistency in bi-axial flexure data may be expected.

2.2.6 Elastic Modulus

Elastic modulus relates to stiffness or rigidity of material and may be described as the ratio of uniaxial stress to strain in a material at small strain levels (Watts, 1994). It is determined from the slope of the elastic region of stress-strain curve (Chung et al., 2005).

Ideally, the elastic modulus of RBCs should be matched with dental tissues to allow uniform stress distribution across the restoration-tooth interface during mastication (Nakayama et al., 1974; Jones and Rizkalla, 1996). The mismatch of elastic modulus between tooth hard tissues and RBCs in a restored tooth may result in fracture of surrounding tooth structure (Jones and Rizkalla, 1996). In addition, disruption of interfacial tooth/restoration bonding may occur, which may consequently result in microleakage, secondary caries and postoperative sensitivity (Nakayama et al., 1974; Jones and Rizkalla, 1996). In previous literature, the elastic modulus of dentine and enamel has been reported as 13-19 GPa (Watts, 1994; Xu et

al., 1998) and 80-94 GPa (Xu et al., 1998) respectively. Therefore, an optimal restoration may only be achieved when two different restorative materials with appropriate elastic modulus distribution related to enamel and dentine are combined simultaneously. However, RBCs are viscoelastic in nature, which may likely exhibit different behaviour compared with enamel and closer match to that of dentine at body temperature. Consequently, dentine has been considered as the standard for the investigation of viscoelastic restorative materials (Watts, 1994).

The elastic modulus of RBCs has been determined using different static and dynamic techniques. The static methods include three-point bending, tensile, compressive (Chabrier et al., 1999; Sabbagh et al., 2002; Wu et al., 2002) and indentation (Chung et al., 2005, Drummond, 2005) whereas, ultrasonic pulse method (Nakayama et al., 1974) mechanical resonance frequencies technique (Spinner and Tefft, 1961), dynamic mechanical thermal analysis (DMTA) (Braem et al., 1987) and impulse excitation technique (Braem et al., 1986; Sabbagh et al., 2002) are employed dynamically. For impulse excitation techniques, a specimen is set in flexural vibration by a light mechanical impulse. Subsequently, the signal produced is collected by a microphone located below the specimen and fundamental frequency under flexure is displayed on the screen of apparatus (Sabbagh et al., 2002; Leprince et al., 2010). In the ultrasonic pulse method, ultrasound is applied to specimens and elastic modulus is calculated from velocity of longitudinal and transverse waves generated at resonant frequency (Nakayama et al., 1974; Jones and Rizkalla, 1996). In DMTA, generally, bending loads are applied to a clamped specimen in single cantilever mode at different frequencies and temperature range (Emami and Söderholm, 2005). The analyser unit compares the applied stresses and the related strain signals (Braem et al., 1987) and then elastic modulus, viscous modulus and loss tangent are collected and

plotted against temperature (Mesquita et al., 2006). In general, dynamic tests are simple and non-destructive but require special equipment and are sensitive to the position of the specimen. For example, in the ultrasonic method, specimen position may change during water immersion and cause difficulty in signal measurement (Braem et al., 1986). The advantage of uniaxial static methods is that strength properties of a material can also be determined in addition to elastic properties (Chung et al., 2004). However, the strains produced by the static methods are difficult to record in materials with high elastic modulus (Suansuwan and Swain, 2001) and thus high stresses are needed to produce enough deformation. Among the testing methods, three-point bending test stipulated by ISO for the evaluation of flexural strength of RBCs is frequently employed to determine the elastic modulus (Manhart et al., 2000; Sabbagh et al., 2002; Kim et al., 2002; Beun et al., 2007; Rodrigues Junior et al., 2008b).

The elastic modulus values of RBCs vary greatly between studies, which are likely due to significant differences in testing methodologies. Sabbagh et al. (2002) evaluated the elastic modulus of a wide range of RBCs using static and dynamic techniques. The dynamic moduli of elasticity of RBCs ranged from 3.0 to 28.6 GPa, which was considerably greater than static moduli of elasticity of RBCs, which ranged from 1.4 to 18.5 GPa, which may be due to variation in the deformation rate of specimens. At low strain rate or frequency, the elastic modulus of RBC decreases, which suggests that RBCs have sufficient time for relaxation that allows stress relief to occur. In contrast, at high strain rate, the time available for viscous flow decreases, which reduces the level of stress relief and thus increases the elastic modulus.

Many studies have evaluated the elastic modulus of RBCs with respect to filler content (Braem et al., 1985; Ferracane et al., 1998; Masouras et al., 2008a) size

(Tanimoto et al., 2006; Masouras et al., 2008a ; Masouras et al., 2008b) and shape (Masouras et al., 2008b; Leprince et al., 2010). Braem et al. (1985), Ferracane et al. (1998), Ikejima et al. (2003) and Masouras et al. (2008a) identified an increase in elastic modulus with increasing filler volume fraction. Tanimoto et al. (2006) determined the flexural modulus of RBCs with different filler sizes at constant volume fraction and no difference between flexural modulus of RBCs was observed. On the other hand, Masouras et al. (2008a, b) identified an increase in the flexural modulus of RBCs with increasing filler particle size but authors have not offered any explanation. It may be speculated from this work that large filler particles are likely to bear greater load and reduce the deformation of polymer network compared with small filler particles, which may result in increased elastic modulus of RBCs.

The effect of filler morphology on elastic modulus has been investigated in several studies, however, the results are contradictory. Masouras et al. (2008b) stated that RBCs with irregular fillers exhibit greater elastic modulus compared with RBCs comprised of spherical fillers. The authors suggested that irregular shape fillers may have potential to interlock and thus not rearrange their position which ultimately results in high elastic modulus. On the contrary, Leprince et al. (2010) identified an opposite trend and authors have advocated a possibility of silane infiltration in porous spherical nanoclusters, which may improve the elastic modulus.

2.2.7 Viscoelastic behaviour of resin-based composites

For materials that exhibit both viscous and elastic properties during deformation are characterised as ‘viscoelastic’. The stress application on viscoelastic materials generally leads to some storage of energy (elastic behaviour) and dissipation of a part of the energy (viscous behaviour). Subsequently, the removal of stress results in a combination of time-dependent recovery of the elastic energy and permanent

deformation of viscous characteristics of the material (Mesquita and Gerstorfer, 2008).

In polymeric composites, the matrix has a dominating effect on the viscoelastic nature of materials (Kumar and Talreja, 2003). This time dependent deformation of polymeric materials can be determined by measuring the creep and recovery characteristics of material. Creep can be defined as a generation of strain in a material under a continuous application of stress over a selected time. In contrast, the 'recovery' of a viscoelastic material is its relaxation over a certain period after stress relief (Vaidyanathan and Vaidyanathan, 2001). Viscoelastic properties have greater significance in terms of mechanical performance of RBCs because of their time-dependent deformation under masticatory forces in oral environment (Cock and Watts, 1985). There are various factors that may affect the viscoelastic response of RBCs, for instance; temperature, aging, vibration frequency and dynamic strain rate (Mesquita and Gerstorfer, 2008).

Cock and Watts (1985) measured the creep of six RBCs including microfilled and traditional types (Section 1.2-1.3) in compression and reported a decreased viscoelastic response of traditional RBCs, which possess increased filler loads. Similar findings were found by Baroudi et al. (2007) who identified a greater creep strain for flowable RBCs which contained a low filler load. Vaidyanathan and Vaidyanathan (2001) evaluated elastic, viscoelastic and viscous deformation of three RBCs microfilled (low filler content), minifilled (medium filler content) and midifilled (high filler content) under creep and recovery parameters. The deformation was decreased in order of increasing filler content. It is known that slippage, decoupling and disentanglements of polymer chains cause creep and plastic deformation in polymeric materials (Baroudi et al., 2007). Therefore, filler

incorporation into the resin matrix reduces the volume of resin content and therefore leads to a decrease in the occurrence of plastic deformation. Consequently, the viscoelastic response of RBCs is significantly affected. Viscoelastic characteristics of four different packable RBCs were evaluated using a resonant dynamic mechanical analysis technique in torsion at various frequencies and temperature range. All materials exhibited significant difference in viscoelastic response, which could be suggestive of variation in monomer and filler composition and filler loading (Papadogiannis et al., 2004). The effect of temperature and water on viscoelastic characteristics of three nanofilled, one packable and one ormocer RBC were investigated and the results highlighted that increased temperature was responsible for a substantial decrease in the moduli of all materials, however, water affected the materials at different rates (Papadogiannis et al., 2008). The authors suggested that the effect of water on moduli of RBCs is likely to be material specific and depend upon filler load. However, Ferracane et al. (1998) proposed that there was less effect of water on flexural modulus of RBCs over prolonged storage periods, which may suggest that filler content has a significant role while factors affecting the polymer matrix may have less significance in determining flexural modulus. Viscoelastic properties of direct and indirect RBCs were evaluated at different frequencies between 0.1 to 10 Hz using dynamic mechanical analysis (Mesquita et al., 2006). The elastic modulus of all RBCs increased with increasing frequency, a low-frequency range materials have sufficient time to flow therefore viscous behaviour predominates. Whereas, at high-frequency there is less time for materials to flow in a viscous manner and therefore materials behave more elastically and lead to an increase in elastic modulus. Musanje and Darvell (2004) determined the elastic modulus of four commercially-available light-cured RBCs at a wide range of cross-

head speeds and identified a marked and steady rise in elastic modulus with increasing cross-head speed. The investigators explained their findings similarly as Mesquita et al. (2006) described above.

2.2.8 Deformation rates for resin-based composite testing

Deformation rates (cross-head speeds) during mechanical property testing vary widely between studies (Table 2.2), which may lead to difficulty in comparison and interpretation of results between operators and research laboratories. RBCs placed clinically experience cyclic loading of varying magnitudes during their lifetime due to forces from mastication and grinding. Para-functional habits, such as bruxism, result in RBCs being subjected to constant forces (Ruyter and Øysæd, 1982) for several minutes in contrast to the intermittent forces in normal mastication (Glaros and Rao, 1977). Moreover, the effect of deformation rate on mechanical properties of polymer-based materials has been reported (Chen and Cheng, 2002; Jacob et al., 2004). However, mechanical properties of RBCs have been usually determined at one deformation rate and even ISO 4049 has suggested a limited range (0.75±0.25 mm/min) for the determination of flexural strength of RBCs. A reason for the selection of a lower deformation rate for mechanical testing of RBCs may be the occurrence of inertial effects at higher deformation rates. It is believed that inertial responses of the testing machine increase with increasing test speed, which may lead to erroneous results and difficulty in interpretation of data. Therefore, accurate characterisation of machine compliance for deformation rate associated studies is important and should be conducted.

It is clear that mechanical testing of RBCs at one deformation rate may not provide sufficient information to elucidate the material behaviour in the real clinical

environment. Thus determination of mechanical properties of RBCs with regard to deformation rate should be standardised.

Table 2.2. Cross-head speeds used in some mechanical tests for resin-based materials studies.

Reference	Year	Test type	Cross-head speed (mm/min)
Aguiar et al.	2005	Diametral	10.0
Asmussen and Peutzfeldt	2004	Three-point flexure	1.0
Beun et al.	2007	Three-point flexure	0.75
Chabrier et al.	1999	Compression	0.2
Curtis et al.	2008	Bi-axial flexure	1.0
Deepa and Krishnan	2000	Compression Diametral	10.0
Ferracane et al.	1998	Fracture toughness Three-point flexure	0.13 0.254
Kim et al.	1994	Three-point flexure	0.1
Labella et al.	1994	Three-point flexure	5.0
Li et al.	2009	Compression	0.1
Lohbauer et al.	2003	Four-point flexure	0.75
Manhart et al.	2001	Three-point flexure	0.5
Peutzfeldt and Asmussen	2000	Diametral Three-point flexure	10.0 1.0
Pilliar et al.	1987	Fracture toughness	5.0
Sabbagh et al.	2002	Three-point flexure	0.75
Sandner et al.	1997	Three-point flexure	5.0
Tian et al.	2008	Three-point flexure	0.5
Yesilyurt et al.	2009	Three-point flexure	0.05
Zhang and Xu	2008	Three-point flexure	0.5
Zhang et al.	2010	Three-point flexure	0.5

2.2.8 Specimen Storage Variability

The International Standard Organization has recommended storage of RBCs specimens in distilled water at 37 ºC for 24 h prior to flexural strength testing (ISO 4049, 2000) and this protocol has been employed in many studies. The reasons for storage of specimens in distilled water are to simulate the oral environment and to allow for the elution of all leachable and unreacted constituent and post-polymerisation of RBCs (Ferracane and Condon, 1990). However, many investigators have conducted the mechanical properties of RBCs after storage of specimen in different storage media such as ethanol (Ferracane and Berge, 1995; Zhang and Xu, 2008), food simulating-liquids (Deepa and Krishnan, 2000) and artificial saliva (Musnaje and Darvell, 2003) at varying temperatures (Watts et el., 1987) and pH (Prakki et al., 2005) in an attempt to introduce a clinically relevant environment compared with distilled water. Moreover, selection of specimen storage time prior to mechanical test is arbitrary and varies widely between studies. Therefore, the differences in results may be expected between different operators and research laboratories and the comparison of data may be difficult.

According to ISO 4049 each specimen is to be suspended by its diametral axis for the studies related to water sorption and solubility of RBCs. However, there is not any criterion for specimen alignment prior to flexural strength testing and it has rarely been considered in the dental literature. As water sorption is known to be diffusion controlled (Asaoka and Hirano, 2003), it can be argued that any difference between surface areas of specimens exposed to water may significantly affect water uptake and ultimately mechanical strength of RBCs following storage. Therefore, it is essential to address the effect of specimen alignment on mechanical properties, which may consequently aid in the accurate assessment of data among researchers.

Studies have reported that water uptake of RBCs is dependent upon the resin matrix chemistry and degree of conversion (Ferracane, 1994), filler particle size and distribution (Calais and Söderholm, 1988) and filler/matrix bonding (Beatty et al., 1998). Palin et al. (2005b) identified a decrease in water uptake of Filtek Z250 compared with Z100 and the differences were attributed to variation in resin chemistry since filler morphology was comparable. Cutis et al. (2008) found an increased water uptake of Filtek supreme 'translucent' shade (FST) compared with Filtek supreme 'body' shade (FSB) and the increased water uptake of FST was likely to be result of the greater volume percentage of individually dispersed nanoparticles and resultant larger surface area availability for water sorption.

2.3 Summary and general aims

In vitro mechanical characterisation of RBCs is a common approach in order to predict their clinical performance. The data acquired may only be considered as meaningful when reproducible and relevant testing and data analysis methods are employed among investigators. Several investigators have used Weibull statistics for the analysis of RBCs strength data, however their applicability might be questioned as many RBCs contain greater resin content and may exhibit sufficient viscous deformation prior to brittle failure. Moreover, variability in the selection of cross-head speed is common and, consequently, differences in the data and associated interpretation may occur. The storage of specimen in distilled water in an attempt to simulate with oral environment is a common practice prior to mechanical properties testing. However, specimen alignment during the storage regime has rarely been reported in literature. It is reasonable to expect that any differences between specimen alignment and resulting surface areas exposed to water may cause variation in the

water sorption and ultimately affect the mechanical properties. Thus, it is essential to understand the relevance of testing and data analysis methods for the accurate characterisation of mechanical properties of RBCs which may aid in the understanding and development of materials.

References

Addison O, Marquis PM, Fleming GJP. The impact of hydrofluoric acid surface treatments on the performance of a porcelain laminate restorative material. Dental Materials, 2007; 23: 461-468.

Aguiar FHB, Braceiro ATB, Ambrosano GMB, Lovadino JR. Hardness and diametral tensile strength of a hybrid composite resin polymerised with different modes and immersed in ethanol or distilled water media. Dental Material, 2005; 21: 1098-1103.

Asaoka K, Hirano S. Diffusion coefficient of water through dental composite resin. Biomaterials, 2003; 24: 975-979.

Asmussen E. Softening of BISGMA based polymer by ethanol and by organic acids of plaque. Scandinavian Journal of Dental Research, 1984; 92:257-261.

Asmussen E, Peutzfeldt A. Influence of UEDMA, BisGMA and TEGDMA on selected mechanical properties of experimental resin composites. Dental Materials, 1998; 14: 51-56.

Ban S, Anusavice KJ. Influence of test method on failure stress of brittle dental materials. Journal of Dental Research, 1990; 69: 1791-1799.

Ban S, Hasegawa J, Anusavice KJ. Effect of loading conditions on bi-axial flexure strength of dental cements. Dental Materials, 1992; 8: 100-104.

Baran GR, McCool JI, Paul D, Boberick K, Wunder S. Weibull models of fracture strengths and fatigue behaviours of dental resins in flexure and shear. Journal of Biomedical Materials Research (Applied Biomaterials), 1998; 43: 226-233.

Baran G, Boberick K, McCool J. Fatigue of restorative materials. Critical Reviews on Oral Biology and Medicine, 2001; 12: 350-360.

Baroudi K, Silikas N, Watts DC. Time-dependent visco-elastic creep and recovery of flowable composites. European Journal of Oral Science, 2007; 115:517-521.

Beatty MW, Swartz ML, Moore BK, Philips RW, Roberts TA. Effect of microfiller fraction and silane treatment on resin composite properties. Journal of Biomedical Materials Research, 1998; 40: 12-23.

Berenbaum R, Brodie I. Measurement of the tensile strength of brittle materials. British Journal of Applied Physics, 1959; 10: 281-287.

Beun S, Glorieux T, Jacques D, Vreven J, Leloup G. Characterisation of nanofilled compared to universal and microfilled composites. Dental Materials, 2007; 23:51-59.

Bhamra GS, Fleming GJP. Effects of halogen light irradiation variables (tip diameter, irradiance, irradiation protocol) on flexural strength properties of resin-based composites. Journal of Dentistry, 2008; 36: 643-650.

Braem M, Lambrechts P, Van Doren V, Vanherle G. The impact of composite structure on its elastic response. Journal of Dental Research, 1986; 65: 648-653.

Braem M, Davidson CL, Vanherle G, Van Doren V, Lambrechts P. The relationship between test methodology and elastic behaviour of composites. Journal of Dental Research, 1987; 66: 1036-1039.

Brosh T, Ganor Y, Belov I, Pilo R. Analysis of strength properties of light-cured resin composites. Dental Materials, 1999; 15: 174-179.

Calais JG, Söderholm KJM. Influence of filler type and water exposure on flexural strength of experimental composite resins. Journal of Dental Research, 1988; 67: 836-840.

Cattell MJ, Clarke RL, Lynch EJR. The biaxial flexural strength and reliability of four dental ceramics- part II. Journal of Dentistry, 1997; 25: 409-414.

Chabrier F, Lloyd CH, Scrimgeour SN. Measurement at low strain rates of the elastic properties of dental polymeric materials. Dental Materials, 1999; 15: 33-38.

Chadwick RG, McCabe JF, Walls AWG, Storer R. The effect of placement technique upon the compressive strength and porosity of a composite resin. Journal of Dentisty, 1989; 17: 230-233.

Chen W, Cheng FLM. Tension and compression tests of two polymers under quasi-static and dynamic loading. Polymer Testing, 2002; 21: 113-121.

Chung SM, Yap AUJ, Koh WK, Tsai KT, Lim CT. Measurment of poisson's ratio of dental composite restorative materials. Biomaterials, 2004; 25: 2455-2460.

Chung SM, Yap AUJ, Tsai KT, FL Yap. Elastic modulus of resin-based dental restorative materials: A microindentation approach. Journal of Biomedical Materials Research Prat B: Applied Biomaterials, 2005; 72B: 246-253.

Cock DJ, Watts DC. Time-dependent deformation of composite restorative material in compression. Journal of Dental Research, 1985; 64: 147-150.

Curtis AR, Shortall AC, Marquis PM, Palin WM. Water uptake and strength charactersistics of nanofilled resin-based composites. Journal of Dentistry, 2008; 36:186-193.

Curtis AR, Palin WM, Fleming GJP, Shortall ACC, Marquis PM. The mechanical properties of nanofilled resin-based composites: Characterising discrete filler particles and agglomerates using a micromanipulation technique. Dental Materials, 2009a; 25: 180-187.

Curtis AR, Palin WM, Fleming GJP, Shortall ACC, Marquis PM. The mechanical properties of nanofilled rein-based composites: The impact of dry and wet cyclic pre-loading on bi-axial flexure strength. Dental Materials, 2009b; 25:188-197.

Darvell BW. Uni-axial compression tests and the validity of indirect tensile strength. Journal of Material Science, 1990; 25: 757-780.

Darvell BW. Mechanical testing. In: Darvell BW. Materials Science for Dentistry (7^{th} Edition). Hong Kong: The University of Hongkong, 2002; Chapter 1:1-35.

Deepa CS, Krishnan VK. Effect of resin matrix ratio, storage medium and time upon the physical properties of a radiopaque dental composite. Journal of Biomaterials applications, 2000; 14: 296-315.

de With G, Wagemans HHM. Ball-on-ring test revisited. Journal of American Ceramic Society, 1989; 72: 1538-1541.

Douglas WH. Considerations for modeling. Dental Materials, 1996; 12: 203-207.

Drummond JL, Mlescke KJ. Weibull models for the statistical analysis of dental composite data: aged in physiologic media and cyclic-fatigued. Dental Materials, 1991; 7: 25-29.

Drummond JL. Nanoindentation of dental composites. Journal of Biomedical Materials Research Part B: Applied Biomaterials, 2006; 78: 27-34.

Emami N, Söderholm KJM. Dynamic mechanical thermal analysis of two light-cured dental composites. Dental Materials, 2005; 21: 977-983.

Ferracane JL, Condon JR. Rate of elution of leachable components from composite. Dental Materials, 1990; 6: 282-287.

Ferracane JL, Condon JR. Post-cure heat treatments for composites: properties and fractography. Dental Materials, 1992; 8: 290-295.

Ferracane JL. Elution of leachable components from composites. Journal of Oral Rehabilitation, 1994; 21: 441-452.

Ferracane JL, Berge HX. Fracture toughness of experimental dental composites aged in ethanol. Journal of Dental Research, 1995; 74: 1418-1423.

Ferracane JL, Berge HX, Condon JR. In vitro aging of dental composites in water-Effect of degree of conversion, filler volume, and filler/matrix coupling. Journal of Biomedical Material Research, 1998; 42: 465-472.

Ferracane JL, Ferracane LL, Musanje L. Effect of light activation method on flexural properties of dental composites. American Journal of Dentistry, 2003; 16: 318-322.

Glaros AG, Rao SM. Effects of bruxism: A review of the literature. Journal of Prosthetic Dentistry, 1977; 38: 149-157.

Griffith AA. The phenomena of rupture and flow in solids. Philosophical Transaction of the Royal Society of London, 1921; 221: 163-198.

Hammant B. The use of 4-point loading tests to determine mechanical properties. Composites, 1971; 2: 246-249.

Harrington E, Wilson HJ. Depth of cure of radiation-activated materials-effect of mould material and cavity size. Journal of Dentistry, 1993; 21: 305-311.

Higgs WAJ. Lucksanasombool P, Higgs RJED, Swain MV. A simple method of determining the modulus of orthopaedic bone cement. Journal of Biomedical Materials Research (Applied Biomaterials), 2001; 58: 188-195.

Ikejima I, Nomoto R, McCabe JF. Shear punch strength and flexural strength of model composites with varying filler volume fraction, particle size and silanation. Dental Materials, 2003; 19: 206-211.

Ilie N, Hickel R. Macro-, micro-, and nano-mechanical investigations on silorane and methacrylate-based composites. Dental Materials, 2009; 25: 810-819.

International Standards Organisation. Dentistry- Polymer-based filling, restorative and luting materials. ISO 4049, 2000; (3rd Edition): 15-18.

Jacob GC, Starbuck JM, Fellers JF, Simunovic S, Boeman RG. Strain rate effects on the mechanical properties of polymer composite materials. Journal of Applied Polymer Science, 2004; 94: 296-301.

Jandt KD, Mills RW, Blackwell GB, Ashworth SH. Depth of cure and compressive strength of dental composites cured with blue light emitting diodes (LEDs). Dental Materials, 2000; 16: 41-47.

Jones DW, Rizkalla AS. Characterisation of experimental composite biomaterials. Journal of Biomedical Materials Research (Applied Biomaterials), 1996; 33: 89-100.

Kawano F, Ohguri T, Ichikawa T, Matsumoto N. Infuence of thermal cylces in water on flexural strength of laboratory-processed composite resin. Journal of Oral Rehabilitation, 2001; 28: 703-701.

Kim KH, Ong JL, Okuno O. The effect of filler loading and morphology on the mechanical properties of contemporary composites. Journal of Prosthetic Dentistry, 2002; 87: 642-649.

Kirsten AF, Woolley RM. Symmetrical bending of thin circular elastic plates on equally spaced point supports. Journal of Research of National Bureau of standards, 1967; 71C: 1-10.

Kumar RS, Talreja R. A continuum damage model for linear viscoelastic composite materials. Mechanics of Materials, 2003; 35: 463-480.

Kusy RP, Dilley GJ. Materials science elastic modulus of a triple-stranded stainless steel arch wire via three- and four-point bending. Journal of Dental Research, 1984; 63: 1232-1240.

Labella R, Lambrechts P, Van Meerbeek B, Vanherle G. Polymerisation shrinkage and elasticity of flowable composite and filled adhesives. Dental Materials, 1999; 15: 128-137.

Leprince J, Palin WM, Mullier T, Devaux J, Vreven J, Leloup G. Investigating filler morphology and mechanical properties of new low-shrinkage resin composite types. Journal of Oral Rehabilitation, 2010; 37: 364-376.

Lohbauer U, Horst TVD, Frankenberger R, Krämer N, Petschelt A. Flexural fatigue behaviour of resin composite dental restoratives. Dental Materials, 2003; 19: 435-440.

Manhart J, Kunzelmann KH, Chen HY, Hickel R. Mechanical properties and wear behaviour of light-cured packable composite resins. Dental Materials, 2000a; 16: 33-40.

Manhart J, Kunzelmann KH, Chen HY, Hickel R. Mechancial properties of new composite restorative materials. Journal of Biomedical Materials Research (Applied Biomaterials), 2000b; 53:353-361.

Masouras K, Silikas N, Watts DC. Correlation of filler content and elastic properties of resin-composites. Dental Materials, 2008; 24: 932-939.

Masouras K, Akhtar R, Watts DC, Silikas N. Effect of fiiler size and shape on local indentation modulus of resin-composites. Journal of Materials Science: Materials in Medicine, 2008b; 19:3561-3566.

McCabe JF, Carrick TE. A statistical approach to the mechanical testing of dental materials. Dental Materials, 1986; 2: 139-142.

McCabe JF, Ogden AR. The relationship between porosity, compressive fatigue limit and wear in composite resin restorative materials. Dental Materials, 1987; 3: 9-12.

Mehl A, Hickel R, Kunzelmann KH. Physical properties and gap formation of light-cured composite with and without ‘softstart-polymerisation’. Journal of Dentistry, 1997; 25: 321-330.

Mesquita RV, Axmann D, Gerstorfer JG. Dynamic visco-elastic properties of dental composite resins. Dental Materials, 2006; 22:258-267.

Mesquita RV, Gerstorfer JG. Influence of temperature on the visco-elastic properties of direct and indirect dental composite resins. Dental Materials, 2008; 24: 623-632.

Moore BK, Platt JA, Borges G, Chu TMG, Katsilieri I. Depth of cure of dental resin composites: ISO 4049 depth and microhardness of types of materials and shades. Operative Dentistry, 2008; 33: 408-412.

Musanje L, Darvell BW. Aspects of water sorption from the air, water and artificial saliva in resin composite restorative materials. Dental Materials, 2003; 19: 414-422.

Musnaje L, Darvell BW. Effects of strain rate and temperature on the mechanical properties of resin composites. Dental Materials, 2004; 20: 750-765.

Nakayama WT, Hall DR, Grenoble DE, Lawrence Katz J. Elastic properties of dental restorative materials. Journal of Dental Research, 1974; 53: 1121-1126.

Opdam NJM, Roeters JJM, Peters TCRB, Burgersdijk RCW, Kuijs RH. Consistency of resin composites for posterior use. Dental Materials, 1996; 12: 350-354.

Opdam NJM, Roeters JJM, Joosten M, Veeke OV. Porosities and voids in Class I restorations placed by six operators using a packable or syringable composite. Dental Materials, 2002; 18: 58-63.

Ortengren U, Anderson F, Elgh U. Influence of pH and storage time on sorption and solubility behaviour of three composite resin materials. Journal of Dentistry, 2001; 29:35-41.

Palin WM, Fleming GJP, Burke FJT, Marquis PM, Randall RC. The reliability in flexural strength testing of a novel dental composite. Journal of Dentistry, 2003; 31:549-557.

Palin WM, Fleming GJP, Marquis PM. The reliability of standardised flexural strength testing procedure for a light-activated resin-based composite. Dental Materials, 2005a; 21: 911-919.

Palin WM, Fleming GJP, Burke FJT, Marquis PM, Randall RC. The influence of short and medium-term immersion on hydrolytic stability of novel low-shrink dental composites. Dental Materials, 2005b; 21:852-863.

Papadogiannis Y, Antoniades MH, Lakes RS. Dynamic mechanical analysis of viscoelastic functions in packable composite resins measured by torsional resonance. Wiley Periodicals, Inc. Journal of the Biomedical material research Part B: Applied Biomaterials, 2004; 71B: 327-335.

Papadogiannis DY, Lakes RS, Papadogiannis Y, Palaghias G, Antoniades MH. The effect of temperature on the viscoelastic properties of nano-hybrid composites. Dental Materials, 2008; 24: 257-266.

Penn RW, Craig RG, Tesk JA. Diametral tensile strength and dental composites. Dental Materials, 1987; 3: 46-48.

Peutzfeldt A, Asmussen E. The effect of posturing on quantity of remaining double bonds, mechanical properties, and in vitro wear of two resin composites. Journal of Dentistry, 2000; 28: 447-452.

Pick B, Meira JBC, Driemeier L, Braga RR. A critical view on biaxial and short-beam uniaxial flexural strength tests applied to resin composites using Weibull, fractographic and finite element analyses. Dental Materials, 2010; 26: 83-90.

Piddock V, Marquis PM, Wilson HJ. The mechanical strength and microstructure of all-ceramic crowns. Journal of Dentistry, 1987; 15: 153-158.

Pilliar RM, Vowles R, Williams DF. The effect of environmental aging on the fracture toughness of dental composites. Journal of Dental Research, 1987; 66: 722-726.

Prakki A, Cilli R, Mondelli RFL. Influence of pH on polymer based dental material properties. Journal of Dentistry, 2005; 33: 91-98.

Quinn GD. Weibull strength scaling for standardised rectangular flexure specimens. Journal of the American Ceramic Society, 2003; 86: 508-510.

Ritter JE, Jakus K, Batakis A, Bandyopadhyay N. Appraisal of biaxial strength testing. Journal of Non-crystalline Solids, 1980; 38&39: 419-424.

Rodrigues Junior SA, Ferracane JL, Bona AD. Flexural strength and Weibull analysis of a microhybrid and nanofill composite evaluated by 3- and 4-point bending tests. Dental Materials, 2008a; 24:426-431.

Rodrigues Junior SA, Scherrer SS, Ferracane JL, Bona AV. Microstructural characterisation and fracture behaviour of a microhybrid and a nanofill composite. Dental Materials, 2008b; 24:1281-1288.

Ruyter IE, Øysæd H. Compressive creep of light cured resin based restorative materials. Acta Odontologica Scandinavica, 1982; 40: 319-324.

Sabbagh J, Vreven J, Leloup G. Dynamic and static moduli of elasticity of resin based materials. Dental Materials, 2002; 18: 64-71.

Sandner B, Baudach S, Davy KWM, Braden M, Clarke RL. Synthesis of BISGMA derivatives, properties of their polymers and composites. Journal of Materials Science: Materials in Medicine, 1997; 8: 39-44.

Shetty DK, Rosenfield AR, McGuire P, Duckworth WH. Bi-axial flexure tests for ceramics. Ceramic Bulletin, 1980; 59: 1193-1197.

Sideridou I, Tserki V, Papanastasiou. Study of water sorption, solubility and modulus of elasticity of light-cured dimethacrylate-based dental resins. Biomaterials, 2003; 24: 655-665.

Spinner S, Tefft WE. A method for determining mechanical resonance frequencies and for calculating elastic moduli for these freqencies. American Society for Testing and Materials, 1961; 61: 1221-1238.

Suansuwan N, Swain MV. Determination of elastic properties of metal alloys and dental porcelains. Journal of Oral Rehabilitation, 2001; 28: 133-139.

Stansbury JW, Trujillo-Lemon M, Lu H, Ding X, Lin Y, Ge J. Conversion-dependent shrinkage stress and strain in dental resins and composites. Dental Materials, 2005; 21: 56-67

Tanimoto Y, Kitagawa T, Aida M, Nishiyama N. Experimental and computational approach for evaluating the mechanical characteristics of dental composite resins with various filler sizes. Acta Biomaterialia, 2006; 2: 633-639.

Tian M, Gao Y, Liu Y, Liao Y, Hedin NE, Fong H. Fabrication and evaluation of Bis-GMA/TEGDMA dental resin/composites containing nano fibrillar silicate. Dental Materials, 2008; 24: 235-243.

Toledano M, Osorio R, Osorio E, Fuentes V, Prati C, Gracía-Godoy F. Sorption and solubility of resin-based restorative dental materials. Journal of Dentistry, 2003; 31: 43-50.

Tsai PCL, Meyers IA, Walsh LJ. Depth of cure and surface microhardness of composite resin cured with blue LED curing lights. Dental Materials, 2004; 20: 364-369.

Vaidyanathan J, Vaidyanathan TK. Flexural Creep deformation and recovery in dental composites. Journal of Dentistry, 2002; 29: 545-551.

Wagner WC, Chu TM. Biaxial flexural strength and indentation fracture toughness of three new dental core ceramics. Journal of Prosthetic Dentistry, 1996; 76: 140-144.

Watts DC, Amer OM, Combe EC. Surface hardness development in light-cured composites. Dental Material, 1987; 3: 265-269.

Watts DC. Elastic moduli and visco-elastic relaxation. Journal of Dentistry, 1994; 22: 154-158.

Weibull W. A statistical distribution function of wide applicability. Journal of Applied Mechanics, 1951; 18-293-297.

Williams PD, Smith DC. Measurement of the tensile strength of dental restorative materials by use of a diametral compression test. Journal of Dental Research, 1971; 50: 436-442.

Wu W, Sadeghipour K, Boberick K, Baran G. Predictive modelling of elastic properties of particulate-reinforced composites. Materials Science and Engineering, 2002; A332: 362-370.

Xu HHK, Smith DT, Jahanmir S, Romberg E, Kelly JR, Thompson VP, Rekow ED. Indentation damage and mechanical properties of human enamel and dentin. Journal of Dental Research, 1998; 77: 472-480.

Yap AUJ. Resin-modified glass ionomer cements: a comparison of water sorption characteristics. Biomaterials, 1996; 17: 1897-1900.

Yap AUJ, Teoh SH. Comparison of flexural properties of composite restoratives using the ISO and mini-flexural tests. Journal of Oral Rehabilitation, 2003; 30: 171-177.

Yesilyurt C, Yoldas O, Altintas SH, Kusgoz A. Effects of food-simualting liquids on the mechanical properties of a silorane based dental composite. Dental Materials Journal, 2009; 28: 362-367.

Yoshida Y, Shiari K, Nakayama Y, Itoh M, Okazaki M, Shintani H, Inoue S, Lambrechts P, Vanherle G, Van Meerbeek B. Improved filler-matrix coupling in resin composites. Journal of Dental Research, 2002; 81: 270-273.

Zhang Y, Xu J. Effect of immersion in various media on the sorption, solubility, elution of unreacted monomers, and flexural properties of two model dental composite compositions. Journal of Materials Science: Materials in Medicine, 2008; 19: 2477-2483.

Zhang L, Gao Y, Chen Q, Tian M, Fong H. Bis-GMA/TEGDMA dental composites reinforced with nano-scaled single crystals of fibrillar silicate. Journal of Materials Science, 2010; 45: 2521- 2524.

Zhao D, Botsis J, Drummond JL. Fracture studies of selected dental restorative composites. Dental Materials, 1997; 13: 198-207.

Chapter 3 The Applicability of Weibull Statistics for the Mechanical Characterisation of Dental Resin-Based Composites

3.1 Introduction

The 'strength' of dental resin-based composites (RBCs) is traditionally determined by various static load-to-failure techniques including diametral tensile, compressive loading and uni-axial and bi-axial flexure and each technique has its merits and demerits (Section 2.2). The fracture of brittle materials or materials which exhibit brittle-like failure originates from flaws distributed at the surface or within the material. The size, distribution and geometry of flaws, on which the strength of the material is determined, vary from specimen to specimen and therefore a range of strength values is expected. However, the strength data of RBCs is usually only reported as mean strength values and associated standard deviations based on an assumption that the mean strength is a true value and a normal strength distribution is present. In reality, the defect population may lack this level of homogeneity and as a result the failure of material may occur at lower stresses (McCabe and Carrick, 1986). Therefore, it has been suggested that the strength of RBCs may only become meaningful when it is evaluated by a probability function such as Weibull statistics (Weibull, 1951; McCabe and Carrick, 1986) and there is an increasing trend of the use of this statistical function within the dental literature.

Weibull statistics are well established and provide a useful analytical approach in materials science. The strength data of dental ceramics have been widely reported by Weibull statistics (Cattell et al., 1997; Bhamra et al., 2002; Lohbauer et al., 2002; Bona et al., 2003; Addison et al., 2007ab) and there is significant interest in using this analysis for the evaluation of failure behaviour of RBCs (Palin et al., 2003; Palin et al., 2005; Rodrigues Junior et al., 2008; Curtis et al., 2009; Ilie and Hickel, 2009a).

Weibull statistics are based on the weakest link theory which assumes that failure at any individual flaw leads to total failure (Danzer, 2006) and the probability of failure increases with an increase in specimen size, because of the increased likelihood of encountering a larger flaw (Griffith, 1921).

There has been significant variability in the selection of an appropriate specimen sample size between researchers in the dental materials science literature. Commonly, ten (Ban and Anusavice, 1990; Bona et al., 2003) or twenty (Palin et al., 2005; Curtis et al., 2009) specimens are employed for Weibull statistics. However, it has been stated that it is not possible to differentiate between a Weibull, a Gaussian, or any other similar distribution function on the basis of such a small sample size (Danzer, 2006). Indeed the experimental sample sizes utilized by Waloddi Weibull in his original work were often in excess of ten times this number (Weibull, 1939, 1951). A sample size of at least thirty specimens for Weibull statistics with due consideration of material and testing cost has been suggested and seems to have been accepted in the dental materials literature (Quinn, 1990; Ritter, 1995). However, this 'magic' number lacks validation for the majority of materials, systems or testing methods employed in dental materials science. Furthermore, Danzer et al. (2008) has used the term "Weibull material" for a material which possesses a single flaw type and the associated distribution follows the inverse power law. However, brittle materials containing multi-mode defect distributions; a combination of surface and volume critical flaws; or exhibiting heterogeneous internal residual stress fields are likely to deviate from Weibull distributions (Danzer et al., 2008). Moreover, Weibull distributions may not necessarily be valid in small specimens or those presenting high stress gradients (Danzer et al., 2007), both of which may be applicable to the dental

materials and common dental materials testing methods. In all these cases the Weibull modulus depends on "the applied stress amplitude" (Danzer et al., 2007).

At the most basic level, Weibull statistics can be used to predict the changes in strength data distributions according to the physical size of the individual test specimens under stress so that strength values of particular specimen size, shape or stress configuration may be scaled to predict corresponding values for different test specimen sizes, shapes or stress configurations (Quinn and Quinn, 2010). Consequently, the validity of the use of Weibull statistics for a particular system can be tested by investigating the consistency of the experimental and theoretical distributions when volume effects are introduced.

Polymers are characterized as visco-elastic materials, therefore some viscous deformation is expected in a RBC prior to brittle-like failure (Watts, 1994; Mesquita et al., 2006). In addition, a variety of RBCs have been developed with different formulations and wide variation in intrinsic properties such as elastic modulus is observed (Sabbagh et al., 2002; Ilie and Hickel, 2009b). Consequently, the use of Weibull statistics might be questioned for less brittle and viscoelastic materials such as RBCs compared with ceramic-based materials, for which Weibull statistics are established (Cattell et al., 1997; Bhamra et al., 2002; Lohbauer et al., 2002; Bona et al., 2003; Addison et al., 2007ab). Until now, no researcher has considered the effect of such characteristics on the applicability of Weibull statistics in RBC related research. Therefore, the aim of the current study was to investigate the applicability of Weibull statistics in different classes of RBCs likely to exhibit a variation in viscoelasticity.

The application of feldspathic porcelain is considered as a traditional approach to high strength ceramic materials. It is commonly used for the fabrication of

Porcelain Laminate Veneers (PLVs) and Dentine Bonded Crowns (DBCs), which requires adhesive bonding agent for the cementation with prepared tooth. The mechanical strength of porcelain is determined using different tests such as three-point flexure (Sherrill and O'Brien, 1974), four-point flexure (Bona et al., 2003), and bi-axial flexure (Cattell et al., 1997). The strength scaling of ceramics has been carried out in previous studies using three and four-point flexure tests, however, until now, no researcher has employed bi-axial flexure testing for strength scaling. Thus, in the current investigation, strength scaling of feldspathic porcelain will also be conducted using ball-on-ring and ring-on-ring bi-axial flexure testing.

3.2 Experimental procedure

3.2.1 Materials

In the current investigation, three commercial resin-based composite (RBC) materials, namely a microhybrid (Z100 MP Restorative^{TM}, Z100; batch 8YR; shade A3), a "nanofilled" (Filtek^{TM} Supreme XT, FST; batch 9BW; shade CT) and a "flowable" (Filtek^{TM} Supreme XT, FSF; batch N163221; shade A3) RBC were evaluated. The resin chemistry of FST comprised of bisphenol-A diglycidyl ether dimethacrylate (BisGMA), triethyleneglycol dimethacrylate (TEGDMA), bisphenol-A hexaethoxylated dimethacrylate ($BisEMA_6$) and urethane dimethacrylate UDMA). In contrast, FSF possessed BisGMA, TEGDMA and $BisEMA_6$, while Z100 comprised of BisGMA and TEGDMA only. The resin matrix of FST is loaded with 'nanocluster' particles with a size distribution of 0.6-1.4 μm and dispersed nanosized silica with a mean size of 75 nm to 30 and 40 mass% respectively. The 'nanocluster' in FST is an agglomeration of nanosized (75 nm) silica particles. The total filler loading FST was reported as 70.0 mass% (57.5 volume%) (Mitra et al., 2003; Filtek^{TM} Supreme

Product Report 2003). The filler in FSF is a combination of 75 nm diameter non-agglomerated silica, 5-10 nm diameter non-agglomerated zirconia, 0.6 -1.4 microns loosely bound nanoclusters, consisting of 5-20 nm primary zirconia/silica particles. The total filler loading was approximately 65% by mass and 55% by volume (Filtek^{TM} Supreme XT Flowable Restorative Product Report 2005). Z100 was reported as being loaded with fused spheroidal zirconia-silica filler particles to 84.5 mass% and 66 volume% and filler particles size ranged from 0.01-3.5 μm with an average of 0.6 μm (Filtek^{TM} Z100 Product Report 1996) (Table 3.1).

The failure characteristics of a feldspathic porcelain was also examined in the current investigation: Vitadur-Alpha dentine powder (batch 7290; shade A2) and Vitadur Modelling-P liquid (batch 11290) (Vita Zahnfabrik, Bad Säckingen, Germany). As a comparative brittle control material, glass cover slips (13 mm diameter, 0.22 mm thickness) were also tested (Agar Scientific Ltd, Essex, England) and used as received.

Table 3.1. RBCs constituents used in the current investigation.

Material	Classification	Resin	Filler	Total filler content
Filtek Z100	Microhybrid	BisGMA TEGDMA	Zirconia/silica; 0.01-3.5 µm (84.5 weight%)	84.5 weight% 66.0 volume%
Filtek supreme translucent	Nanofilled	BisGMA UDMA $BisEMA_6$ TEGDMA	Silica; 75 nm nanoparticles (40.0 weight%) Silica; 0.6-1.4 µm nanoclusters (30.0 weight%)	70.0 weight% 57.5 volume%
Filtek supreme flowable	Flowable	BisGMA TEGDMA $BisEMA_6$	Silica; 75 nm nanoparticles Zirconia; 5-10 nm nanoparticles Zirconia/silica; 0.6-1.4 µm nanoclusters	65.0 weight% 55.0 volume%

BisGMA, bisphenol-A diglycidyl ether dimethacrylate; TEGDMA, triethyleneglycol dimethacrylate; $BisEMA_6$, - bisphenol-A hexaethoxylated dimethacrylate; UDMA, urethane dimethacrylate.

3.2.2 Specimen preparation

For each RBC, one hundred and eighty nominally identical disc-shaped specimens (12 mm diameter, 1 mm thickness) consisting of two groups (n=90) were fabricated. Split black nylon moulds were used to allow specimen removal without introducing spurious bending stresses. For each specimen 0.24±0.005 g of RBC paste was weighed using electronic scales (Mettler-Toledo Ltd, Leicester, UK) accurate to 0.001 g and then packed into the nylon mould. Upper and lower surfaces of each specimen were covered with cellulose acetate strip (approximately 0.1 mm thick) to lessen the impact of oxygen inhibition (Shawkat et al., 2009). The filled mould was placed within a black nylon alignment ring to ensure concentric placement of the curing-tip for each successive specimen irradiation. This was placed on a steel platen and irradiated from either side for 20 s using a halogen curing unit (Elipar Trilight, ESPE, Seefeld, Germany) with a 10 mm diameter curing tip at an ambient temperature 23±2 ºC. The irradiance of the curing-unit was measured prior to fabrication of each sample set using the built-in radiometer and remained at ~700 mW/cm^2 throughout the experiment. Following irradiation, the cellulose acetate strips were discarded, each specimen immediately removed from the mould and flash cut away using a sharp blade. Prior to testing, the RBC specimens were stored dry for 1 week at room temperature using a cylindrical light-proof container.

One hundred and eighty nominally identical feldspathic porcelain disc-shaped specimens consisting of two groups (n=90) were manufactured by condensing a powder and liquid slurry into a plastic ring mould (14 mm diameter, 1 mm thickness) firmly secured to burnished aluminum on a Perspex assembly. 0.6 g of Vitadur-Alpha dentine powder was manipulated with 0.22 ml of Vitadur Modelling Fluid to form a slurry with an optimum powder to liquid mixing ratio (Fleming et al., 2000). The

slurry mix was condensed by placing the mould assembly on a vibrating table (Croform Techniques Ltd., London, UK) and removing any liquid. The condensed specimen was levelled with a razor blade and then transferred to a flat silicon nitride slab and fired in accordance with the manufacturer instructions. Specimens were pre-heated at 600 °C for 360 s and then temperature was raised from 600 °C to 960 °C with 60 °C/min increase for 360 s, and held for further 60 s at 960 ºC in a vacuum furnace (Vita Vacumat 40, Vita Zahnfabrik , Bad Säckingen, Germany). The specimen's surface which faced toward the burnished aluminium exhibited a 'glazed' surface whereas a 'fit' surface resulted by the levelling of the other specimen surface with a razor blade. The specimens were stored in a dessicator maintained at 23±1°C for 1 week prior to testing.

Two hundred glass cover-slip specimens (13 mm diameter, 0.22 mm thickness) consisting of two groups (n=100) were tested as received.

3.2.3 Bi-axial flexure strength testing

The bi-axial flexure strength (BFS) of each material group was determined at the cross-head speed of 1.0 mm/min in either a ball-on-ring or ring-on-ring configuration using a universal testing machine (Model 5544, Instron Ltd, High Wycombe, Bucks, England). In the ball-on-ring configuration, a 3 mm ball-indenter was used to centrally load the disc-shaped specimens supported on a 10 mm diameter knife-edge support. Whereas, a loading ring of 3.5 mm inner diameter was employed to centrally load the disc-shaped specimens in ring-on-ring configuration. The porcelain specimens were aligned so that the glazed surface was placed under compression during test. A thin sheet of rubber was placed between the specimen and the support to ensure uniform loading and to accommodate variations in the peripheral

thickness. The load (N) at failure of each specimen was recorded and mean specimen thickness (mm) was measured at the point of fracture of each fragment with a screw-gauge micrometer (Moore and Wright, Sheffield, UK) accurate to 10 μm. The thickness of glass specimens was measured prior to failure, due to the number and small size of the fracture fragments. The ball-on-ring BFS was calculated according to Equation 3.1 (Timoshenko et al., 1959),

$$\sigma_{\max} = \frac{p}{h^2}\{(1+\nu)[0.485\times\ln\left(\frac{a}{h}\right)+0.52]+0.48\} \qquad \text{Equation 3.1}$$

where σ_{max} was the maximum tensile stress (MPa), P the measured load at fracture (N), a the radius of knife-edge support (mm), h the specimen thickness at the point of fracture (mm) and ν the Poisson's ratio for the material.

The ring-on-ring BFS was calculated according to Equation 3.2 (Morrell et al., 1999),

$$\sigma_{\max} = \frac{3P}{4\pi t^2}\left[2(1+\nu)\ln\frac{a}{b}+\frac{(1-\nu)(a^2-b^2)}{R^2}\right] \qquad \text{Equation 3.2}$$

where σ_{max} was the maximum tensile stress (MPa), P the measured load at fracture (N), a the radius of knife-edge support (mm), b the loading ring radius (mm), t the disc thickness (mm), R the radius of disc specimen (mm) and ν the Poisson's ratio for the material. In literature, the Poisson's ratio values of 0.24 (Ban and Anusavice, 1990) and 0.25 (Anusavice et al., 1980) have been substituted for BFS determination of RBCs and porcelain respectively. In previous study, Poisson's ratio of a microhybrid and a flowable RBC was identified as 0.30 and 0.39 respectively and higher Poisson's ratio of the flowable RBC was attributed to its low filler content and resultant decrease in elastic modulus (Chung et al., 2004). The elastic modulus of porcelain is reported to be in the range of 64-70 GPa (Lawn et al., 2002; Fleming et al., 2005). Consequently, in the current investigation, a Poisson's ratio value of 0.23

for porcelain and glass cover slips, 0.25 for FST and Z100 and 0.27 for FSF was utilized arbitrarily and was justified with their associated elastic modulus.

3.2.4 Statistical analyses

The statistical theory described by Weibull (1951) is a commonly used approach to analyse failure probabilities of brittle materials. The Weibull distribution for a body failing under tensile stress can be expressed as

$$P_f = 1 - \exp\left[-V\left(\frac{\sigma - \sigma_{\min}}{\sigma_o}\right)^m\right] \qquad \text{Equation 3.3}$$

where σ is the applied stress at failure (MPa) and σ_{min}, σ_o and m are the Weibull parameters. V is the specimen volume. The Weibull modulus (m) characterises the brittleness of a material (Trustrum and Jayatilaka 1979). The Weibull modulus parameter is a function of the flaw size, orientation and distribution and therefore the resultant scatter and associated reliability of the flexure strength data. σ_{min} is the threshold stress parameter at which failure probability approaches zero and σ_o is the scale parameter of the Weibull distribution, which is also referred as the normalising constant. P_f is the probability of failure, which varies from zero to one and was calculated according to Equation 3.4

$$P_f = \left(\frac{n}{N^* + 1}\right) \qquad \text{Equation 3.4}$$

N^* is the total number of specimens and n is the ranking number of the specimen when the flexural strength of the specimens is ranked in ascending order. Davies (1973) and Stanley et al. (1973) have previously demonstrated that $\sigma_{min} = 0$ is a safe assumption for brittle materials as there is a finite probability of the presence of a

critical flaw in a specimen prior to stressing. Therefore, Equation 3.3 can be reduced to the form of Equation 3.5

$$P_s = 1 - P_f = 1 - \left(1 - \exp\left[-\frac{\sigma}{\sigma_o}\right]^m\right) \qquad \text{Equation 3.5}$$

Equation 3.4 may further be rearranged using natural logarithms of straight line y = mx + c to allow the flexure strength data and resultant Weibull analysis to be presented in graphical form

$$\ln\ln\left(\frac{1}{Ps}\right) = m\ln\sigma - m\ln\sigma_o \qquad \text{Equation 3.6}$$

Where Ps is the probability of survival since Ps is equal to 1-P_f. The intercept of the y-axis when x= 0 is $-m\ln\sigma_o$ and *m* was the gradient of the line. In the current investigation bi-axial flexure strength data was ranked in ascending order and a Weibull analysis performed on the resultant data by plotting lnln(1/Ps) against lnσ. m becomes the gradient of the linearised data and was calculated by superimposing a regression line along the data points to provide the Weibull modulus for each group of specimens tested.

To determine statistical differences between the Weibull modulus of the flexure strength data, the 95% confidence intervals for the specimen groups under investigation were calculated by a least square regression analysis. The differences in the Weibull modulus of the flexure strength data was considered to be significantly different when the 95% confidence intervals failed to overlap.

Strength scaling was conducted on ring-on-ring configuration using Weibull statistics to determine related BFS for ball-on-ring configuration. According to Weibull weakest link theory, the size-strength relationship can be written as following (Davies, 1973),

$$\frac{\sigma_1}{\sigma_2} = \left(\frac{V_{E2}}{V_{E1}} \right)^{1/m}$$ Equation 3.7

where m is the Weibull modulus, σ_1 and σ_2 are the mean strength of two different test configurations, and V_{E1} and V_{E2} are the related effective volumes. If surface flaws are greater than volume flaws, then effective volumes can be replaced with effective surfaces i.e. S_{E1} and S_{E2} in Equation 3.8.

In previous literature, equations for effective volumes and effective areas are available for rectangular bars tested in uniaxial flexure such as three-point flexure or four-point flexure (Quinn, 2003). If bar-shaped specimens with similar width, height and span length are utilized in three-point and four-point flexure tests, the ratio of effective volume is,

$$\frac{V_{E4-pt}}{V_{E3-pt}} = \frac{m+2}{2}$$ Equation 3.8

where $V_{E4\text{-}pt}$ and $V_{E3\text{-}pt}$ are the effective volumes of four-point and three-point flexure test configurations, respectively. No scaling relationships to date have been presented for ball-on-ring and ring-on-ring bi-axial flexure testing. However, it may be assumed that the relationship would approximate to an equi-biaxial version of the relationship between three-point and four-point bending. Therefore, it is reasonable to assume that a similar consideration may be applied in current study as nominally identical disc-shaped specimens and supporting ring were employed in both ball-on-ring and ring-on-ring configuration. Thus, it may be written as,

$$\frac{V_{EROR}}{V_{EBOR}} = \frac{m+2}{2}$$ Equation 3.9

where V_{EROR} and V_{EBOR} are the effective volumes of ring-on-ring and ball-on-ring flexure test configurations, respectively. This can be substituted in Equation 3.7 in order to predict the strength for ball-on-ring configuration.

$$\sigma_{BOR} = \sigma_{ROR}\left(\frac{V_{EROR}}{V_{EBOR}}\right)^{1/m}$$ Equation 3.10

$$\sigma_{BOR} = \sigma_{ROR}\left(\frac{m+2}{2}\right)^{1/m}$$ Equation 3.11

Within the dental literature, although the appropriateness is debatable, Weibull statistics are frequently performed and presented complementary to parametric methods. Therefore a one-way ANOVA and post hoc Tukey multiple comparison tests were performed on the BFS data (P=0.05) to highlight any differences between ball-on-ring and ring-on-ring BFS of each material investigated.

3.3 Results

The Weibull modulus and associated 95% confidence intervals, characteristic strength (σ_o), mean BFS and associated standard deviations of all materials evaluated using ball-on-ring and ring-on-ring are shown in Table 3.2. The ball-on-ring test revealed significantly increased (σ_o) and mean BFS when compared with ring-on-ring test for all materials (P<0.001) except flowable resin composite (P=0.207) (Table 3.2). The ball-on-ring BFS of microhybrid RBC, nanofilled RBC, porcelain and glass cover slips was 19%, 17%, 50%, 47% greater compared with ring-on-ring BFS of related materials respectively. In contrast, the flowable resin composite exhibited a non-significant 2% increase in ball-on-ring BFS in relation to the corresponding ring-on-ring BFS.

For both the flowable resin-composite and porcelain materials, the Weibull moduli of ring-on-ring was significantly decreased when compared with ball-on-ring BFS data as the 95% confidence intervals of m did not overlap. However, no

significant difference between the Weibull moduli of BFS data was identified between ball-on-ring and ring-on-ring for either microhybrid, nanofilled or the glass cover slips (Table 3.2). Examination of the Weibull plots revealed that the microhybrid RBC, nanofilled RBC and glass cover slips exhibited similar distributions following ball-on-ring and ring-on-ring testing when compared with the flowable RBC and the porcelain specimens (Figure 3.2).

The predicted BFS of microhybrid and nanofilled RBCs using strength scaling was 173 MPa and 154 MPa respectively for ball-on-ring configuration, which is in agreement with the corresponding experimental BFS (Table 3.2). The strength scaling for glass cover slips revealed the 884 MPa BFS for ball-on-ring configuration, which is 19% lower than associated experimental BFS (Table 3.2). The Weibull strength scaling on flowable RBC and porcelain data was not performed due to the significant difference between Weibull modulus of ball-on-ring and ring-on-ring test configurations (Table 3.2).

Table 3.2. The characteristic strength, mean BFS, associated Weibull modulus, 95% confidence intervals of microhybrid, nanofilled, flowable RBCs, porcelain and glass cover slips tested using the ball-on-ring and ring-on-ring configuration. The predicted ball-on-ring BFS of microhybrid RBC, nanofilled RBC and glass cover slips is also shown.

Material	Test	Weibull modulus (m)	95% Confidence intervals	Mean BFS (MPa)	Predicted BFS (MPa)	Characteristic strength (MPa)
Microhybrid RBC (Z100)	Ball-on-ring	7.6	7.4-8.0	172(26)	173	178
	Ring-on-ring	7.2	7.0-7.4	140(22)	---	146
Nanofilled RBC (FST)	Ball-on-ring	8.5	8.2-8.8	151(20)	154	159
	Ring-on-ring	8.0	7.8-8.3	126(18)	---	131
Flowable RBC (FSF)	Ball-on-ring	12.0	11.6-12.4	169(16)	---	175
	Ring-on-ring	8.2	7.8-8.6	165(24)	---	168
Porcelain	Ball-on-ring	6.7	6.5-7.0	129(22)	---	134
	Ring-on-ring	3.9	3.9-4.0	64(18)	---	67
Glass cover slips	Ball-on-ring	2.3	2.2-2.4	1197(646)	884	1244
	Ring-on-ring	2.4	2.4-2.5	635(289)	---	692

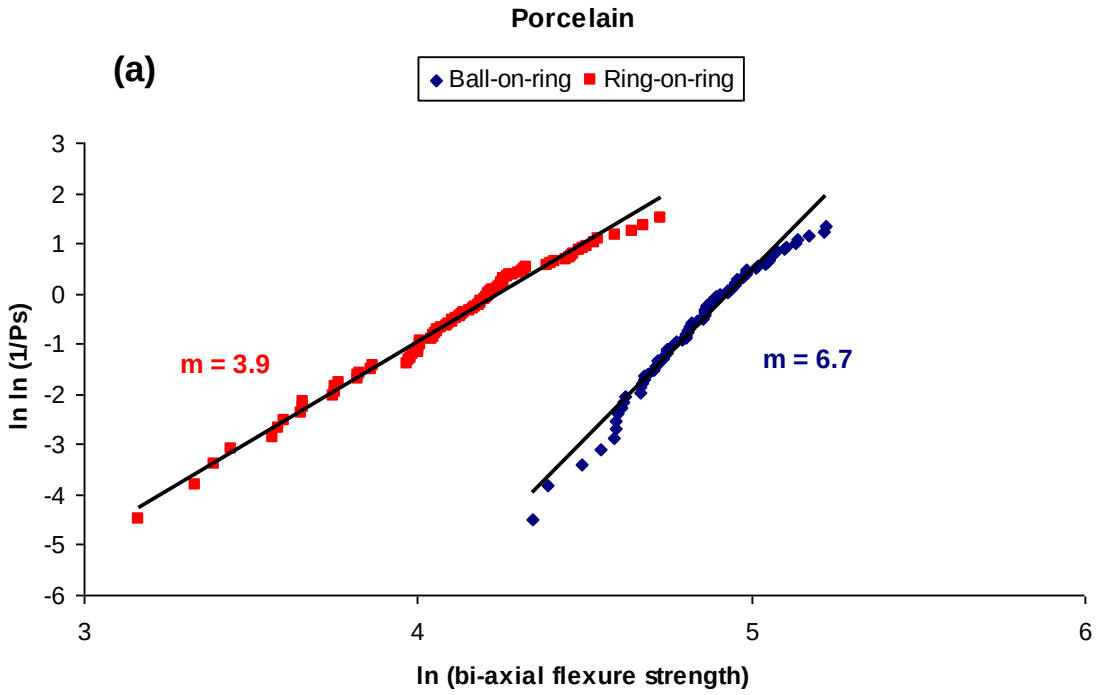
Porcelain
(a)
Ball-on-ring
Ring-on-ring
m = 3.9
m = 6.7
ln ln (1/Ps)
ln (bi-axial flexure strength)

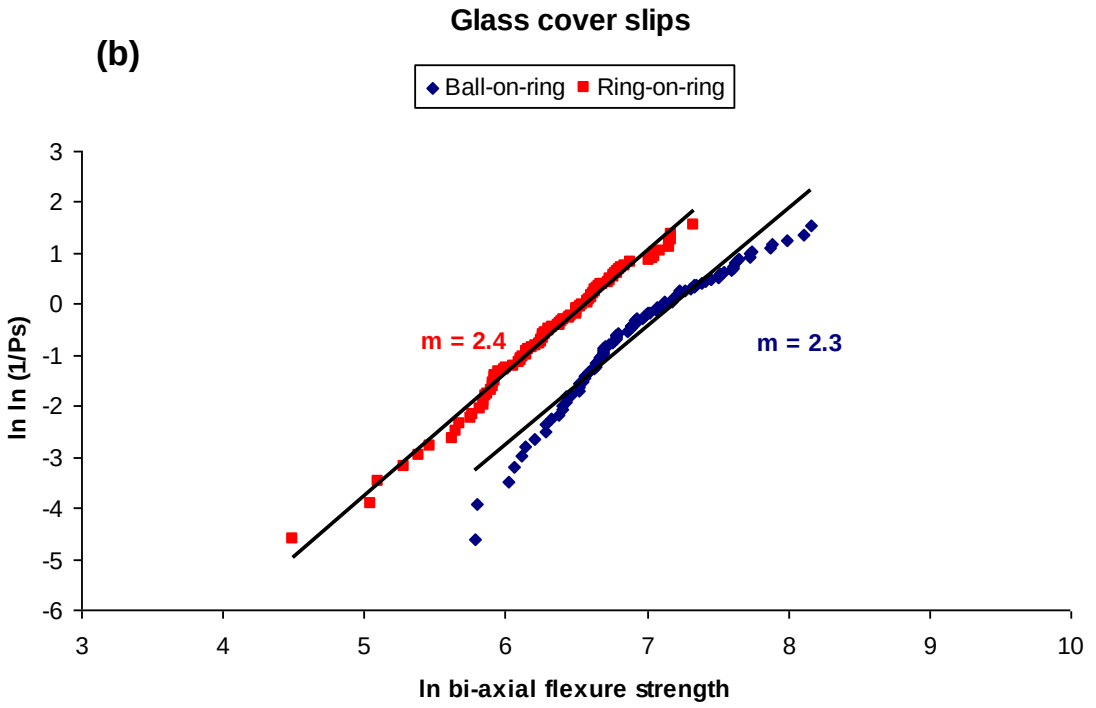
Glass cover slips
(b)
Ball-on-ring
Ring-on-ring
m = 2.4
m = 2.3
ln ln (1/Ps)
ln bi-axial flexure strength

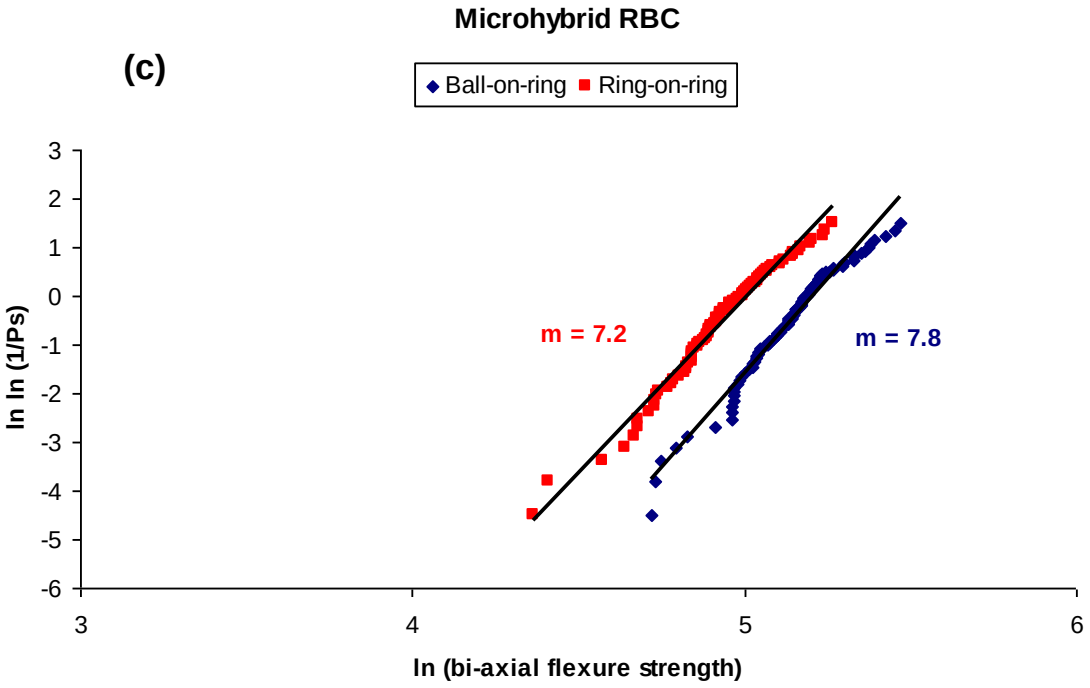
Microhybrid RBC
(c)
Ball-on-ring
Ring-on-ring
m = 7.2
m = 7.8
ln ln (1/Ps)
ln (bi-axial flexure strength)
3
2
1
0
-1
-2
-3
-4
-5
-6
3
4
5
6

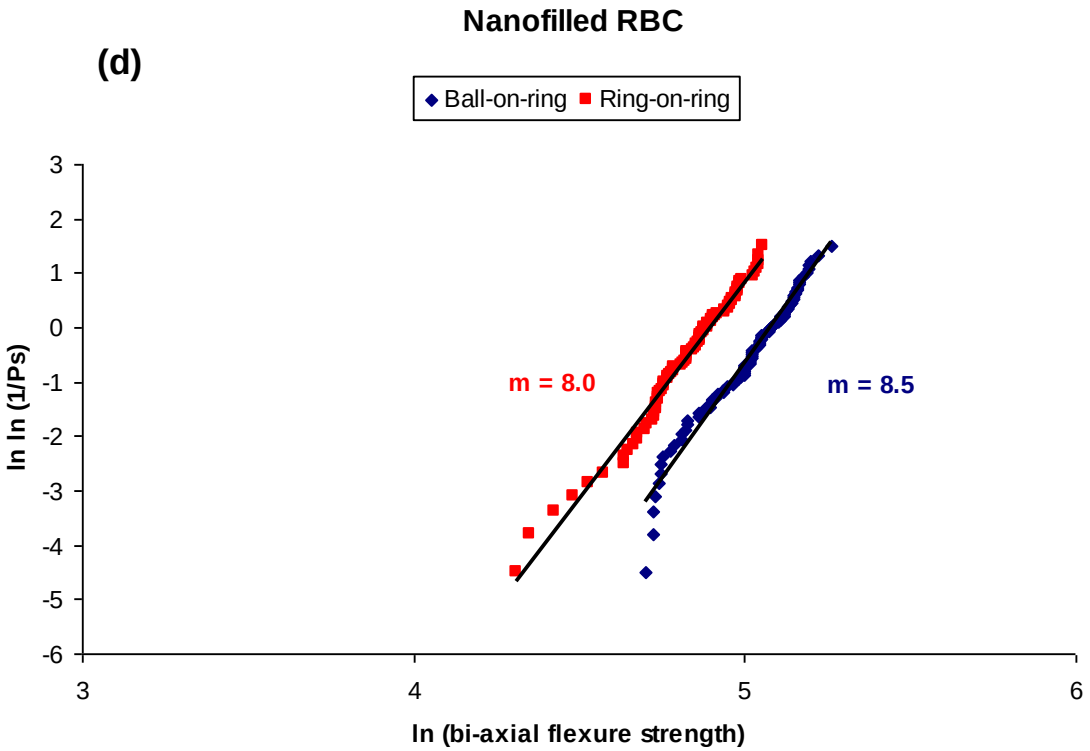
Nanofilled RBC
(d)
Ball-on-ring
Ring-on-ring
m = 8.0
m = 8.5
ln ln (1/Ps)
ln (bi-axial flexure strength)
3
2
1
0
-1
-2
-3
-4
-5
-6
3
4
5
6

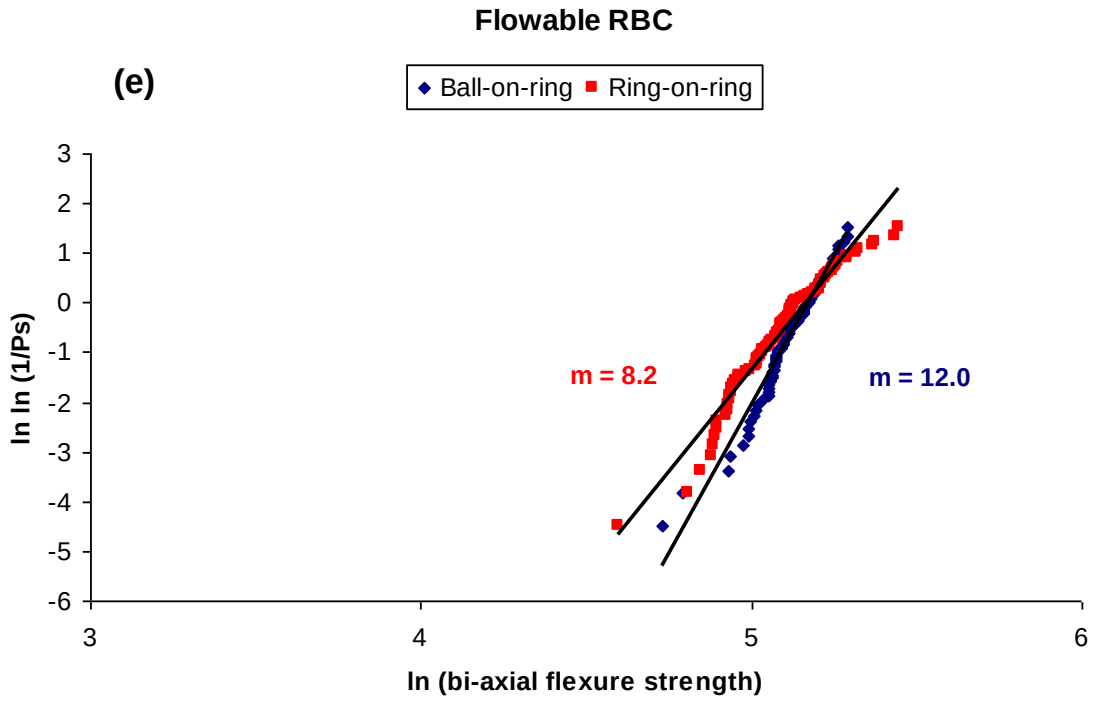

Figure 3.1. The combined Weibull plots of (a) porcelain, (b) glass cover slips, (c) microhybrid RBC, (d) nanofilled RBC and (e) flowable RBC specimens tested in bi-axial flexure using ball-on-ring and ring-on-ring configurations. All materials except flowable RBC failed at significantly lower stresses with ring-on-ring configuration in contrast to ball-on-ring configuration. Porcelain and flowable RBC specimens exhibited significant difference between their ball-on-ring and ring-on-ring Weibull modulus.

3.4 Discussion

An increase in the characteristic strength (σ_o) (and mean BFS of porcelain and glass cover slips) following ball-on-ring compared with ring on ring test was expected since specimens in the former were loaded under a smaller volume or surface areas at the maximum tensile stress. This is in accordance with previous investigators who identified significantly increased strength values of ceramics for three-point flexure compared with four-point flexure test methods and attributed their findings to a smaller volume of three-point flexure specimens subjected to high tensile stresses compared with four-point flexure test (Jin et al., 2004). In contrast, the reduced Weibull modulus of the porcelain following ring-on-ring compared with the ball-on-ring test was not expected as ceramics are often assumed to follow Weibull theory (Danzer et al., 2007). The findings suggest that for the ring-on-ring loading the critical defect population differed from that encountered in the ball-on-ring test. During the sintering and cooling of the porcelain disc specimens, transient and residual stresses are introduced (Isgró et al., 2010) and lead to a slight deformation of the specimen. As, ring-on-ring testing stresses a larger area radial to the centre point of the disc specimen compared with ball-on-ring, it is likely that different defects or defects subjected to differing residual stress states may be encountered leading to the observed decrease in the Weibull modulus. This finding supports that inconsistent machining or handling of specimens do not represent a specific flaw population and thus do not provide a suitable data for Weibull statistics (Quinn and Quinn, 2010).

The glass cover slips were included in the current study as a model system in terms of reproducibility as precise machining by the manufacturers is expected. The similar Weibull distributions demonstrated by an overlap in 95% confidence intervals of ball-on-ring and ring-on-ring of glass cover slips suggest that similar flaw types

were involved in both configurations and support the applicability of Weibull statistics. The lower than predicted ball-on-ring BFS of glass cover slips when compared with the associated experimental ball-on-ring BFS (Table 3.2) could possibly be explained by the thickness of specimens. For very thin specimens the impact of contact stresses between supports and loading tools play a greater role particularly in a ring-on-ring configuration. The large number of fracture fragments observed when compared with dental porcelain or RBC specimens supports this suggestion have been attributed to increased energy storage prior to failure (Kelly, 1999) and may have led to the reduction in BFS which may then predict lower ball-on-ring BFS. The magnitude of the decrease in the ring-on-ring BFS of porcelain and glass cover slips compared with their corresponding ball-on-ring BFS (approximately 50 %) suggests a significant role of pre-existing surface defects in determining failure. The major involvement of surface flaws in the failure of porcelain specimens has also been reported by researchers, who identified a significant reduction in the BFS of porcelain following alumina particle air-abrasion (Addison et al., 2007a) and hydrofluoric acid etching (Addison et al., 2007b). In ball-on-ring only small region at the centre-point of the lower surface of the specimen reaches the maximum tensile stress when compared with a significantly larger region in ring-on-ring loading.

The greater ball-on-ring BFS of microhybrid and nanofilled RBCs when compared with ring-on-ring BFS can also be explained in a similar manner to porcelain and glass cover slips. The comparable Weibull plots and no significant difference between Weibull modulus of ball-on-ring and ring-on-ring test of either microhybrid and nanofilled RBCs indicate similar flaw types dictate failure in both test configurations. These findings in addition to related strength scaling results (Table 3.2) confirm the applicability of Weibull statistics with both the microhybrid

and nanofilled RBCs tested within the limits of the present investigation. The significant change in Weibull modulus of the flowable RBC following ring-on-ring test compared with corresponding ball-on-ring test suggests a wider variation in the strength distribution using the ring-on-ring configuration. It was also evident from the distribution that failure of some flowable RBC specimens increased at higher stresses in ring-on-ring configuration when compared with ball-on-ring and thus resulted in an increased BFS. A possible explanation could be that a greater amount of energy is required to generate or propagate the critical defect in the flowable RBC compared with microhybrid and nanofilled specimens in ring-on-ring configuration. A flowable RBC comprises of a low amount of fillers in contrast to microhybrid and nanofilled RBCs and therefore a lower elastic modulus of a flowable RBC is expected. A higher proportion of resin in a flowable RBC would be expected to exhibit increased plastic deformation and a viscoelastic response as a result of energy-absorbing molecular rearrangements at the crack tip which may slow crack propagation and toughen the material. Lee et al. (2010) suggested that flexural strength reflects both toughness and flaw size, therefore any mechanism which slows crack propagation is likely to cause an increase in flexural strength. It is important to note that there is no significant difference between Weibull modulus of nanofilled and flowable RBCs following ring on-ring test, so one could speculate that both materials are equally ‘reliable’. In reality, that would not be the case if both materials were tested in ball-on-ring configuration. The findings of the current investigation suggest that test of a material on different levels of effective volumes may confirm the existence of a Weibull distribution, which has also been suggested by different investigators (Danzer, 2006; Quinn and Quinn, 2010).

3.6 Conclusions

1. This study suggests that Weibull statistics may not necessarily applicable for all RBCs. Thus, their use for characterisation of a wide range of RBCs may cause wrong interpretation of data among researchers.
2. To ensure the validity of the Weibull approach for RBCs, a material may be tested on different level of effective volumes using different test configurations.

References

Addison O, Marquis PM, Fleming GJP. The impact of hydrofluoric acid surface treatments on the performance of a porcelain laminate restorative material. Dental Materials, 2007a; 23: 461-468.

Addison O, Marquis PM, Fleming GJP. The impact of modifying alumina air abrasion parameters on the fracture strength of a porcelain laminate restorative material. Dental Materials, 2007b; 23: 1332-1341.

Anusavice KJ, Dehoff PH, Fairhurst CW. Materials science: Comparative evaluation of ceramic-metal bond tests using finite element stress analysis. Journal of Dental Research, 1980; 59: 608-613.

Ban S, Anusavice KJ. Influence of test method on failure stress of brittle dental materials. Journal of Dental Research, 1990; 69: 1791-1799.

Bhamra G, Palin WM, Fleming GJP. The effect of surface roughness on the flexure strength of an alumina reinforced all-ceramic crown material. Journal of Dentistry, 2002; 30: 153-160.

Bona AD, Anusavice KJ, DeHoff PH. Weibull analysis and flexural strength of hot-pressed core and veneered ceramic structures. Dental Materials, 2003; 19: 662-669.

Cattell MJ, Clarke RL, Lynch EJR. The biaxial flexural strength and reliability of four dental ceramics- part II. Journal of Dentistry, 1997; 25: 409-414.

Chung SM, Yap AUJ, Koh WK, Tsai KT, Lim CT. Measurment of poisson's ratio of dental composite restorative materials. Biomaterials, 2004; 25: 2455-2460.

Curtis AR, Palin WM, Fleming GJP, Shortall ACC, Marquis PM. The mechanical properties of nanofilled rein-based composites: The impact of dry and wet cyclic pre-loading on bi-axial flexure strength. Dental Materials, 2009; 25:188-197.

Danzer R. Some notes on the correlation between fracture and defect statistics: Are Weibull statistics valid for very small specimens? Journal of the European Ceramic Society, 2006; 26: 3043-3049.

Danzer R, Supancic P, Pascual J, Lube T. Fracture statistics of ceramics-Weibull statistics and deviation from Weibull statistics. Engineering Fracture Mechanics, 2007; 74: 2919-2932.

Danzer R, Lube T, Supancic P, Damani R. Fracture of ceramics. Advanced Engineering Materials, 2008; 10: 275-297.

Davies DGS. The statistical approach to engineering design in ceramics. Proceedings of the British Ceramic Society, 1973; 22: 429-451.

Fleming GJP, Shaini FJ, Marquis PM. An assessment of the influence of mixing induced variability on the bi-axial flexure strength of dentine porcelain discs and the implications for laboratory testing of porcelain specimens. Dental Materials, 2000; 16: 114-119.

Fleming GJP, El-Lakwah SFA, Harris JJ, Marquis PM. The effect of core: dentine thickness ratio on the bi-axial flexure strength and fracture mode and origin of bilayered dental ceramic composites. Dental Materials, 2005; 21: 164-171.

Griffith AA. The phenomena of rupture and flow in solids. Philosophical Transaction of the Royal Society of London, 1921; 221: 163-198.

Griggs JA, Zhang Y. Determining the confidence intervals of Weibull parameters estimated using a more precise probability estimator. Journal of Materials Science letters, 2003; 22:1771-1773.

Ilie N, Hickel R. Macro-, micro- and nano-mechanical investigations on silorane and methacrylate-based composites. Dental Materials, 2009a; 25: 810-819.

Ilie N, Hickel R. Investigations on mechanical behaviour of dental composites. Clinical Oral Investigations, 2009b; 13: 427-438.

Isgró G, Addison O, Fleming GJP. Transient and residual stresses induced during the sintering of two dentine ceramics. Dental Materials, 2010 (Article in press).

Jin Jingyue, Takahashi H, Iwasaki N. Effect of test method on flexural strength of recent dental ceramics. Dental Materials Journal, 2004; 23: 490-496.

Kelly JR . Clinically relevant approach to failure testing of all-ceramic restorations. Journal of Prosthetic Dentistry, 1999; 81: 652-661.

Lawn BR, Deng Y, Lloyd IK, Janal MN, Rekow ED, Thompson VP. Materials design of ceramic-based layer structures for crowns. Journal of Dental Research, 2002; 81: 433-438.

Lee VA, Lee Cardenas H, Ralph Rawls H. Rubber-toughening of dimethacrylate dental composite resin. Journal of Biomedical Materials Research Part B: Applied Biomaterials, 2010; 94B: 447-454.

Lohbauer U, Petschelt A, Greil P. Life time prediction of CAD/CAM dental ceramics. Journal of Biomedical Materials Research (Applied Biomaterials), 2002; 63: 780-785.

McCabe JF, Carrick TE. A statistical approach to the mechanical testing of dental materials. Dental Materials, 1986; 2: 139-142.

Mesquita RV, Axmann D, Gerstorfer JG. Dynamic visco-elastic properties of dental composite resins. Dental Materials, 2006; 22:258-267.

Mitra SB, Dong WU, Holmes BN. An application of nanotechnology in advanced dental materials. Journal of the American Dental Association, 2003; 134:1382-1390.

Morrell R, McCormick NJ, Bevan J, Lodeiro M, Margetson J. Bi-axial disc flexure-modulus and strength testing. British Ceramic Trnasactions, 1999; 98: 234-240.

Palin WM, Fleming GJP, Burke FJT, Marquis PM, Randall RC. The reliability in flexural strength testing of a novel dental composite. Journal of Dentistry, 2003; 31:549-557.

Palin WM, Fleming GJP, Marquis PM. The reliability of standardised flexural strength testing procedure for a light-activated resin-based composite. Dental Materials, 2005; 21: 911-919.

Papargyris AD. Estimator type and population size for estimating the Weibull modulus in ceramics. Journal of European Ceramic Society, 1998; 18: 451-455.

Quinn G. Advance structural ceramics: A round robin. Journal of American Ceramic Society, 1990; 73: 2374-2384.

Quinn JB, Quinn GD. A practical and systemic review of Weibull statistics for reporting strengths of dental materials. Dental Materials, 2010; 26: 135-147.

Ritter JE. Critique of test methods for life time predictions. Dental Materials, 1995; 11: 147-151.

Rodrigues Junior SA, Ferracane JL, Bona AD. Flexural strength and Weibull analysis of a microhybrid and nanofill composite evaluated by 3- and 4-point bending tests. Dental Materials, 2008; 24:426-431.

Sabbagh J, Vreven J, Leloup G. Dynamic and static moduli of elasticity of resin based materials. Dental Materials, 2002; 18: 64-71.

Shawkat ES, Shortall AC, Addison O, Palin WM. Oxygen inhibition and incremental layer bond strengths of resin composites. Dental Materials, 2009; 25: 1338-1346.

Sherrill CA, O'Brien WJ. Transverse strength of aluminous and feldspathic porcelain. Journal of Dental Research, 1974; 53: 683-690.

Stanley P, Fessler H, Sivill AD. An Engineer's approach to the prediction of failure probability in brittle components. Proceedings of the British Ceramic Society, 1973; 22:452-487.

Timoshenko S, Woinowsky-Krieger S. Symmetrical bending of circular plates. In: Theory of Plates and Shells. McGraw-Hill; New York, 1959; (2nd Edition).

Trustrum K, Jayatilaka A. Applicability of Weibull analysis for brittle materials. Journal of Materials Science, 1983; 18:2765-2770.

Watts DC. Elastic moduli and visco-elastic relaxation. Journal of Dentistry, 1994; 22: 154-158.

Weibull W. A statistical theory of the strength of materials. Ingeniörsvetenkapsakademiens Handlingar Nr 151, 1939; Page: 1-45

Weibull W. A statistical distribution function of wide applicability. Journal of Applied Mechanics, 1951; 18-293-297.

Chapter 4 Effects of Deformation Rate on the Bi-axial Flexural Strength of Dental Resin-Based Composites

4.1 Introduction

Amalgam is traditionally the material of choice for the restoration of posterior teeth, however, there is a trend towards more cosmetic resin-based composite (RBC) restorations because of patients increased demand for tooth-coloured restorations, fear concerning mercury vapours released from amalgam and the associated biological and environmental considerations relating to waste removal (Chin et al., 2000; Burke, 2004; Hörsted-Bindslev, 2004). The advantages of RBCs include the ability to be bonded to tooth structure (Leinfelder, 1996) and the availability in tooth-coloured shades (Uchida et al., 1998). Despite the desirable features of RBCs, there are deficiencies such as polymerisation shrinkage (Davidson and Feilzer, 1997; Kleverlaan and Feilzer, 2005) and in fracture resistance (Ferracane et al., 1987) which cause concern to researchers and clinicians in terms of the restoration performance in service. Several attempts have and are being made to address these shortcomings mainly through the development of the filler technology. As a consequence, microhybrid and nanofilled RBCs have been developed and are believed to possess improved aesthetics and mechanical properties compared with traditional RBC materials.

Considerable effort has been undertaken to determine the fracture behaviour of RBCs in terms of static strength, cyclic loading, fatigue crack growth and fracture resistance (Curtis et al., 2008; Curtis et al., 2009; Shah et al., 2009ab). Different patterns of fracture have been observed between materials and attributed to the different filler sizes, filler morphologies and their associated interfacial adhesion with the resins matrix (Curtis et al., 2008). The filler particles have not simply modified the

strength values but have greatly changed the mechanisms of fracture in RBCs (Kim et al., 1994; Drummond, 2008; Curtis et al., 2009; Shah et al., 2009ab).

In the oral environment, RBCs will experience cyclic loading of varying magnitudes during the lifetime of the restoration due to the heterogeneous forces from mastication and grinding. The nature of the forces encountered will vary from patient to patient according to their anatomy, physiological chewing patterns, diet (Yamashita et al., 1999; Koolstra, 2002) and position of restoration within the dentition. For example, when a patient exhibits para-functional habits such as bruxism, RBC restorations may be subjected to sustained forces (Ruyter and Øysæd, 1982) for extended periods at low deformation rates in contrast to the much more transient loading forces in normal mastication (Glaros and Rao, 1977). However, the mechanical properties of RBCs are almost universally determined at a single deformation rate and even the International Standard for Dental Polymer-Based Filling, Restorative and Luting Materials (ISO 4049, 2000) has suggested a narrow range of testing rates (0.75±0.25 mm/min) for the determination of the flexural strength of RBCs. It is clear that to investigate the mechanical characteristics of RBCs at one deformation rate is not sufficient to elucidate the material behaviour in the real clinical environment. Moreover, it is understood that many classes of dental restorative material will exhibit a strain-rate dependence on their strength. Therefore, the aim of the study is to investigate the influence of deformation rate on the bi-axial flexure strength (BFS) of two microhybrid and two nanofilled RBCs.

4.2 Experimental procedure

4.2.1 Materials

Four commercial RBCs, Z100 MP Restorative™ (Z100; batch 8YR; shade A3), Filtek™ Z250 (Z250; batch 8MA, 9UX; shade A3) and Filtek™ Supreme XT 'body' (FSB; batch 8NU; shade A3) and 'translucent' shades (FST; batch 6CL, 7EA; shade YT) (3M ESPE Dental Products, St. Paul, MN, USA) were used in the current investigation. Z250, FSB and FST possessed an identical resin chemistry, consisting of Bisphenol A diglycidyl ether dimethacrylate (BisGMA), triethyleneglycol dimethacrylate (TEGDMA), Bisphenol A polyethylene glycol diether dimethacrylate ($BisEMA_6$) and Urethane dimethacrylate (UDMA). In contrast, Z100 comprised of BisGMA and TEGDMA only. Z100 and Z250 were loaded with fused zirconia-silica filler particles (84.5 weight%; 66.0 volume%) and (84.5 weight%; 60.0 volume%) respectively and the filler particles size ranged from 0.01-3.5 µm with an average of 0.6 µm. FSB contained a mixture of individually dispersed nanosized silica particles (8.0 weight%) and distinct agglomerations of nanosized zirconia and silica (nanoclusters) (71.0 weight%), which became (79.0 weight% and 59.5 volume%) in total. The size of individual nanoparticles and nanoclusters was in range of 5-20 nm and 0.6-1.4 µm respectively. The fillers of FST consisted of silica nanoparticles of 75 nm size (40.0 weight%) and silica nanoclusters of 0.6-1.4 µm size (30.0 weight%) which was collectively (70.0 weight% and 57.5 volume%). The RBCs constituents are summarised in Table 4.1.

Table 4.1. Material constituents used in the current investigation.

Material	**Classification**	**Resin**	**Filler**	**Total filler content**
Filtek Z100 (Z100)	Microhybrid	BisGMA TEGDMA	Zirconia/silica; 0.01-3.5 µm (84.5 weight%)	84.5 weight% 66.0 volume%
Filtek Z250 (Z250)	Microhybrid	BisGMA UDMA $BisEMA_6$ TEGDMA	Zirconia/silica: 0.01-3.5 µm (84.5 weight%)	84.5 weight% 60.0 volume%
Filtek supreme body (FSB)	Nanofilled	BisGMA UDMA $BisEMA_6$ TEGDMA	Silica; 5-20 nm nanoparticle (8.0 weight%); Zirconia/silica; 0.6-1.4 µm nanocluster (71.0 weight%)	79.0 weight% 59.5 volume%
Filtek supreme translucent (FST)	Nanofilled	BisGMA UDMA $BisEMA_6$ TEGDMA	Silica; 75 nm nanoparticle (40.0 weight%) Silica; 0.6-1.4 µm nanocluster (30.0 weight%)	70.0 weight% 57.5 volume%

4.2.2 Bi-axial flexure strength: Specimen preparation

Four groups of each RBC comprising of one hundred and twenty nominally identical disc-shaped specimens (12 mm diameter, 1 mm thickness) each were fabricated. Split black nylon moulds were used to allow specimen removal without introducing spurious bending stresses. For each specimen approximately 0.24±0.005 g of RBC paste was weighed using a Mettler AE 163 analytical balance (Mettler-Toledo Ltd, Leicester, UK) accurate to 0.001 g and packed into mould. The top and bottom surfaces of each specimen were covered with cellulose acetate strip (0.1 mm thickness) to lessen the effects of oxygen inhibition (Shawkat et al., 2009). All specimens were light irradiated from one side by a quartz-tungsten-halogen curing unit (Optilux 501, Kerr, Orange, CA, USA) with a 12 mm diameter curing tip placed in contact with acetate strip using a light guide to allow for concentric alignment. The irradiance of the curing-unit was measured prior to fabrication of each sample set (780-880 mW/cm^2) using a radiometer (Coltolux C-7900 Coltene/Whaledent Inc, Mahwah, NJ, US). Following irradiation at an ambient temperature 23±2 ºC for 20 s, the cellulose acetate strips were discarded, each specimen immediately removed from the mould and flash cut away using a sharp blade. Prior to testing, four groups of each RBC (n=120) were stored for short (1 week dry and 1 week wet), medium (13 weeks wet) and long-term (52 weeks wet) storage regimes at 37±1 ºC in a polystyrene cylindrical 30 ml container. To allow wet storage of specimens, distilled water was employed throughout the study to provide a reproducible reference solution (Martin et al., 2003). Specimens were aligned so that they were stacked directly on top of each other. To avoid the potential accumulation of leached RBC constituents in container, distilled water was replaced on weekly basis for 13 weeks ‘wet’ and 52 weeks ‘wet’ storage regimes.

4.2.3 Determination of bi-axial flexure strength

The bi-axial flexure strength (BFS) of each RBC group was determined at a range of deformation rates by setting the cross-head speed to 0.01, 0.1, 1.0 or 10.0 mm/min (n=30) using a ball-on-ring configuration in a universal testing machine (Model 5544, Instron Ltd, High Wycombe, Bucks, England). A 3 mm ball-indenter was used to centrally load the disc-shaped specimens supported on a 10 mm diameter knife-edge support. The irradiated surface of each specimen was placed uppermost, with the non-irradiated surface under tension. The load (N) at failure was recorded and the mean specimen thickness was measured at the point of fracture of each fragment with a screw-gauge micrometer (Moore and Wright, Sheffield, UK) accurate to 10 µm. The BFS (MPa) was calculated according to equation 4.1 (Timoshenko and Woinowsky-Krieger, 1959).

$$\sigma_{max} = \frac{p}{h^2}\{(1+\nu)[0.485 \times \ln\left(\frac{a}{h}\right) + 0.52] + 0.48\} \qquad \text{Equation 4.1}$$

Where σ_{max} was the maximum tensile stress (MPa), P the measured load of fracture (N), a the radius of knife-edge support (mm), h the sample thickness (mm) and ν Poisson's ratio for the material and a value of 0.25 was substituted for all RBCs investigated in the current experiment (Section 3.2.3).

4.2.4 Flexural modulus: Specimen preparation

Four groups of each RBC consisting of ten nominally identical bar-shaped specimens (25 mm length, 2 mm width and 2 mm thickness) were fabricated using nylon split mould. For each specimen, 0.26±0.005 g of RBC was used to slightly overfill the bar-shaped mould. The mould was packed with RBC and both upper and

lower surfaces were covered with cellulose acetate strips (0.1 mm thickness) to reduce oxygen inhibition of the outer layers of specimen. An overlapping curing pattern in accordance with ISO 40409, 2000 was utilized due to increased length of bar-shaped specimens (25 mm) compared with the diameter of curing-light tip (12 mm). Firstly the central portion of the bar-shaped specimen was irradiated for 20 s and then specimen was irradiated at two overlapping irradiation positions for 20 s each immediately after first shot to cure the entire length of the bar-shaped specimen. All specimens were irradiated from one side by a quartz-tungsten-halogen curing unit (Optilux 501, Kerr, Orange, CA, USA) utilizing a 12 mm diameter curing tip at an ambient temperature 23±2 ºC . The irradiance of the curing-unit was measured prior to fabrication of each sample set (780-880 mW/cm^2) using a radiometer (Coltolux C-7900 Coltene/Whaledent Inc, Mahwah, NJ, US). Following irradiation, the cellulose acetate strips were detached, each specimen was immediately removed from the mould and flash cut away using a sharp blade. Prior to testing, RBCs specimens were stored for short (1 week dry and 1 week wet), intermediate (13 weeks wet) and long-term (52 weeks wet) storage regimes at 37±1 ºC. To allow wet storage of specimens, distilled water was employed throughout the study.

4.2.5 Determination of flexural modulus

Three-point flexure data was achieved in accordance with ISO 4049, 2000. The bar- shaped specimens were centrally loaded using a 3 mm diameter cylindrical roller across a support span of 20 mm at a cross-head speed of 1.0 mm/min using a universal testing machine (Model 5544, Instron Ltd, High Wycombe, Bucks, England). The irradiated surface of specimen was placed uppermost, with the non-irradiated surface under tension. After failure of each specimen, the width and

thickness of the specimen at the point of fracture (mm) was measured using a screw-gauge micrometer (Moore and Wright, Sheffield, UK) accurate to 10 µm. The load-deflection curve was plotted for each specimen in order to calculate load (N) and deflection (mm) values at most linear part of curve, subsequently flexural modulus (GPa) was determined using Equation 4.2.

$$E = \frac{Fl^3}{4bh^3d} \qquad \text{Equation 4. 2}$$

Where F was the load (N), l was the span distance (20 mm), b was the width of the specimen (mm), h was the thickness of specimen (mm) and d was the deflection (mm).

4.2.6 Statistical analysis

Two-way analyses of variance (ANOVA) were conducted on complete BFS data sets for each storage regime with materials (4 levels) and deformation rates (4 levels) as independent variables. Additional one-way ANOVA and post-hoc Tukey tests were performed on the BFS data to highlight the differences between BFS of each material at the four deformation rates and also differences between the BFS of materials at each deformation rate following the four storage regimes. Flexural modulus data was assessed by one-way ANOVA and post-hoc Tukey tests, to identify the differences between flexural modulus of each material at the four storage regimes and also to highlight the differences between materials.

4.3 Results

4.3.1 Bi-axial flexure strength

A two-way ANOVA highlighted that mean BFS was significantly influenced by material type ($P<0.001$) and deformation rate ($P\leq0.010$) following all storage regimes and a significant factorial interaction was identified ($P\leq0.011$) between deformation rate and storage. A one-way ANOVA revealed significant difference between the mean BFS of all RBC materials at different deformation rates ($P\leq 0.047$) except for Z100 following one week 'dry' ($P=0.083$) and 52 weeks 'wet' ($P=0.299$) and for Z250 following 1 week 'dry' ($P=0.380$) storage regimes respectively (Figure 4.1; Table 4.2). Further one-way ANOVA revealed significant differences between the mean BFS of materials at each deformation rate ($P\leq0.016$) except at 1.0 mm/min following 'dry' storage ($P=0.073$), 0.01 mm/min following 1 week 'wet' ($P=0.438$) and 52 weeks 'wet' ($P=0.062$) storage regimes (Figure 4.1; Table 4.2).

4.3.2 Flexural modulus

The flexural moduli of all materials following the 'dry' storage regime was significantly higher when compared with all three 'wet' storage regimes ($P<0.001$), whereas no significant difference between the flexural moduli following 'wet' storage was observed in all materials ($P>0.001$) (Table 4.3). Following 'dry' storage, Z100 and Z250 revealed no significant difference between moduli ($P>0.001$), however, both materials exhibited a significantly higher modulus when compared with FSB and FST ($P<0.001$) (Table 4.3). During all 'wet' storage regimes, FSB and FST showed lower flexural modulus in contrast to Z100 and Z250 and a significant difference was observed between the moduli of Z100 and Z250 ($P<0.001$) (Table 4.3). FSB and FST

revealed no significance difference in modulus when tested after storage at all storage regimes ($P>0.001$) (Table 4.3).

Table 4.2. The mean BFS (MPa) and associated standard deviations of Z100, Z250, FSB and FST determined at 0.01, 0.1, 1.0 and 10.0 mm/min deformation rates following 1 week dry and 1 week wet storage regimes.

1 week dry

	Deformation rate (0.01 mm/min)	Deformation rate (0.1 mm/min)	Deformation rate (1.0 mm/min)	Deformation rate (10.0 mm/min)	One-way ANOVA
Z100	150(25)^{1ab}	161(23)^{1ab}	163(25)^{1a}	151(27)^{1b}	P=0.083
Z250	162(23)^{1a}	169(26)^{1a}	174(30)^{1a}	169(26)^{1ab}	P=0.380
FSB	136(18)^{2b}	150(18)^{2b}	158(23)^{1a}	160(25)^{1ab}	P=0.001
FST	163(16)^{12a}	154(25)^{2ab}	161(23)^{12a}	171(29)^{1a}	P=0.047
One-way ANOVA	P=0.001	P=0.009	P=0.073	P=0.016	

1 week wet

	Deformation rate (0.01 mm/min)	Deformation rate (0.1 mm/min)	Deformation rate (1.0 mm/min)	Deformation rate (10.0 mm/min)	One-way ANOVA
Z100	88(18)^{2a}	132(21)^{1a}	135(20)^{1a}	138(24)^{1a}	P=0.001
Z250	95(17)^{3a}	133(26)^{2a}	137(21)^{2a}	155(25)^{1a}	P=0.001
FSB	88(24)^{2a}	102(19)^{2b}	117(22)^{1b}	118(17)^{1b}	P=0.001
FST	94(23)^{2a}	126(17)^{1a}	142(27)^{1a}	141(32)^{1a}	P=0.001
One-way ANOVA	P=0.438	P=0.001	P=0.001	P=0.001	

P-value less than 0.05 at the end of each row and column indicate statistically significant difference. In addition, superscript notation with similar numbers across rows and similar letters down columns indicate no statistically significant difference (P>0.05).

Table 4.2 (continued). The mean BFS (MPa) and associated standard deviations of Z100, Z250, FSB and FST determined at 0.01, 0.1, 1.0 and 10.0 mm/min deformation rates following 13 weeks wet and 52 weeks wet storage regimes.

13 weeks wet

	Deformation rate (0.01 mm/min)	Deformation rate (0.1 mm/min)	Deformation rate (1.0 mm/min)	Deformation rate (10.0 mm/min)	One-way ANOVA
Z100	114(17)^{2a}	134(24)^{1a}	125(20)^{12b}	134(25)^{1ab}	P=0.001
Z250	114(17)^{3a}	135(14)^{2a}	150(23)^{1a}	149(25)^{1a}	P=0.001
FSB	96(12)^{2b}	115(11)^{1b}	117(16)^{1b}	122(15)^{1b}	P=0.001
FST	114(18)^{23a}	111(18)^{3b}	128(21)^{12b}	142(27)^{1a}	P=0.001
One-way ANOVA	P=0.001	P=0.001	P=0.001	P=0.001	

52 weeks wet

	Deformation rate (0.01 mm/min)	Deformation rate (0.1 mm/min)	Deformation rate (1.0 mm/min)	Deformation rate (10.0 mm/min)	One-way ANOVA
Z100	102(21)^{1a}	110(20)^{1b}	103(22)^{1b}	99(23)^{1b}	P=0.299
Z250	105(17)^{2a}	133(23)^{1a}	112(21)^{2b}	114(22)^{2a}	P=0.001
FSB	94(15)^{2a}	98(15)^{2b}	103(16)^{2b}	114(17)^{1a}	P=0.001
FST	101(12)^{2a}	110(21)^{2b}	133(19)^{1a}	127(22)^{1a}	P=0.001
One-way ANOVA	P=0.062	P=0.001	P=0.001	P=0.001	

P-value less than 0.05 at the end of each row and column indicate statistically significant difference. In addition, superscript notation with similar numbers across rows and similar letters down columns indicate no statistically significant difference (P>0.05).

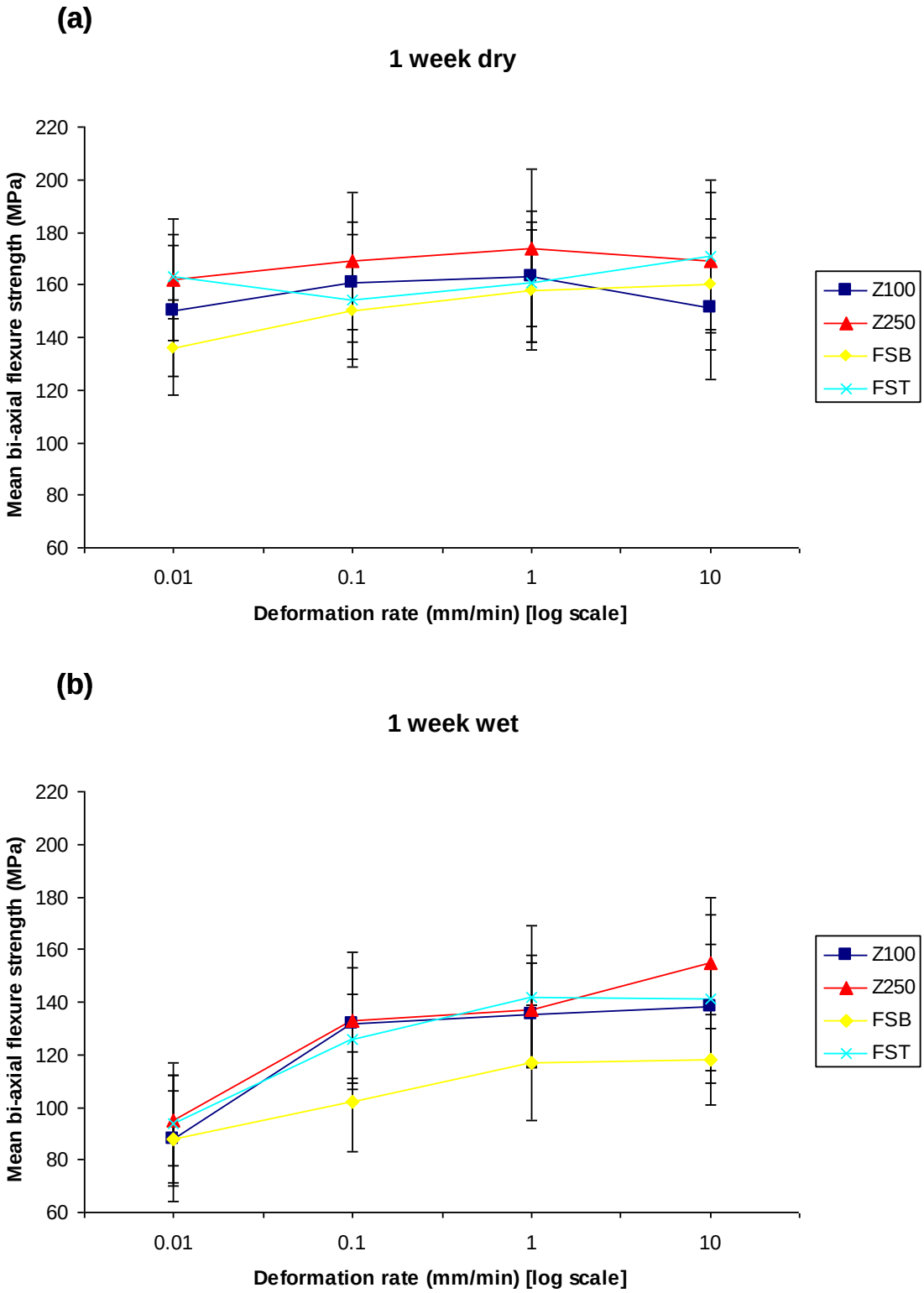

Figure 4.1. Plots illustrating the mean bi-axial flexure strength (and associated standard deviations) of Z100, Z250, FSB and FST determined at 0.01, 0.1, 1.0 and 10.0 mm/min deformation rates following (a) 1 week dry and (b) 1 week wet storage regimes.

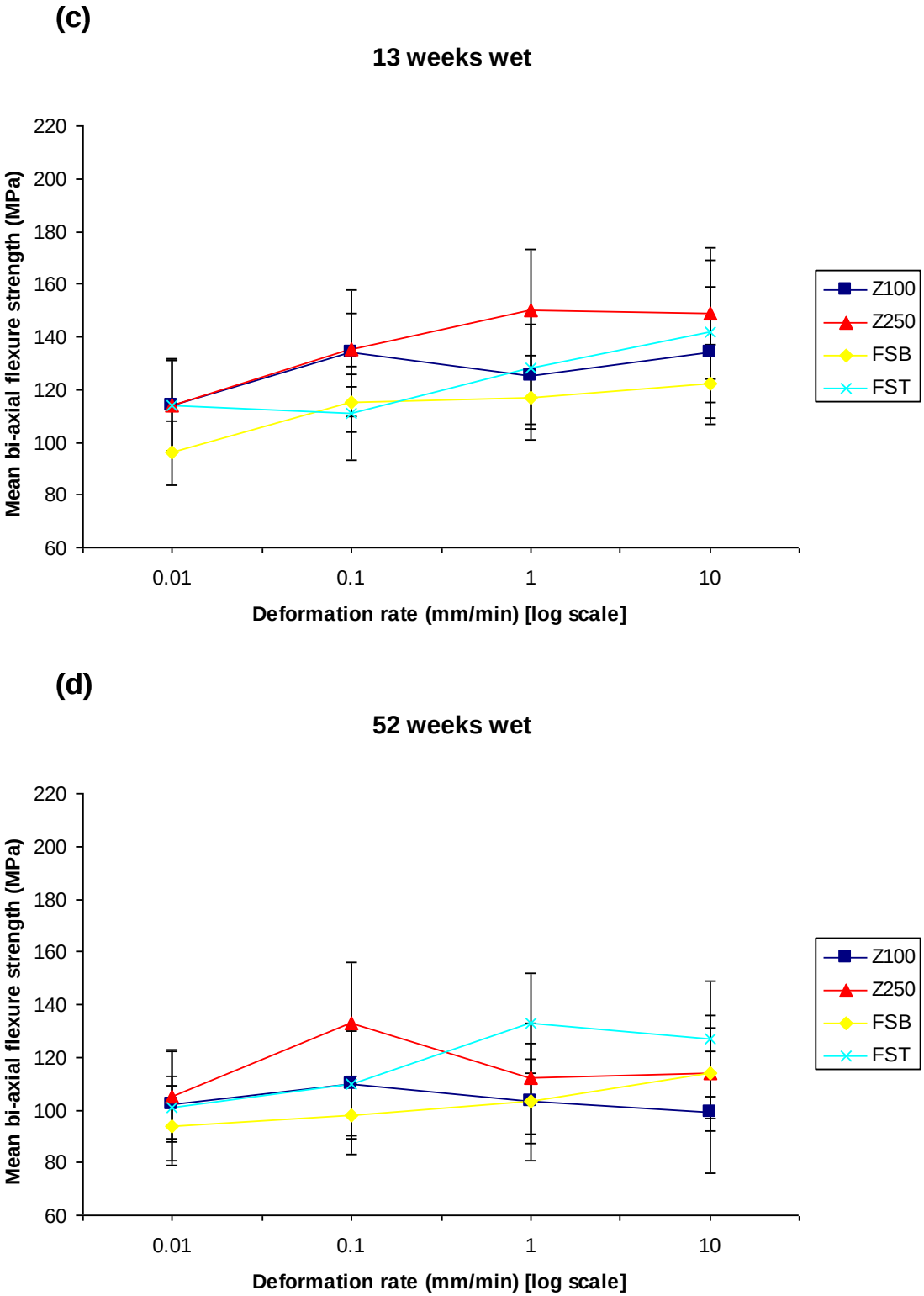

Figure 4.1 (continued). Plots illustrating the mean bi-axial flexure strength (and associated standard deviations) of Z100, Z250, FSB and FST determined at 0.01, 0.1, 1.0 and 10.0 mm/min deformation rates and following (a) 13 weeks wet and (b) 52 weeks wet storage regimes.

Table 4.3. The mean flexural modulus (GPa) and associated standard deviations of Z100, Z250, FSB and FST following 1 week dry, 1 week wet, 13 weeks wet and 52 weeks wet storage regimes. All specimens tested at a deformation rate of 1.0 mm/min.

	Z100	Z250	FSB	FST
Mean flexural modulus(GPa) 1 week dry	18.3(1.2)^{1a}	16.7(0.8)^{1a}	13.7(0.6)^{2a}	12.7(2.3)^{2a}
Mean flexural modulus(GPa) 1 week wet	15.7(0.8)^{1b}	13.3(1.4)^{2b}	11.0(2.1)^{3b}	10.4(1.0)^{3b}
Mean flexural modulus(GPa) 13 weeks wet	15.5(1.0)^{1b}	14.0(0.7)^{2b}	10.5(0.7)^{3b}	10.7(0.5)^{3b}
Mean flexural modulus(GPa) 52 weeks wet	16.2(1.0)^{1b}	13.2(0.9)^{2b}	11.5(0.9)^{3b}	10.5(0.7)^{3b}

Superscript with similar numbers across rows and similar letters down columns indicate no statistically significant difference (P>0.05).

4.4 Discussion

The findings of the current study highlight the variation observed in the BFS of all RBCs tested, as a function of both the deformation rate and storage regime. Only when Z100 and Z250 specimens were stored dry for 1 week or when Z100 specimens were stored wet for 52 weeks were no differences between the BFS determined at different deformation rates observed (Table 4.2). The general changes in BFS with deformation rate and particularly the increase in BFS at high deformation rates in all four materials suggests the importance of the polymer prior to catastrophic specimen fracture. At higher deformation rates there will be reduced time for materials to flow in viscous manner, which subsequently lowers the extent to which stress relief can occur and thereby leads to an increase in the measured BFS values (Musanje and Darvell, 2004).

The pattern of the BFS sensitivity to deformation rate, between RBCs also varied widely (Figure 4.1; Table 4.2) and has the potential to significantly influence the interpretation of BFS data. There was no significant difference between BFS of all

four RBCs at 1.0 mm/min deformation rate following 1 week ‘dry’ storage of specimens, whereas, materials exhibited significant differences for the remainder of deformation rates to differing extents (Table 4.2). Following 52 weeks ‘wet’ storage, the BFS of all materials was statistically comparable at a 0.01 mm/min deformation rate whereas significant differences were identified at all other deformation rates (Table 4.2). Consequently, it can be argued that ranking of materials on the basis of mechanical properties by researchers (Sabbagh et al., 2002; Ilie and Hickel, 2009) and industrial manufacturers, who tested materials at single deformation rate, would be different if alternative load rate parameters were employed. In simple terms, if two researchers evaluate the mechanical properties of identical materials and test specimens but at different deformation rates, their findings and associated interpretations may be completely different. Therefore, a significant effect on the future research and development of RBCs may be expected. However, this matter has rarely been addressed by the dental materials research community.

In current study, three RBCs, namely Z250, FSB and FST comprised of identical resin matrices, but different filler sizes and distributions, whereas as two RBCs, Z100 and Z250 comprised of comparable filler sizes and distributions with distinct resin matrices. Consequently, it may be expected that the influence of the filler and resin could be explored. However, in the current investigation, the sensitivity of the recorded BFS to deformation rate was extremely complex for these commercial materials with no obvious relationships to reported constituents and microstructures observed. To elucidate mechanistic pathways it was identified that the examination of model ‘experimental’ RBC systems was required and is reported in Chapter 5. The wide variation in BFS between materials can be explained by the assumption that the overall structure of the RBC varies significantly from one RBC to

another RBC as a result of different constituents, which may thus modify the susceptibility of each material towards environment and lead to differences in degradation mechanisms of RBCs. Various chemically and mechanistically-induced failure mechanisms of RBCs have been reported in previous studies and rate of those mechanisms is based on the type of monomer (Asmussen et al., 1998), degree of monomer conversion (Asmussen and Peutzfeldt , 2002, 2003), filler morphology (Bagheri et al., 2007), and silanisation of filler/resin interface (Söderholm , 1983; Söderholm et al., 1984). Several studies have compared the nanofilled and microhybrid RBCs. However, controversial data is available in terms of their mechanical properties. Most studies reveal similarities between nanohybrid and microhybrid RBCs which may be due to similar filler morphologies and volume fraction (Beun et al., 2007; Rodrigues Junior et al., 2008). Whereas some researchers have reported superior (Curtis et al., 2009) or inferior (Shah et al., 2009ab) properties of nanofilled RBCs compared with microhybrid RBCs. These differences in results may be explained, in-part, by the different testing methods employed between investigators. In the majority of studies, commercial nanofilled RBCs have been investigated, therefore, the effect of confounding variables such as resin and photo-initiator chemistry on the material properties may be expected during comparison of materials. Hence, determination of experimental nanohybrid or nanofilled RBCs with controlled variables is essential to understand novel aspects of future nanocomposite technology.

A previous study determined the BFS of Z250, FSB and FST at the cross-head speed of 1.0 mm/min following different storage regimes and the investigators employed a similar specimen size, light curing unit and storage medium used in current study (Curtis et al., 2008). However, the authors identified greater strength

degradation following 52 weeks immersion in water compared with ‘dry’ storage, (Z250, FSB, FST; 47%, 65%, 49%) in contrast to current study (Z250, FSB, FST; 36%, 35%, 17%) respectively at the cross-head speed of 1.0 mm/min. The significant differences in strength degradation of RBCs between the two studies may be attributed to the difference in specimen alignment during storage. In previous study, the specimens were held on their diametral axis (Curtis, 2008) therefore water may greatly diffuse through the specimen cross-section compared with the stacked alignment utilized in the current study. Consequently, the effect of the specimen alignment on BFS of RBCs warrants further study and is explored and reported in Chapter 6.

The flexural modulus of all RBCs was determined following four corresponding storage regimes at 1.0 mm/min deformation rate to identify whether it has any effect on the BFS results. A significantly greater flexural modulus of Z100 and Z250 ‘dry’ specimens was identified in contrast to FSB and FST (Table 4.3) which may explain the 1 week ‘dry’ BFS results, since no significant difference between BFS of Z100 and Z250 was revealed across the range of deformation rates compared with FSB and FST. Due to a relative high brittleness, there may be less capacity for stress relief in the region of the critical defect even at low deformation rates which consequently led to an increase in the BFS values. In contrast, all RBCs exhibited no significant difference between flexural modulus at all ‘wet’ storage regimes (Table 4.3), while significant differences were found between BFS of all materials except 52 weeks ‘wet’ Z100 at different deformation strain rates following corresponding storage regimes (Table 4.2). This suggests that there was little correlation between the elastic response and BFS results.

A significant reduction in the flexural modulus of all RBCs following 'wet' storage regimes compared with 'dry' specimens was identified (Table 4.3). The deterioration of tensile strength (Soderholm and Roberts, 1990), flexural strength (Curtis et al., 2008; Calais and Soderholm, 1988) flexural modulus, fracture toughness and hardness (Ferracane et al., 1998) have been frequently attributed to water-related degradation of the resin matrix (Ferracane, 2006), resin/filler interface (Söderholm , 1983; Söderholm et al., 1984) and filler particle surface (Söderholm, 1981). The degradation of mechanical properties of RBCs after immersion in various storage media have been explained by two mechanisms. Firstly, water sorption causes a softening and swelling of the polymer resin component and subsequently reduces the frictional forces between polymer chains (Ferracane et al., 1998) and leads to monomer leaching (Bastioli et al., 1990; Santerre et al., 2001). Secondly, mechanical properties of RBC may be compromised by failure of bond between resins and fillers (Söderholm et al., 1984; Söderholm and Roberts, 1990). However, the lack of significant difference between flexural modulus of each material following three wet storage regimes (Table 4.3) implies equilibration of the polymer network (Ferracane et al., 1998). Moreover, Ferracane et al. (1998) proposed that there was less effect of water on the flexural modulus of RBCs over prolonged storage periods which may suggest that filler content/filler integration has a significant role while factors affecting the polymer matrix may have less significance in determining flexural modulus. Z100 exhibited the highest flexural modulus compared with all materials (Table 4.3) which is likely to be as a consequence of the presence of a greater quantity of TEGDMA and a related increased conversion of carbon double bonds (Asmusssen and Peutzfeldt, 1998). Z250, FSB, FST possessed identical resin chemistries, however, both FSB and FST highlighted a lower flexural modulus in contrast to Z250

(Table 4.3) which may be acknowledged to reduced filler mass fraction in both nanofilled RBCs compared with Z250. In previous studies, a correlation between weight percentage of fillers and elastic modulus has been reported (Sabbagh et al., 2002; Beun et al., 2007; Rodrigues Junior et al., 2008). Rodrigues Junior et al. (2008) compared the elastic modulus of a microhybrid with a nanofilled RBC and identified a significantly greater elastic modulus of the microhybrid. Authors have explained this finding with increased weight percentage of fillers in microhybrid RBC in contrast to nanofilled RBC.

It is clear that all RBCs are deformation rate dependent but to different extents and that the pattern of dependence is a function of additional variables including storage parameters. Thus, determination of experimental RBCs with controlled variables is essential to get further insight into the behaviour of materials and is reported in chapter 5.

4.5 Conclusions

1. All RBCs exhibited differences in BFS as a function of deformation rate.
2. Generally, the pattern of BFS between RBCs also varied with respect to deformation rate (Figure 4.1; Table 4.2) which has the potential to significantly impact on the interpretation of the BFS data.
3. No correlation between elastic response and the BFS data of all RBCs was found.

References

Asmussen E, Peutzfeldt A. Influence of UEDMA, BisGMA and TEGDMA on selected mechanical properties of experimental resin composites. Dental Materials, 1998; 14: 51-56.

Asmussen E, Peutzfeldt A. Influence of composition on rate of polymerisation contraction of light-curing resin composites. Acta Odontologica Scandinavica, 2002; 60: 146-150.

Asmussen E, Peutzfeldt A. Two-step curing: influence on conversion and softening of a dental polymer. Dental Materials, 2003; 19: 466-470.

Bagheri R, Tyas MJ, Burrow MF. Subsurface degradation of resin-based composites. Dental Materials, 2007; 23: 944-951.

Bastioli C, Romano G, Migliaresi C. Water sorption and mechanical properties of dental composites. Biomaterials, 1990; 11: 219-223.

Beun S, Glorieux T, Devaux J, Vreven J, Leloup G. Characterization of nanofilled compared to universal and microfilled composites. Dental Materials, 2007; 23: 51-59.

Burke FJT. Amalgam to tooth-coloured materials-implications for clinical practice and dental education: governmental restrictions and amalgam-usage survey results. Journal of Dentistry, 2004; 32:343-350.

Calais JG, Söderholm KJM. Influence of filler type and water exposure on flexural strength of experimental composite resin. Journal of Dental Research, 1988; 67:836-840.

Chin G, Chong J, Kluczewska A, Lau A, Gorjy S, Tennant M. The environmental effects of dental amalgam. Australian Dental Journal, 2000; 45:246-249.

Curtis AR. The influence of ‘nanocluster’ reinforcement on the mechanical properties of a resin-based composite material. PhD Thesis, University of Birmingham, 2008; Page.76

Curtis AR, Shortall AC, Marquis PM, Palin WM. Water uptake and strength charactersistics of nanofilled resin-based composites. Journal of Dentistry, 2008; 36:186-193.

Curtis AR, Palin WM, Fleming GJP, Shortall ACC, Marquis PM. The mechanical properties of nanofilled rein-based composites: The impact of dry and wet cyclic pre-loading on bi-axial flexure strength. Dental Materials, 2009; 25:188-197.

Davidson CL, Feilzer AJ. Polymerisation shrinkage and polymerisation shrinkage stress in polymer-based restoratives. Journal of Dentistry, 1997; 25:435-440.

Drummond JL. Degradation, fatigue, and failure of resin dental composite materials. Journal of Dental Research, 2008; 87: 710-719.

Ferracane JL, Antonio RC, Matsumoto H. Varibales affecting the fracture toughness of dental composites. Journal of Dental Research, 1987; 66:1140-1145.

Ferracane JL, Berge HX, Condon JR. In vitro aging of dental composites in water-Effect of degree of conversion, filler volume, and filler/matrix coupling. Journal of Biomedical Material Research, 1998; 42: 465-472.

Ferracane JL. Hygroscopic and hydrolytic effects in dental polymer networks. Dental Materials, 2006; 22: 211-222.

Glaros AG, Rao SM. Effects of bruxism: A review of the literature. Journal of Prosthetic Dentistry, 1977; 38: 149-157.

Hörsted-Bindslev P. Amalgam toxicity-environmental and occupational hazards. Journal of Dentistry, 2004; 32:359-365.

Ilie N, Hickel R. Investigations on mechanical behaviour of dental composites. Clinical Oral Investigations, 2009; 13: 427-438.

International Standards Organisation. Dentistry – Polymer-based filling, restorative and luting materials. ISO 4049, 2000; (3rd Edition): 15-17.

Kim KH, Park JH, Imai Y, Kishi T. Microfracture mechanisms of dental resin composites containing spherically-shaped filler particles. Journal of Dental Research, 1994; 73: 499-504.

Kleverlaan CJ, Feilzer AJ. Polymerisation shrinkage and contraction stress of dental resin composites. Dental Materials, 2005; 21:1150-1157.

Koolstra JH. Dynamics of the human masticatory system. Critical Reviews in Oral Biology & Medicine, 2002; 13: 366-376.

Leinfelder KF. A conservative approach to placing posterior composite resin restorations. Journal of American Dental Association, 1996; 127:743-748.

Martin N, Jedynakiewicz NM, Fisher AC. Hygroscopic expansion and solubility of composite restoratives. Dental Materials, 2003; 19: 77-86.

Musnaje L, Darvell BW. Effects of strain rate and temperature on the mechanical properties of resin composites. Dental Materials, 2004; 20: 750-765.

Rodrigues Junior SA, Scherrer SS, Ferracane JL, Bona AV. Microstructural characterisation and fracture behaviour of a microhybrid and a nanofill composite. Dental Materials, 2008; 24:1281-1288.

Ruyter IE, Øysæd H. Compressive creep of light cured resin based restorative materials. Acta Odontologica Scandinavica, 1982; 40: 319-324.

Sabbagh J, Vreven J, Leloup G. Dynamic and static moduli of elasticity of resin-based materials. Dental Materials, 2002; 18: 64-71.

Santerre JP, Shajii L, Leung BW. Relation of dental composite formulation to their degradation and the release of hydrolyzed polymeric-resin-derived products. Critical Reviews in Oral Biology and Medicine. 2001; 12: 136-151.

Shah MB, Ferracane JL, Kruzic JJ. Mechanistic aspects of fatigue crack growth behaviour in resin based dental restorative composites. Dental Materials, 2009a; 25: 909-916.

Shah MB, Ferracane JL, Kruzic JJ. R-curve behaviour and toughening mechanism of resin-based dental composites: Effects of hydration and post-cure heat treatment. Dental Materials, 2009b; 25:760-770.

Shawkat ES, Shortall AC, Addison O, Palin WM. Oxygen inhibition and incremental layer bond strengths of resin composites. Dental Materials, 2009; 25: 1338-1346.

Söderholm KJM. Degradation of glass filler in experimental composites. Journal of Dental Research, 1981; 60: 1867-1875.

Söderholm KJM. Leaking of fillers in dental composites. Journal of Dental Research, 1983; 62: 126-130.

Söderholm KJM, Zigan M, Ragan M, Fischlschweiger W, Bergman M. Hydrolytic degradation of dental composites. Journal of Dental Research, 1984, 63:1248-1254.

Söderholm KJM, Roberts MJ. Influence of water exposure on the tensile strength of dental composites. Journal of Dental Research, 1990; 69:1812-1816.

Timoshenko S, Woinowsky-Krieger S. Symmetrical bending of circular plates. In: Theory of Plates and Shells. McGraw-Hill; New York, 1959; (2nd Edition).

Uchida H, Vaidyanathan J, Viswandhan T, Vaidyanathan TK. Colour stability of dental composites as a function of shade. Journal of Prosthetic Dentistry, 1998; 79: 372-377.

Yamashita S, Hatch JP, Rugh JD. Does chewing performance depend upon a specific masticatory pattern? Journal of Oral Rehabilitation, 1999; 26: 547-553.

Chapter 5 Mechanical Properties of Experimental Resins and Resin-Based Composites as a Function of Deformation Rate

5.1 Effect of filler addition on the bi-axial flexural strength and deformation rate dependence of resins

5.1.1 Introduction

It is well known that mechanical properties of polymer-based materials are sensitive to deformation rate applied during testing (Jacob et al., 2004; Chen and Cheng, 2002). However, this area of research has rarely been addressed in the resin-based dental composites research despite the fact that masticatory forces occur at varying magnitude and rate. In the previous experiment, bi-axial flexural strength (BFS) of four commercial resin-based composites (RBCs) was determined at a wide range of deformation rates following different immersion periods and the effect of both variables was identified (Chapter 4). However, the sensitivity of recorded BFS to deformation rate was complex and no obvious effect of resin or filler constituents was observed. Such complex effects on the final mechanical properties were attributed, in part, to the variation in commercial RBC formulations. Consequently, a systematic investigation of experimental RBCs with controlled variables was proposed in order to understand the influence of material constituents on the BFS with regard to deformation rate and storage time. In the current chapter, BFS of the experimental dimethacrylate-based unfilled resins and filled RBCs with controlled formulation was evaluated with respect to deformation rate and storage time. The selection of the experimental unfilled resins for the current experiment was justified as a variety of RBCs with different resin content are used for numerous applications and a variation in viscoelastic response or creep strain has been reported (Vaidyanathan and Vaidyanathan, 2001; Baroudi et al., 2007). Polymeric materials will have significant effect on the viscoelastic behaviour of RBCs (Cock and Watts, 1985). Therefore, it is

important to understand the behaviour of relevant unfilled co-monomer mixtures at varying deformation rates, which may aid a further understanding of failure mechanisms of RBCs. Therefore, the aim of the current experiment was to evaluate the BFS of experimental unfilled resins and associated RBCs at varying deformation rates.

5.1.2 Experimental procedure

5.1.2.1 Resin formulation

A light-curable experimental resin formulation of bisphenol A diglycidyl ether dimethacrylate (BisGMA) and triethyleneglycol dimethacrylate (TEGDMA) at 60:40 ratio by mass was prepared. The photoinitiator system comprised of camphoroquinone (CQ) (0.2 mass%) and dimethylaminoethyl methacrylate (DMAEMA) (0.3 mass%) and butylated hydroxytoluene (BHT) (0.1 mass%) was employed as an inhibitor (Sigma Aldrich, Gillangham, UK). The resins, CQ, DMAEMA and BHT were weighed using a Mettler AE 163 analytical balance (Mettler-Toledo Ltd, Leicester, UK) accurate to 0.0001 g and transferred to a beaker (150 ml). The beaker was wrapped with silver foil in order to protect the resins from blue light and placed onto a hot plate (Fisher Scientific LTD, Loughborough, UK) at 70 ºC and constituents were mixed using a magnetic stirrer at a speed of 350 rpm until a homogenous mix was achieved.

5.1.2.2 Selection of the mixing technique for model RBCs

Initially, in a preliminary experiment (Appendix), two batches of experimental RBCs, either hand-spatulated and mechanically-mixed, were prepared and investigated. The hand-spatulated RBCs exhibited greater porosity, a lower mean BFS

and reduced reliability of strength data compared with mechanically-mixed RBCs. Consequently, in the current study, RBCs were prepared using reproducible mechanical mixing technique.

5.1.2.3 Experimental resin composite preparation

The resins, (45 volume%) were mixed with 46 volume% of silanised barium silicate glass particles with an average particle size of 0.7 μm (Schott AG, Hattenbergstrasse, Germany) and 9 volume% of silanised fumed silica particles, approximately 14 nm diameter (Aerosil R 711, Evonik Industries, Germany). A centrifugal mixing device (Speed-Mixer, DAC 150 FVZ-K, Hauschild Engineering, Germany) was used to mechanically incorporate the filler. Resins were mixed with fumed silica at the speed of 2300 rpm and 3500 rpm each for 1 min and this regime was repeated following subsequent addition of the barium silicate filler particles into the composite mix.

5.1.2.4 Specimen preparation

Two hundred and seventy nominally identical disc-shaped specimens (12mm diameter, 1mm thickness) of either unfilled resins or experimental RBC comprising of three groups (n=90) were fabricated. Split black nylon moulds were used to allow specimen removal without introducing spurious bending stresses. For each specimen mould was overfilled with composite paste and the top and bottom surfaces of each specimen were covered with cellulose acetate strip (0.1 mm thickness) to lessen oxygen inhibition. All specimens were light irradiated from one side by a quartz-tungsten-halogen curing unit (Optilux 501, Kerr, Orange, CA, USA) with a 12 mm diameter curing tip placed in contact with acetate strip using a light guide to allow for

concentric alignment. The irradiance of the curing-unit was measured prior to fabrication of each sample set (780-880 mW/cm^2) using a radiometer (Coltolux C-7900 Coltene/Whaledent Inc, Mahwah, NJ, US). Following irradiation for 40 s at an ambient temperature of 23±2 ºC, the cellulose acetate strips were discarded, each specimen immediately removed from the mould and flash cut away using a sharp blade. Prior to testing, three groups of each unfilled resin and RBC (n=90) were stored for one week 'dry', one and thirteen weeks 'wet' at 37±1 ºC in a polystyrene cylindrical 30 ml container. To allow wet storage of specimens, distilled water was employed throughout the study. Each group was aligned so that specimens were stacked directly on top of each other. To avoid the potential accumulation of leached unfilled resins and RBC constituents in the container, distilled water was replaced on a weekly basis for the longest storage regime.

5.1.2.5 Bi-axial flexure strength

The bi-axial flexure strength (BFS) of each unfilled resins and RBC group was determined at 0.1, 1.0 and 10.0 mm/min deformation rates (n=30) in a ball-on-ring configuration using a universal testing machine (Model 5544, Instron Ltd, High Wycombe, Bucks, England). A 3 mm ball-indenter was used to centrally load the disc-shaped specimens supported on a 10 mm diameter knife-edge support. The irradiated surface of specimen was placed uppermost, with the non-irradiated surface under tension. The load (N) at failure was recorded and the mean specimen thickness was measured at the point of fracture of each fragment with a screw-gauge micrometer (Moore and Wright, Sheffield, UK) accurate to 10 µm. The BFS (MPa) was calculated according to Equation 5.1 (Timoshenko and Woinowsky-Krieger, 1959).

$$\sigma_{max} = \frac{p}{h^2}\{(1+\nu)[0.485 \times \ln\left(\frac{a}{h}\right) + 0.52] + 0.48\} \qquad \text{Equation 5.1}$$

Where σ_{max} was the maximum tensile stress (MPa), P the measured load of fracture (N), a the radius of knife-edge support (mm), h the sample thickness (mm) and ν Poisson's ratio for the material and a value of 0.25 was substituted for unfilled resins and RBCs investigated in current experiment (Braem et al., 1986). The data were analysed with one-way analysis of variance (ANOVA) and post hoc Tukey tests (P=0.05).

5.1.3 Results

A dependence of deformation rate was observed for unfilled resins since one-way ANOVA of the BFS data revealed significantly lower mean BFS at 0.1 mm/min deformation rate compared with 1.0 and 10.0 mm/min following all storage regimes (Table 5.1, Figure 5.1). However, for filled resins, no significant difference between BFS at all deformation rates was identified following one week 'dry' and 13 weeks 'wet' storage regimes. BFS was significantly decreased at 0.1 mm/min deformation rate compared with 1.0 and 10.0 mm/min for one week 'wet' specimens (Figure 5.1, Table 5.1).

The one week 'wet' unfilled resin specimens exhibited an apparent reduction in BFS compared with 'dry' specimens but no significant difference was identified between one week 'dry' and 'wet' specimens. BFS of unfilled resin was substantially reduced following 13 weeks compared with one week 'dry' and 'wet' storage regimes (Table 5.1). The BFS of filled resins was significantly reduced following one and 13 weeks 'wet' storage compared with 'dry' specimens whereas no significant difference

between BFS of one and 13 weeks 'wet' specimens was identified at 1.0 and 10.0 mm/min deformation rates.

Table 5.1. The mean BFS and associated standard deviations of experimental (a) unfilled resins and (b) resin-based composite at 0.1, 1.0 and 10.0 mm/min deformation rates following 1 week dry, 1 week and 13 weeks wet storage regimes.

(a)

	Deformation rate 0.1 mm/min	**Deformation rate 1.0 mm/min**	**Deformation rate 10.0 mm/min**
1 week dry	126(31)^{2a}	148(34)^{1a}	163(39)^{1a}
1 week wet	117(32)^{2a}	142(37)^{1a}	152(29)^{1a}
13 weeks wet	67(17)^{2b}	84(24)^{1b}	91(26)^{1b}

(b)

	Deformation rate 0.1 mm/min	**Deformation rate 1.0 mm/min**	**Deformation rate 10.0 mm/min**
1 week dry	122(13)^{1a}	131(15)^{1a}	131(16)^{1a}
1 week wet	82(17)^{2c}	95(13)^{1b}	98(21)^{1b}
13 weeks wet	97(17)^{1b}	100(18)^{1b}	106(18)^{1b}

Superscript with similar numbers across rows and similar letters down columns indicate no statistically significant difference ($P>0.05$).

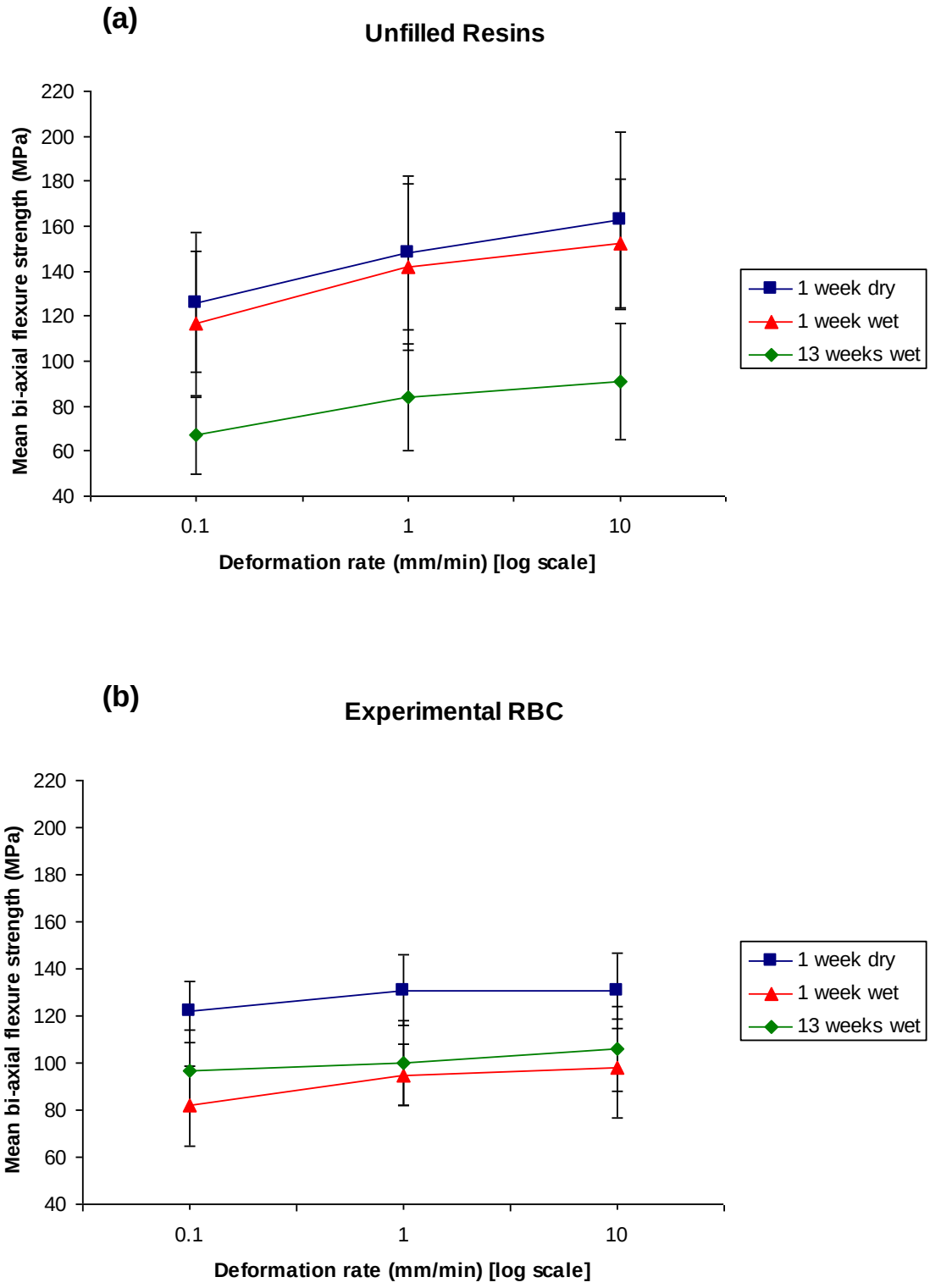

Figure 5.1. Plots illustrating the mean bi-axial flexure strength (and associated standard deviations) of experimental (a) unfilled resins (b) resin-based composite at 0.1, 1.0, 10.0 mm/min deformation rates [log scale] following 1 week dry, 1 week and 13 weeks wet storage regimes.

5.1.4 Discussion

Following one week ‘dry’ and ‘wet’ storage regimes, the unfilled resin exhibited a significantly greater mean BFS compared with the experimental RBC, which was unexpected. There is a common concept of load sharing between resin matrix and fillers, which suggests that the stronger and stiffer fillers are likely to bear a greater load compared with ufilled resin matrices. In addition, many researches have suggested that the incorporation of fillers into RBCs will increase compressive (Li et al., 1985; Germain et al., 1985), diametral tensile (Chung, 1990) and flexural strength (Braem et al., 1989). However, contrary to this common conception, Calais and Söderholm (1988) and O’Donnell et al. (2008) have reported a higher flexural strength of light-cured dimethacrylate-based resins relative to resin composites, which is in agreement with current study. The possible explanation could be poor bonding between resins and fillers as a result of insufficient silane or porosity due to incapability of mixing machine to mix the constituents efficiently. Thus, unbounded interface or porosity in RBCs may act as crack in terms of Griffith’s law and therefore accelerate the crack propagation and reduce the strength of materials. Other possible explanation could be the uneven distribution of filler particles, especially the fumed silica nanoparticles, which tend to agglomerate. The agglomerated particles possess high internal porosity compared with a discrete solid filler and are likely to create regions of stress concentration. Consequently, such regions require less energy to initiate or propagate a crack and lead to failure at low stresses (Huang and Zhang, 2009). In addition, agglomerated particles may create a weak resin/filler interface and lead to insufficient load transfer between matrix and particles (Jumahat et al., 2010), thereby resulting in decreased BFS. Moreover, it may be assumed that fillers in RBC may scatter the light and decrease the degree of cure compared with unfilled resins,

hence reducing the BFS. The aforementioned explanations with regard to silane, mixing device and degree of cure warrant further study, which may give further insight in to the strength property of RBCs. Although a superior BFS of unfilled resins observed here may imply a superior material system, it should be noted that the incorporation of filler particles in resin matrices improves the wear resistance, decreases thermal expansion coefficient and reduces polymerisation shrinkage of RBCs which are essential for longevity of a dental restoration.

Both unfilled resins and RBCs exhibited hydrolytic degradation but to different extents. The water-induced failure of RBCs involves the degradation of resin matrix, silane coupling agent, and filler particles and depends upon on the type of monomer (Asmussen et al., 1998), degree of monomer conversion (Asmussen and Peutzfeldt , 2002, 2003), filler morphology (bagheri et al., 2007), and silanisation of filler/resin interface (Söderholm, 1983; Söderholm et al., 1984). Thus, the degradation of RBCs can be considered as more complex compared with unfilled resins. The significant decrease in BFS of the RBC compared with the unfilled resin following one week storage in water can possibly be explained by two mechanisms. First, the degree of conversion in RBCs is likely to be lower than that of unfilled resins as a result of light scattering which may make the RBCs structure more susceptible to hydrolytic degradation. Second, the hydrolytic degradation of silane coupling agent may occur at resin/filler interface, which leads to interfacial cracking and thus reducing the BFS. The significant decrease in BFS of the experimental RBC following wet storage compared with the dry control is also in accordance with four commercial RBCs tested in the previous experiment (Chapter 4). No further degradation of RBC following 13 weeks compared with one week immersion is also in agreement with previous experiment (Chapter 4) and may be attributed to the

saturation of resin matrix and silane interface and associated reduction in degradation. However, a significant degradation of unfilled reins in contrast to the RBC following 13 weeks storage is likely to be the result of its greater water uptake and dissolution. Since RBCs were comprised of only 45 volume% polymer compared with unfilled resins, therefore lower resin-associated degradation compared with unfilled resins may be expected.

A decrease in BFS of unfilled resins at 0.1 mm/min deformation rate compared with 1.0 and 10.0 mm/min was identified. This suggests that at the low deformation rate, the specimen has sufficient time to deform plastically, as a result slow crack growth which can extend to a larger defect is likely to result in failure at lower stresses and causes the observed reduction in BFS. On the contrary, specimens that exhibit less plastic deformation as a consequence of the reduction in time under load at high deformation rates would fail at higher stresses (Musanje and Darvell, 2004). No deformation rate dependence of dry RBC specimens can be explained with a decreased viscous behaviour of RBCs as a result of load transfer from resins to brittle fillers and also the presence of a lower resin content, which reduces the plastic flow of RBCs at low deformation rate. The decrease in BFS, at lowest deformation rate, of one week wet RBC specimens may be ascribed to plasticisation of the polymer network as a result of water sorption. It is well known that water diffuses into the polymer network and separates the chains, which can then lead to swelling and softening of the polymer network (Ferracane et al., 1998). Therefore, at low deformation rate, the plasticised polymer network of the RBC may deform in viscous manner and cause a reduction in BFS. In the previous experiment (Chapter 4), two commercial nanofilled RBCs also exhibited a comparable pattern of BFS following one week wet storage as described above. However, following 13 weeks immersion

the BFS of commercial RBCs became independent of deformation rate, which may be attributed to the saturation of the polymer network and reduced plasticity, which may subsequently reduce the viscous deformation at 0.1 mm/min and increase strength properties.

This experiment highlights the influence of resin and filler constituents on the deformation rate dependence of RBCs. The incorporation of filler particles resulted in no significant difference between BFS of RBCs across the range of deformation rates following one week 'dry' and 13 weeks 'wet' storage, which suggest that RBCs can perform better at various masticatory rates. However, lower BFS of one week 'wet' RBCs specimens at 0.1 mm/min deformation rate is suggestive of the premature failure of RBC restorations in patients with parafucnctional habits, where restorations may be subjected to sustained forces (Ruyter and Øysæd, 1982) for extended periods at low deformation rates. Consequently, a further experiment is required to evaluate the effect of filler particle size and nanoparticle addition on deformation rate dependence, which may assist in designing RBCs with respect to various masticatory rates (Section 5.2).

5.1.5 Conclusions

1. The unfilled resins revealed a deformation rate dependence following all storage regimes, however, addition of fillers in unfilled resins modified such reliance following 1 week dry and 13 weeks wet storage regimes.
2. Although fillers are considered as strengthening phase of composites, however, in current study, incorporation of fillers in unfilled resins led to a significant decline in BFS following one week storage.

5.2 Effect of filler particle size and nanoparticle addition on deformation rate dependence of experimental RBCs

5.2.1 Introduction

The previous experiment in this Chapter (Section 5.1) demonstrated the effect of filler addition, storage time and deformation rate on the BFS of experimental unfilled resins and associated RBCs. The one week dry and 13 weeks wet RBC specimens exhibited no difference in BFS at varying deformation rates. However, a lower BFS of one week wet specimens was identified at 0.1 mm/min deformation rate compared with 1.0 and 10.0 mm/min deformation rates and this pattern was also found in two nanofilled RBCs investigated in a previous investigation (Chapter 4).

The filler size, filler morphology and filler size distribution of RBCs have been significantly modified since their development in order to improve the material properties. However, studies have mainly tested the mechanical properties of RBCs at a single deformation rate. Therefore, it is important to understand the influence of filler size and distribution on the BFS of RBCs at varying deformation rates, which may assist the development of improved materials for clinical situations where variable masticatory rates may occur. For example, in bruxism, RBC restorations may be subjected to sustained forces (Ruyter and Øysæd, 1982) for extended periods at low rates in contrast to the much more transient loading forces in normal mastication (Glaros and Rao, 1977). Thus, the aim of the current investigation was to highlight the effect of filler particle size and addition of nanoparticles on deformation rate dependence of BFS and flexural modulus of experimental RBCs and also highlight the influence of particle size and nanoparticle addition on BFS and flexural modulus at each deformation rate.

5.2.2 Experimental procedure

Nine experimental resin-based composites (RBC1-RBC9) with constant resin and filler volume ratio (45:55) were prepared by the method outlined in Section 5.1.2.3. A similar resin formulation was used for all RBCs as described in Section 5.1.2.1 However, RBCs were reinforced with varying filler particle size and nanoparticle content. The silanised barium glass filler particles of 0.7, 3.0 and 5.0 μm size were purchased from Schott AG, Hattenbergstrasse, Germany and fumed silica; Aerosil R 711, of approximately 14 nm size was provided by Evonik Industries, Germany. The summary of experimental RBCs is shown in Table 5.2.

Table 5.2. Constituents of the experimental resin-based composites. All RBCs were comprised of similar resin chemistries.

Experimental Resin Composites	Microfiller (diameter/load)	Nanofiller (diameter/load)
RBC1	0.7 µm; 55.0 vol%	14 nm; 0.0 vol%
RBC2	0.7 µm; 50.5 vol %	14 nm; 4.5 vol%
RBC3	0.7 µm; 46.0 vol %	14 nm; 9.0 vol%
RBC4	3.0 µm; 55.0 vol%	14 nm; 0.0 vol%
RBC5	3.0 µm; 50.5 vol %	14 nm; 4.5 vol%
RBC6	3.0 µm; 46.0 vol %	14 nm; 9.0 vol%
RBC7	5.0 µm; 55.0 vol%	14 nm; 0.0 vol%
RBC8	5.0 µm; 50.5 vol%	14 nm; 4.5 vol%
RBC9	5.0 µm; 46.0 vol %	14 nm; 9.0 vol%

5.2.2.1 Bi-axial flexure strength

In total, 810 specimens were prepared and for each RBC, 90 disc-shaped specimens were fabricated as described in section 5.1.2.4. All specimens were stored in distilled water at 37±1 ºC for one week prior to testing. The BFS of each RBC was determined at three deformation rates (0.1, 1.0, 10.0 mm/min) (n=30) using the method outlined in section 5.1.2.5.

5.2.2.2 Flexural modulus

Fifteen nominally identical bar-shaped specimens (25 mm length, 2 mm width and 2 mm thickness) of each RBC were made using nylon split mould. The mould was packed with RBC and both upper and lower surfaces were covered with cellulose acetate strips (0.1 mm thickness) to reduce oxygen inhibition of the outer layers of the specimen. An overlapping curing regime was performed due to increased length of bar-shaped specimens (25 mm) compared with the diameter of curing-light tip (12 mm). Firstly, the central portion of the bar-shaped specimen was irradiated for 40s and then specimen was irradiated at two overlapping irradiation positions for 40s each immediately after first shot to cure the entire length of the bar-shaped specimen. All specimens were irradiated from one side by a quartz-tungsten-halogen curing unit (Optilux 501, Kerr, Orange, CA, USA) at an ambient temperature 23±2 ºC . The irradiance of the curing-unit was measured prior to fabrication of each sample set (780-880 mW/cm^2) using a digital radiometer (Coltolux C-7900 Coltene/Whaledent Inc, Mahwah, NJ, US). Following irradiation, the cellulose acetate strips were detached, each specimen was immediately removed from the mould and flash cut away using a sharp blade. Prior to testing, RBCs specimens were stored in distilled water for one week at 37±1 ºC.

Three-point flexure data was achieved in accordance with the International Standard for Dental Polymer-Based Filling, Restorative and Luting Materials (ISO 4049, 2000). The bar- shaped specimens of each RBC were centrally loaded using a 3 mm diameter cylindrical roller across a support span of 20 mm at three cross-head speeds of 0.1, 1.0 and 10.0 mm/min (n=5) using a universal testing machine (Model 5544, Instron Ltd, High Wycombe, Bucks, England). The irradiated surface of specimen was placed uppermost, with the non-irradiated surface under tension. After failure of each specimen, the width and thickness of the specimen at the point of fracture (mm) was measured using a screw-gauge micrometer (Moore and Wright, Sheffield, UK) accurate to 10 µm. The load-deflection curve was plotted for each specimen in order to calculate load (N) and deflection (mm) values at the most linear part of curve were used to calculate flexural modulus (GPa) using Equation 5.2

$$E = \frac{Fl^3}{4bh^3d} \qquad \text{Equation 5.2}$$

where F was the load (N), l was the span distance (20 mm), b was the width of the specimen (mm), h was the thickness of specimen (mm) and d was the deflection (mm).

5.2.2.3 Statistical analysis

A general linear model (GLM) ANOVA was conducted on the combined BFS and flexural modulus data to highlight the effect of deformation rate (3 levels), filler particle size (3 levels) and nanoparticle addition (3 levels) with post hoc Sidak test comparison (P=0.05). Two-way ANOVA tests were run on BFS and flexural modulus data for each filler particle size with deformation rate (3 levels) and nanoparticle

addition (3 levels). One-way ANOVA and post hoc Tukey tests (P=0.05) were performed on BFS and flexural modulus data at each deformation rate to highlight the difference between RBCs with regard to filler particle size and nanoparticle addition. Main effects plots were produced to highlight the general trends in combined BFS and flexural modulus data.

5.2.3 Results

The GLM-ANOVA highlighted a significant effect of deformation rate, filler particle size and nanoparticle addition on the BFS and flexural modulus ($P<0.001$) (Figure 5.2). A general increase in BFS and flexural modulus was identified with increasing deformation rate whereas a high volume percentage of nanoparticles led to a reduction in BFS and flexural modulus (Figure 5.2). The flexural modulus generally increased with an increase in filler particle size. In contrast, BFS was declined with an increase in filler particle size (Figure 5.2). Two-way ANOVA revealed a significant effect of deformation rate ($P<0.001$) and nanoparticle addition ($P<0.001$) for BFS and flexural modulus data sets for each RBC series with similar filler particle size (Table 5.3, 5.4). The mean BFS and flexural modulus and associated standard deviations of all experimental RBCs at 0.1, 1.0 and 10.0 mm/min deformation rates are shown in Tables 5.3 and 5.4, respectively. In addition, plots are presented to highlight the effect of nanoparticle addition and filler particle size on BFS and flexural modulus at 0.1, 1.0 and 10.0 mm/min deformation rates (Figure 5.3-5.6).

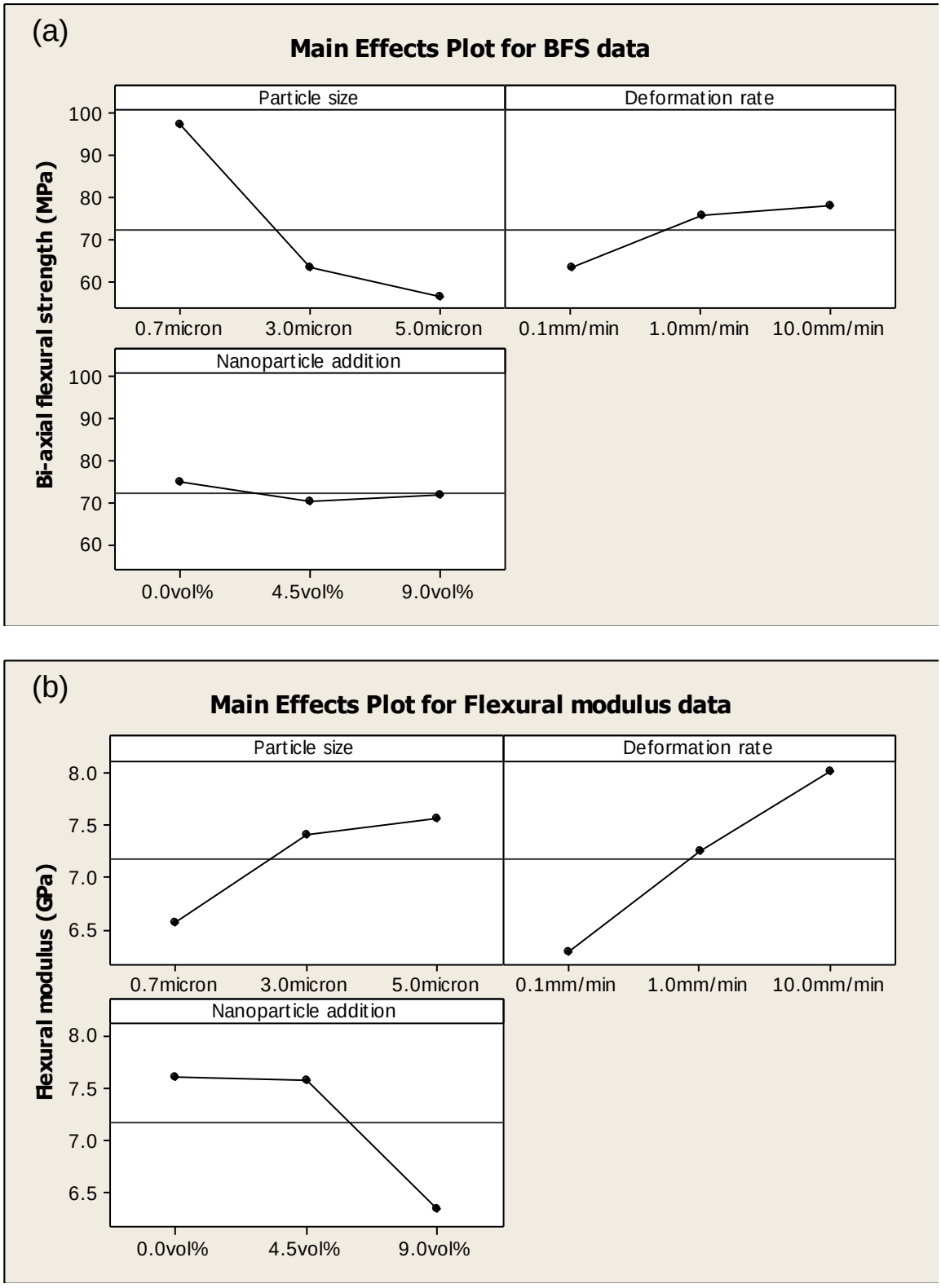

Figure 5.2. The main effects plots highlighting the significant effect of filler particle size, nanoparticle addition and deformation rate on the combined (a) bi-axial flexure strength and (b) flexural modulus data of experimental resin-based composites.

Table 5.3. The mean BFS and associated standard deviations of experimental resin-based composites (RBC1-RBC9) at 0.1, 1.0 and 10.0 mm/min deformation rates.

Experimental Resin Composites	Microfiller (diameter/load)	Nanofiller (diameter/load)	BFS (MPa) 0.1 mm/min	BFS (MPa) 1.0 mm/min	BFS (MPa) 10.0 mm/min
RBC1	0.7 µm; 55.0 vol%	14 nm; 0.0 vol%	89(11)^{12b}	106(14)^{1a}	106(16)^{1a}
RBC2	0.7 µm; 50.5 vol %	14 nm; 4.5 vol%	95(13)^{1b}	103(14)^{12ab}	104(17)^{1a}
RBC3	0.7 µm; 46.0 vol %	14 nm; 9.0 vol%	82(17)^{2b}	95(13)^{2a}	98(21)^{1a}
RBC4	3.0 µm; 55.0 vol%	14 nm; 0.0 vol%	62(9)^{3b}	70(10)^{3a}	75(13)^{2a}
RBC5	3.0 µm; 50.5 vol %	14 nm; 4.5 vol%	47(10)^{4b}	66(12)^{34a}	61(10)^{34a}
RBC6	3.0 µm; 46.0 vol %	14 nm; 9.0 vol%	53(10)^{34b}	69(12)^{3a}	66(15)^{234a}
RBC7	5.0 µm; 55.0 vol%	14 nm; 0.0 vol%	48(6)^{4b}	58(9)^{4a}	61(12)^{34a}
RBC8	5.0 µm; 50.5 vol%	14 nm; 4.5 vol%	45(8)^{4b}	55(7)^{4a}	59(8)^{4a}
RBC9	5.0 µm; 46.0 vol %	14 nm; 9.0 vol%	52(7)^{4c}	59(9)^{4b}	72(14)^{23a}

Superscript notation with similar numbers down columns and similar letters across rows indicate no statistically significant difference ($P>0.05$).

(a)

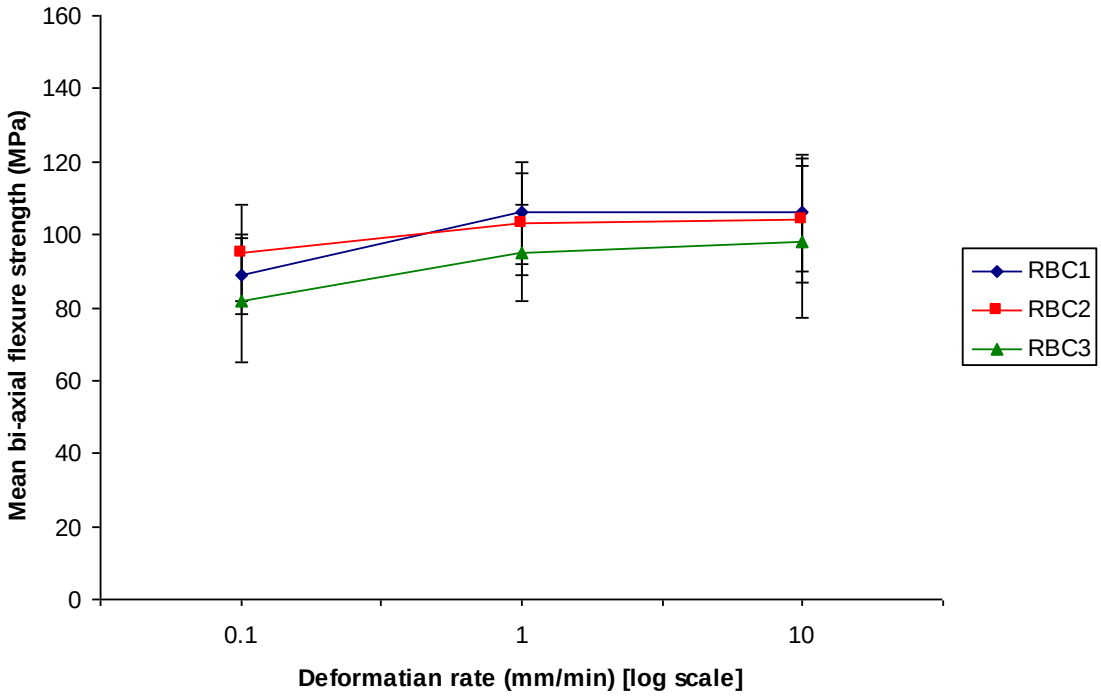
160
140
120
100
80
60
40
20
0
Mean bi-axial flexure strength (MPa)
0.1
1
10
Deformatian rate (mm/min) [log scale]
RBC1
RBC2
RBC3

(b)

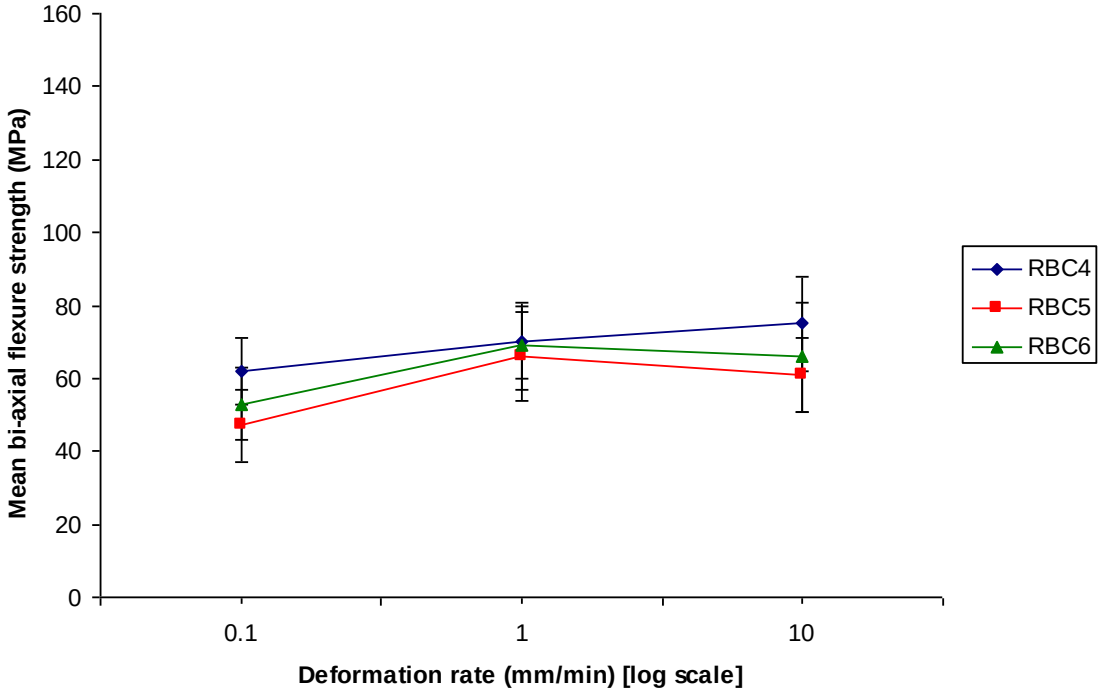
160
140
120
100
80
60
40
20
0
Mean bi-axial flexure strength (MPa)
0.1
1
10
Deformation rate (mm/min) [log scale]
RBC4
RBC5
RBC6

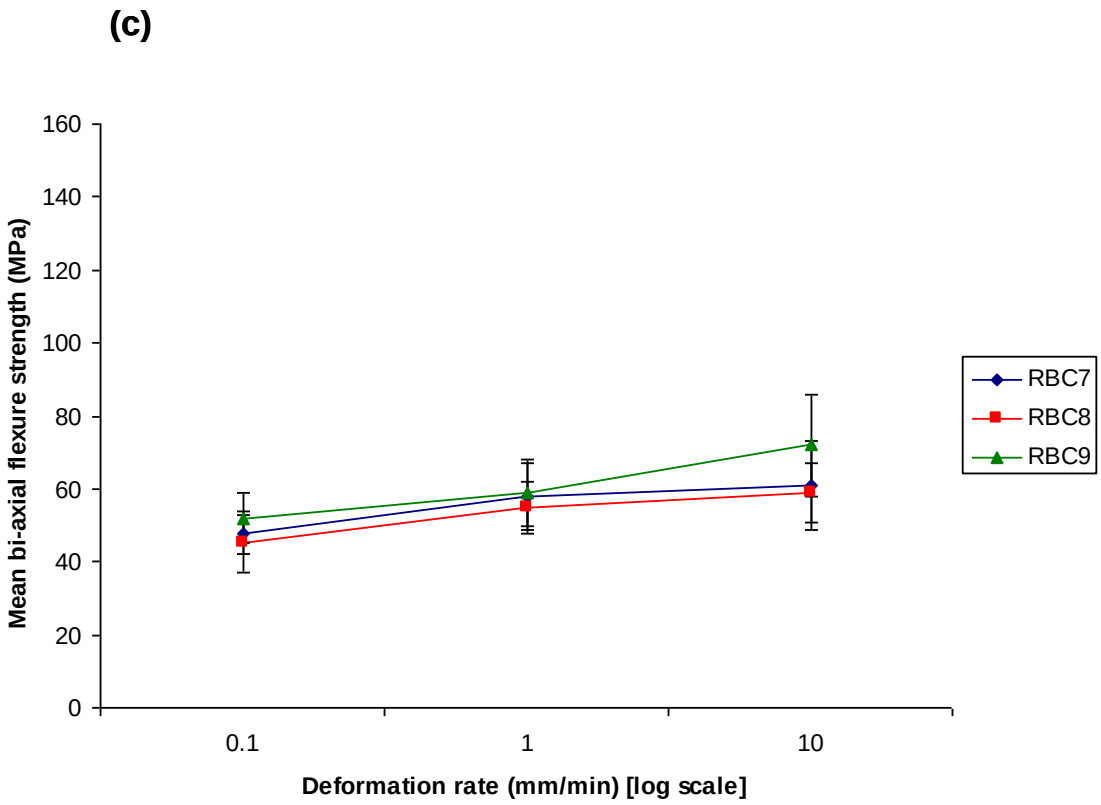

Figure 5.3. Plots illustrating the mean bi-axial flexure strength (and associated standard deviations) of experimental resin-based composite (a) RBC1-RBC3 (b) RBC4-RBC6 and (c) RBC7-RBC9 at 0.1, 1.0, 10.0 mm/min deformation rates [log scale] and highlighting the effect of nanoparticle addition on BFS.

(a)

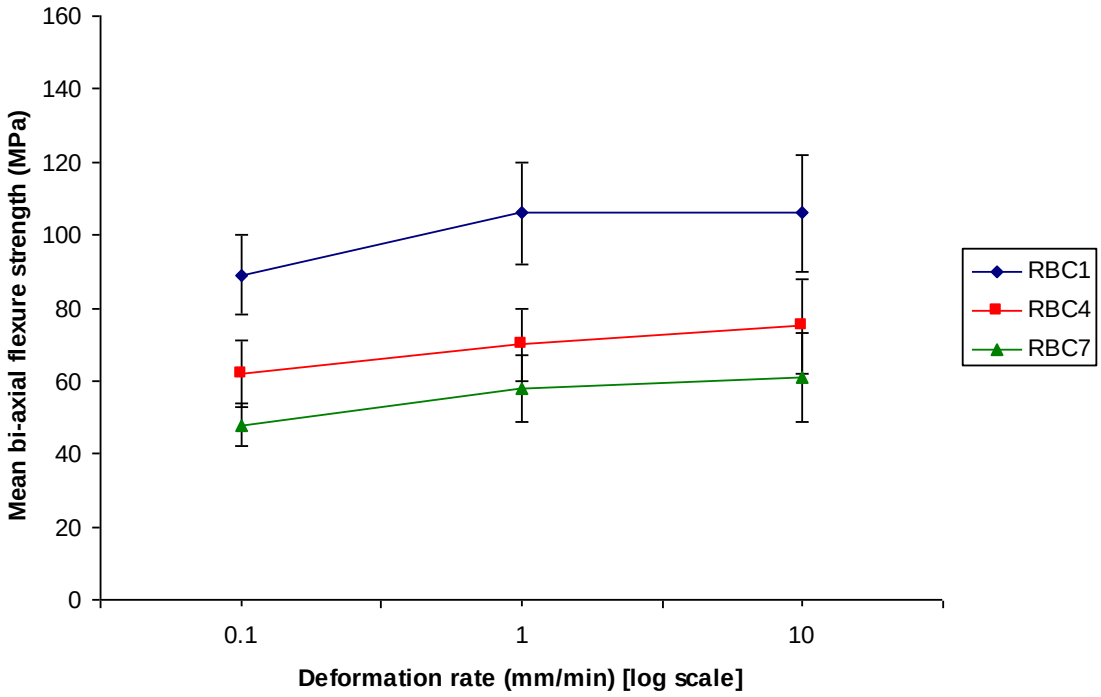
160
140
120
100
80
60
40
20
0
Mean bi-axial flexure strength (MPa)
0.1
1
10
Deformation rate (mm/min) [log scale]
RBC1
RBC4
RBC7

(b)

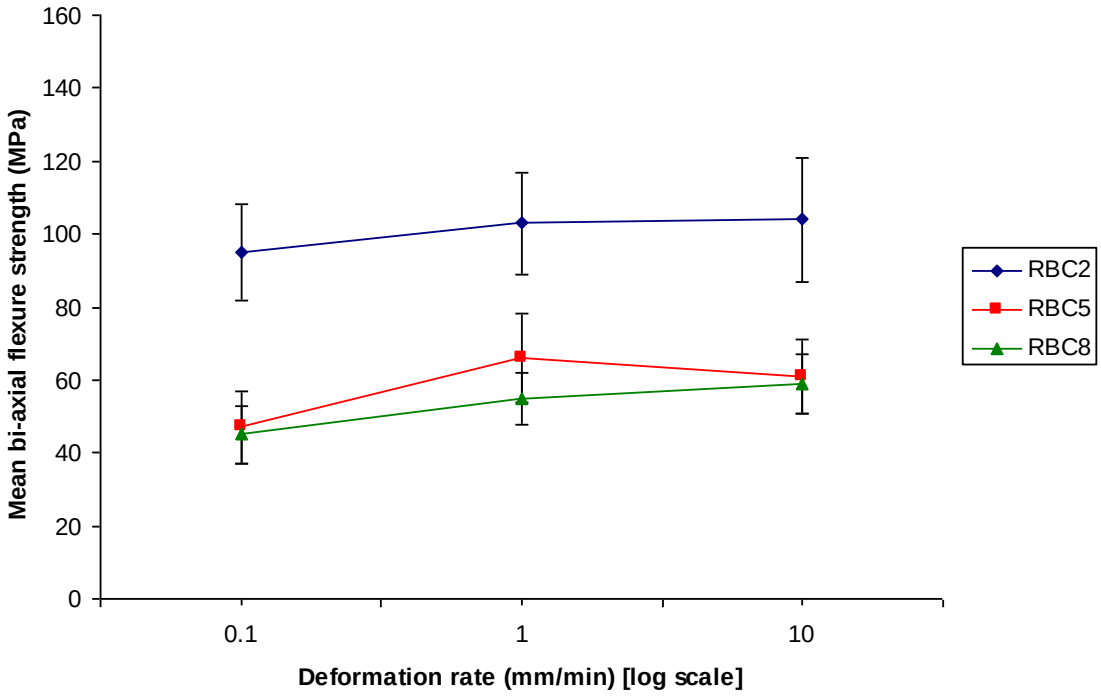
160
140
120
100
80
60
40
20
0
Mean bi-axial flexure strength (MPa)
0.1
1
10
Deformation rate (mm/min) [log scale]
RBC2
RBC5
RBC8

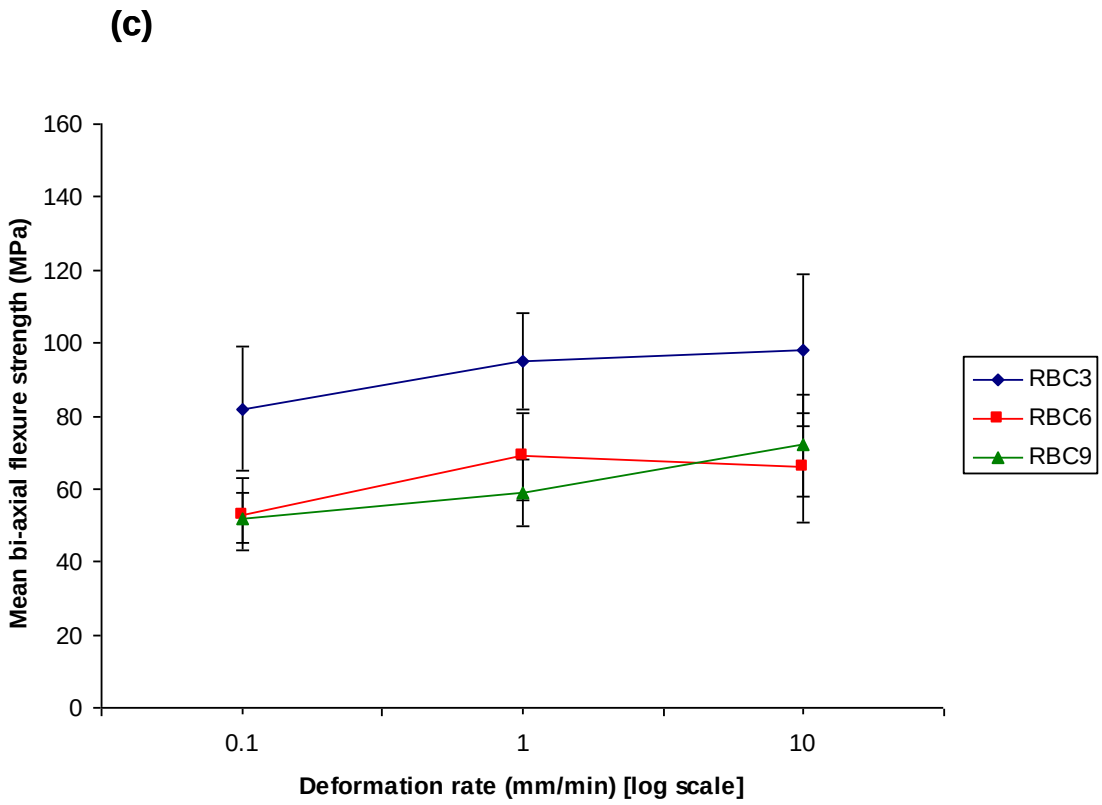

Figure 5.4. Plots illustrating the mean bi-axial flexure strength (and associated standard deviations) of experimental resin-based composite (a) RBC1, RBC4 and RBC7 (b) RBC2, RBC5 and RBC8 (c) RBC3, RBC6 and RBC9 at 0.1, 1.0, 10.0 mm/min deformation rates [log scale] and highlighting the effect of filler particle size on BFS.

Table 5.4. The mean flexural modulus and associated standard deviations of experimental Resin-based composites (RBC1-RBC9) at 0.1, 1.0 and 10.0 mm/min deformation rates.

Experimental Resin Composites	Microfiller (diameter/load)	Nanofiller (diameter/load)	Flexural modulus (GPa) 0.1 mm/min	Flexural modulus (GPa) 1.0 mm/min	Flexural modulus (GPa) 10.0 mm/min
RBC1	0.7 µm; 55.0 vol%	14 nm; 0.0 vol%	5.7(0.2)^{2b}	6.8(0.7)^{2a}	7.0(0.5)^{2a}
RBC2	0.7 µm; 50.5 vol %	14 nm; 4.5 vol%	6.2(0.6)^{2c}	6.9(0.4)^{2b}	8.1(1.0)^{1a}
RBC3	0.7 µm; 46.0 vol %	14 nm; 9.0 vol%	5.6(0.2)^{2b}	5.3(0.8)^{3b}	7.5(0.3)^{12a}
RBC4	3.0 µm; 55.0 vol%	14 nm; 0.0 vol%	6.7(0.9)^{1b}	8.9(0.9)^{1a}	8.8(0.8)^{1a}
RBC5	3.0 µm; 50.5 vol %	14 nm; 4.5 vol%	7.3(0.2)^{1b}	8.3(0.7)^{1a}	8.7(0.8)^{1a}
RBC6	3.0 µm; 46.0 vol %	14 nm; 9.0 vol%	5.2(0.2)^{2b}	5.7(0.6)^{3b}	7.0(0.2)^{2a}
RBC7	5.0 µm; 55.0 vol%	14 nm; 0.0 vol%	6.6(0.2)^{1b}	9.0(1.0)^{1a}	8.9(0.9)^{1a}
RBC8	5.0 µm; 50.5 vol%	14 nm; 4.5 vol%	6.8(1.2)^{1c}	7.4(0.5)^{2b}	8.6(0.8)^{1a}
RBC9	5.0 µm; 46.0 vol %	14 nm; 9.0 vol%	6.3(0.3)^{12b}	6.9(0.3)^{2b}	7.6(0.5)^{1a}

Superscript notation with similar numbers down columns and similar letters across rows indicate no statistically significant difference ($P>0.05$).

(a)

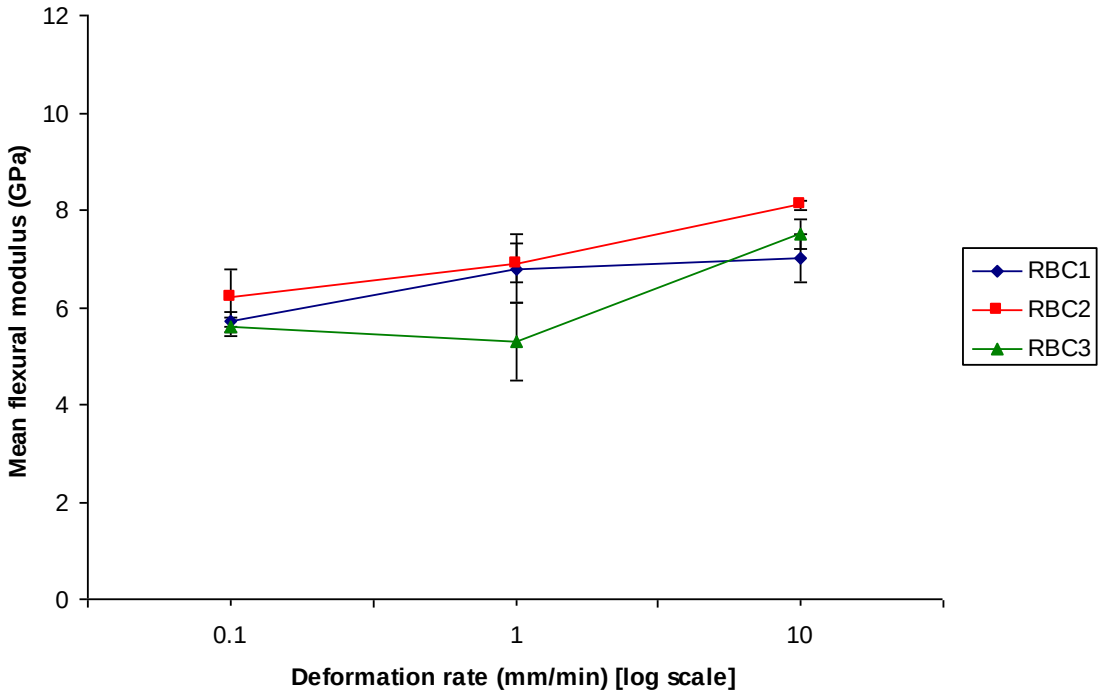
Mean flexural modulus (GPa)
12
10
8
6
4
2
0
0.1
1
10
Deformation rate (mm/min) [log scale]
RBC1
RBC2
RBC3

(b)

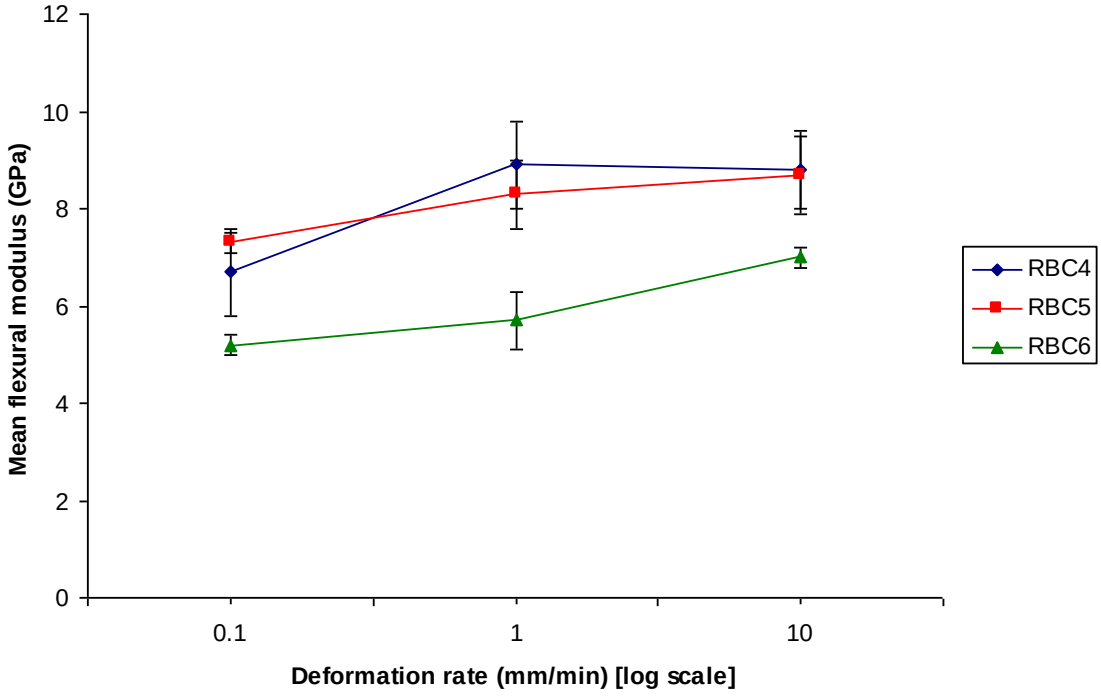
Mean flexural modulus (GPa)
12
10
8
6
4
2
0
0.1
1
10
Deformation rate (mm/min) [log scale]
RBC4
RBC5
RBC6

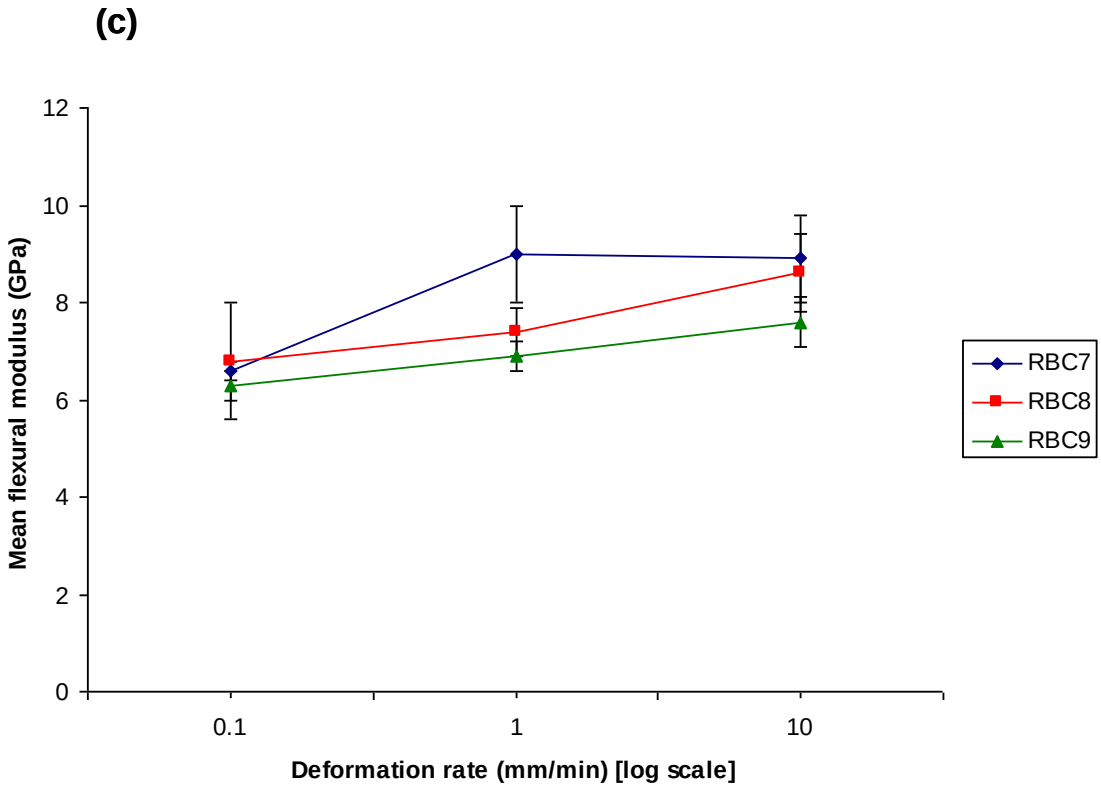

Figure 5.5. Plots illustrating the mean flexural modulus (and associated standard deviations) of experimental resin-based composite (a) RBC1-RBC3 (b) RBC4-RBC6 and (c) RBC7-RBC9 at 0.1, 1.0, 10.0 mm/min deformation rates [log scale] and highlighting the effect of nanoparticle addition on flexural modulus.

(a)

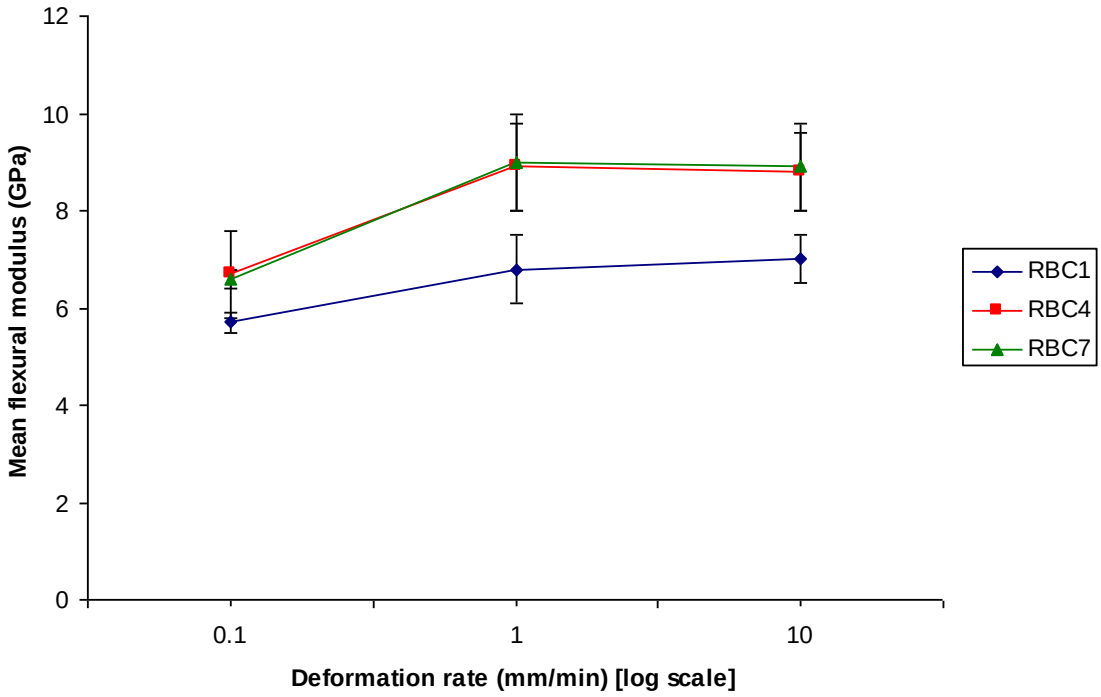
12
10
8
6
4
2
0
Mean flexural modulus (GPa)
0.1
1
10
Deformation rate (mm/min) [log scale]
RBC1
RBC4
RBC7

(b)

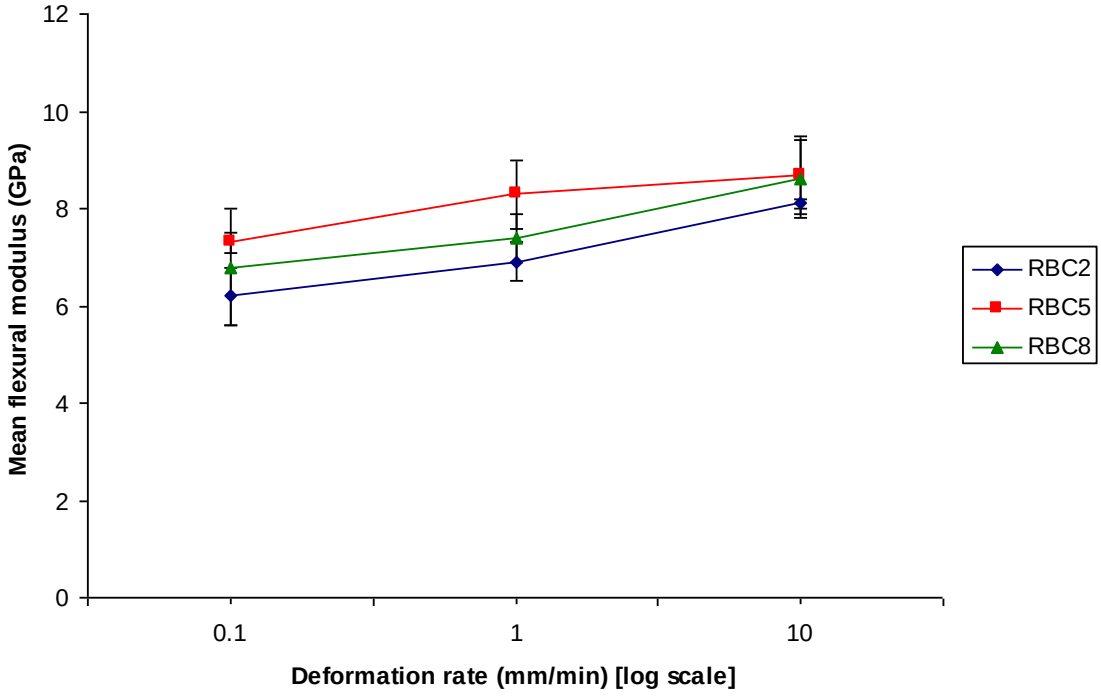
12
10
8
6
4
2
0
Mean flexural modulus (GPa)
0.1
1
10
Deformation rate (mm/min) [log scale]
RBC2
RBC5
RBC8

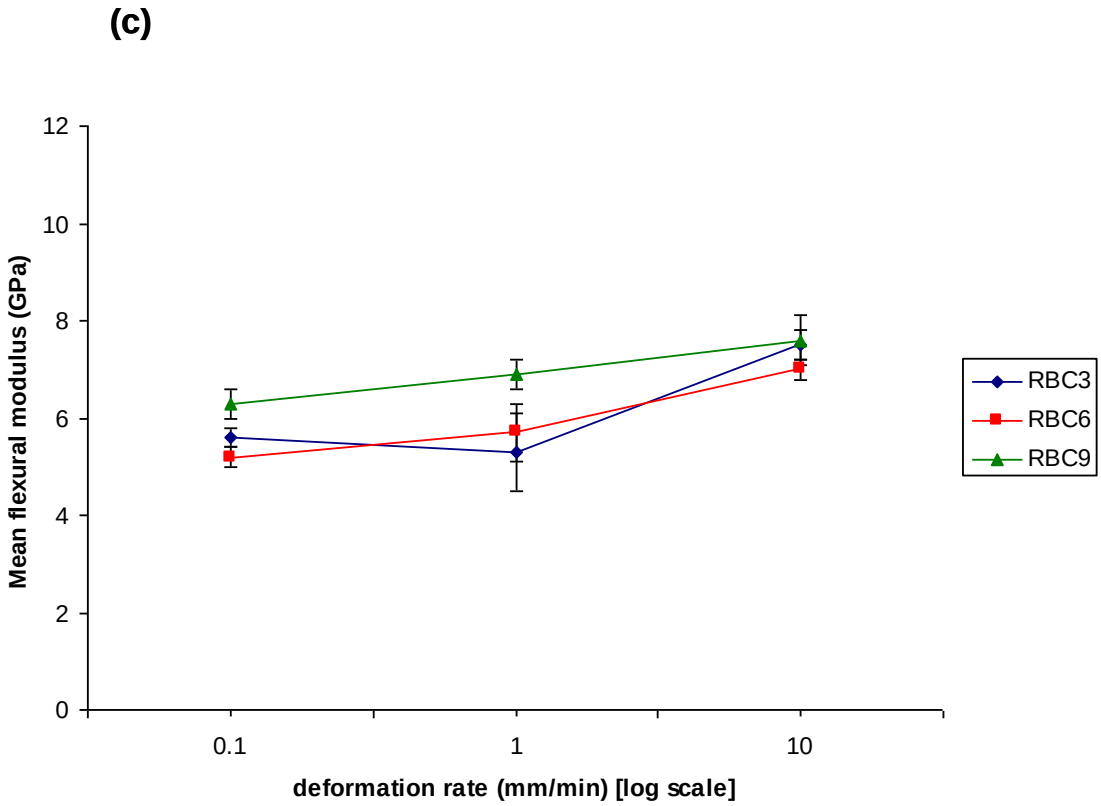

Figure 5.6. Plots illustrating the mean flexural modulus (and associated standard deviations) of experimental resin-based composite (a) RBC1, RBC4 and RBC7 (b) RBC2, RBC5 and RBC8 (c) RBC3, RBC6 and RBC9 at 0.1, 1.0, 10.0 mm/min deformation rates [log scale] and highlighting the effect of filler particle size on flexural modulus.

5.2.4 Discussion

In previous experiments, two commercial nanofilled (Chapter 4) and an experimental RBC (Chapter 5) exhibited a lower mean BFS at 0.1 mm/min deformation rate compared with 1.0 and 10.0 mm/min deformation rates following one week wet storage regime. Consequently, in the current experiment, one week wet immersion was considered the most important storage regime and was chosen to determine the effect of filler particle size and nanoparticle addition on the BFS and flexural modulus at the similar deformation rates.

All RBCs exhibited a decrease in the mean BFS and flexural modulus at 0.1 mm/min deformation rate compared with higher deformation rates which highlight the inherent viscoelastic behaviour of polymer-based materials. The relevant material examples are silicones or silicon-based materials (Askeland and Phulé, 2006) such as polydimethylsiloxane, which exhibits unusual properties dependent upon the speed of force that is used to manipulate the material; if pulled apart slowly the material will stretch, but will fracture if given a sharp blow. At low strain rate, the polymeric chains of materials are allowed to uncoil and move relative to each other and subsequently lead to plastic deformation, whereas at high strain rate, the polymeric chains are not likely to move relative to each other and thus result in brittle failure.

A decrease in the mean BFS and flexural modulus of all RBCs with different filler size and nanoparticle combinations at 0.1 mm/min deformation rate compared with higher deformation rates (Table 5.3, 5.4) suggested that filler particle size and nanoparticle addition have no significant effect on the deformation rate dependence of RBCs at the filler volume fraction used. It may be assumed that an equivalent volume of resin (45 vol%) is likely to be responsible for similar deformation rate dependence pattern across the range of RBCs investigated. Consequently, a further investigation

with different resin formulations is warranted which may give an insight into the material behaviour. In a preliminary study, RBC formulations with various filler/resin ratios were carried out, however the mixing device was capable to mix maximum 55:45 filler/resin volume ratio utilized in the current experiment, which is comparable with many commercially-available RBCs.

Generally, a significant reduction in mean BFS of RBCs with increasing filler particle size was identified at all deformation rates (Table 5.3, Figure 5.4). In previous studies, Miyasak (1996) and Tanimoto et al. (2006) also a found similar pattern. Tanimoto et al. (2006) evaluated the flexural strength of RBCs with varying filler size and also investigated the corresponding stress distribution using three-dimensional finite element (FE) analysis. The authors found increased stress concentration at resin/filler interface and a resultant decrease in flexural strength with increasing particle size of filler. Generally, the addition of nanoparticles either did not exhibit any effect or reduced the BFS (Table 5.3, Figure 5.3). A possible explanation may be that agglomeration of nanoparticles occurred in RBC batches and caused the weakening of the RBC due to increased stress concentration (Section 5.1.4). In a previous study, the influence of various mass fractions of nano fibrillar silicate (1%, 2.5% and 7.5%) on the flexural strength of resin composites was investigated (Tian et al., 2008) and the authors identified an increase in the flexural strength with 1 and 2.5 % nano fibrillar silicate addition while no further increase with 7.5% mass fraction. The increased flexural strength was attributed to highly separated and uniformly distributed nano fibrillar silicate. It was further proposed by authors that two effects, either reinforcing due to highly separated and uniformly distributed nano fibrillar silicate, or weakening due to the agglomeration that may occur in resin composites.

The flexural modulus generally exhibited an opposite trend in contrast to BFS by highlighting an increased flexural modulus with increasing filler particle size (Table 5.4, Figure 5.6). Masouras et al., (2008) have also reported similar pattern, however, Tanimoto et al. (2006) suggested that filler size has no any significant effect on elastic modulus and that filler volume fraction determines the flexural modulus characteristics of a composite material. Here, an increased nanoparticle addition led to a decrease in flexural modulus of RBCs. It is believed that composites with large particles restrain the movement of matrix during load application, whereas in composites with small particles, the matrix bears the sufficient load and the small particles hinder the plastic deformation. It can be assumed that in the current study, large filler particles bear greater load compared with small filler particles and exhibited an increased flexural modulus. Moreover, a reduced flexural modulus in the RBCs with nanoparticle addition (Table 5.4, Figure 5.5) may also be anticipated as the result of greater plastic deformation of matrix.

It is clear that filler particle size and nanoparticle addition have significant effects on the mechanical properties of RBCs, however, various combinations of both variables did not highlight any effect on the dependence of deformation rate. Consequently, a further study is warranted with regard to resin formulations and also a greater filler/resin ratio which may aid the development of improved materials.

5.2.5 Conclusions

1. The deformation rate dependence of experimental RBCs was not significantly affected by various combinations of filler particle size and nanoparticle addition.

2. The BFS of RBCs decreased with increasing filler particle size, while an increase in the flexural modulus of RBCs was observed as a result of increased filler size.
3. The addition of a high volume percentage of nanoparticles resulted in a decreased flexural modulus of RBCs compared with RBCs without nanoparticle addition.

References

Askeland DR, Phulé PP. Mechanical properties: Part one. In: Askeland DR, Phulé PP. The Science and Engineering of Materials (5th Edition). Cengage Learning, 2006; Chapter 6: 183-222

Asmussen E, Peutzfeldt A. Influence of composition on rate of polymerisation contraction of light-curing resin composites. Acta Odontologica Scandinavica, 2002; 60: 146-150.

Asmussen E, Peutzfeldt A. Two-step curing: influence on conversion and softening of a dental polymer. Dental Materials, 2003; 19: 466-470.

Bagheri R, Tyas MJ, Burrow MF. Subsurface degradation of resin-based composites. Dental Materials, 2007; 23: 944-951.

Baroudi K, Silikas N, Watts DC. Time-dependent visco-elastic creep and recovery of flowable composites. European Journal of Oral Science, 2007; 115:517-521.

Braem M, Lambrechts P, Van Doren V, Vanherle G. The impact of composite structure on its elastic response. Journal of Dental Research, 1986; 65: 648-653.

Braem M, Finger W, Van Doren VE, Lambrechts P, Vanherle G. Mechanical properties and filler fraction of dental composites. Dental Materials, 1989; 5: 346-349.

Calais JG, Söderholm KJM. Influence of filler type and water exposure on flexural strength of experimental composite resin. Journal of Dental Research, 1988; 67:836-840.

Chen W, Cheng FLM. Tension and compression tests of two polymers under quasi-static and dynamic loading. Polymer Testing, 2002; 21: 113-121.

Chung KH. The relationship between composition and properties of posterior resin composites. Journal of Dental Research, 1990; 68: 852-856.

Cock DJ, Watts DC. Time-dependent deformation of composite restorative material in compression. Journal of Dental Research, 1985; 64: 147-150.

Ferracane JL, Berge HX, Condon JR. In vitro aging of dental composites in water-Effect of degree of conversion, filler volume, and filler/matrix coupling. Journal of Biomedical Material Research, 1998; 42: 465-472.

Glaros AG, Rao SM. Effects of bruxism: A review of the literature. Journal of Prosthetic Dentistry, 1977; 38: 149-157.

Germain HS, swartz ML, Philips RW, Moore BK, Roberts TA. Properties of microfilled composite resins as influenced by filler content. Journal of Dental Research, 1985; 64: 155-160.

Huang HX, Zhang JJ. Effects of filler-filler and polymer-filler interactions on rheological and mechanical properties of HDPE-Wood composites. Journal of Applied Polymer Science, 2009; 111: 2806-28012.

International Standards Organisation. Dentistry- Polymer-based filling, restorative and luting materials. ISO 4049, 2000; (3rd Edition): 15-18.

Jacob GC, Starbuck JM, Fellers JF, Simunovic S, Boeman RG. Strain rate effects on the mechanical properties of polymer composite materials. Journal of Applied Polymer Science, 2004; 94: 296-301.

Jumahat A, Soutis C, Jones FR, Hodzic A. Effect of silica nanoparticles on compressive properties of an epoxy polymer. Journal of Materials Science, 2010; 45: 5973-5983.

Masouras K, Akhtar R, Watts DC, Silikas N. Effect of fiiler size and shape on local indentation modulus of resin-composites. Journal of Materials Science: Materials in Medicine, 2008b; 19:3561-3566.

Musnaje L, Darvell BW. Effects of strain rate and temperature on the mechanical properties of resin composites. Dental Materials, 2004; 20: 750-765.

Miyasaka T. Effect of shape and size of silanated fillers on mechanical properties of experimental photo cure composite resins. Dental Material Journal, 1996; 15:98:110.

O'Donnell JNR, Langhorst SE, Fow MD, Antonucci JM, Skrtic D. Light-cured dimethacrylate resins and their composites: comparative study of mechanical strength, water sorption and ion release. Journal of Bioactive and Compatible Polymers, 2008; 23: 207-226.

Ruyter IE, Øysæd H. Compressive creep of light cured resin based restorative materials. Acta Odontologica Scandinavica, 1982; 40: 319-324.

Söderholm KJM. Leaking of fillers in dental composites. Journal of Dental Research, 1983; 62: 126-130.

Söderholm KJM, Zigan M, Ragan M, Fischlschweiger W, Bergman M. Hydrolytic degradation of dental composites. Journal of Dental Research, 1984, 63:1248-1254.

Tanimoto Y, Kitagawa T, Aida M, Nishiyama N. Experimental and computational approach for evaluating the mechanical characteristics of dental composite resins with various filler sizes. Acta Biomaterialia, 2006; 2: 633-639.

Tian M, Gao Y, Liu Y, Liao Y, Hedin NE, Fong H. Fabrication and evaluation of Bis-GMA/TEGDMA dental resin/composites containing nano fibrillar silicate. Dental Materials, 2008; 24: 235-243.

Timoshenko S, Woinowsky-Krieger S. Symmetrical bending of circular plates. In: Theory of Plates and Shells. McGraw-Hill; New York, 1959; (2nd Edition).

Vaidyanathan J, Vaidyanathan TK. Flexural Creep deformation and recovery in dental composites. Journal of Dentistry, 2002; 29: 545-551.

Chapter 6 Effect of Specimen Alignment on the Mechanical Properties of Dental Resin-Based Composites

6.1 Introduction

Currently, a wide range of direct and indirect restorative materials are used in restorative dentistry. One of the important requirements for a dental restorative material is stability when it is exposed to the moist oral environment. However, investigators have demonstrated that the exposure of resin-based composites (RBCs) to an aqueous environment can reduce fracture resistance (Ferracane and Berge, 1995) and flexural strength (Calais and Soderholm, 1988; Curtis et al., 2008). Such decline in mechanical properties has been attributed to hydrolytic degradation of the polymer matrix or fillers and debonding of the filler-resin interface (Söderholm et al., 1984; Söderholm et al., 1996; Ferracane et al., 1998). Therefore during the characterisation and development of RBC materials, it is essential that *in vitro* modelling should account for the degradative potential of water on the mechanical properties.

To simulate the perceived clinical environment, studies have been conducted following storage of RBC specimens in distilled water, ethanol (Ferracane and Berge, 1995; Zhang and Xu, 2008), food simulating-liquids (Deepa and Krishnan, 2000), and artificial saliva (Musnaje and Darvell, 2003). The effect of storage time (Örtengren et al., 2001), pH of media (Prakki et al., 2005) and temperature conditions (Watts et el., 1987) on the sorption and solubility , degradation and surface hardness of RBCs have been widely reported but to date the alignment of specimens throughout such storage regimes has rarely been detailed. Moreover, the International Standards Organisation (ISO) has not recommended any specimen alignment criteria for the flexural strength testing of RBCs (ISO 4049, 2000). Hence, to ensure the consistency of strength data of RBCs among different investigators and research laboratories, it is essential to

standardise the specimen alignment throughout the storage regimes which may consequently, aid in the accurate assessment of data. Thus the purpose of the current study was to investigate the influence of different specimen alignments on the bi-axial flexural strength and surface hardness of RBCs and to standardise the clinically relevant specimen alignment for the future RBCs associated research work.

The investigation tested the null hypothesis that differences in specimen alignment during storage regimes would not lead to variation in bi-axial flexure strength and surface hardness of RBCs.

6.2 Experimental procedure

6.2.1 Materials

A micro-hybrid RBC (Filtek^{TM} Z250; batch 8MA; shade A3) was investigated in the current study. The monomer matrix comprised of bisphenol A diglycidyl ether dimethacrylate (BisGMA), triethyleneglycol dimethacrylate (TEGDMA), bisphenol A polyethylene glycol diether dimethacrylate ($BisEMA_6$) and urethane dimethacrylate (UDMA) filled with fused zirconia-silica filler particles ranging from 0.01-3.5 μm with an average of 0.6 μm diameter. The total content of the filler particles was (84.5 weight%; 60 volume%).

6.2.2 Bi-axial flexure strength (BFS)

Two hundred and forty nominally identical disc-shaped specimens (12 mm diameter, 1 mm thickness) of the resin composite were manufactured. Split black Nylotron moulds were used to allow specimen removal without introducing spurious bending stresses. For each specimen 0.24±0.005 g of RBC paste was weighed using a Mettler AE 163 analytical balance (Mettler-Toledo Ltd, Leicester, UK) accurate to

0.001 g and packed into the mould. The top and bottom surfaces of each specimen were covered with cellulose acetate strip (0.1 mm thickness) to lessen the impact of oxygen inhibition (Shawkat et al., 2009). All specimens were light irradiated using a halogen curing unit (Optilux 501, Kerr, Orange, CA, USA) with a 12 mm diameter curing tip placed in contact with the acetate strip using a light guide to allow for reproducible concentric alignment. The irradiance of the curing-unit was measured prior to fabrication of each sample set (780-880 mW/cm^2) using a radiometer (Coltolux C-7900 Coltene/Whaledent Inc, Mahwah, NJ, US). Following irradiation at an ambient temperature 23±2 ºC for 20 s, the cellulose acetate strips were discarded and each specimen carefully removed from the mould and flash cut away using a sharp blade. Specimens were stored in a dessicator (dry control) or in water in three different alignments. One group was aligned so that specimens were stacked directly on top of each other. Specimens from a second group were embedded in polyvinylsiloxane putty so that only the upper surface was exposed to water and a final group was secured at a point at the specimen periphery rendering them upright with upper and lower surfaces directly exposed to water (Figure 6.1). For each condition, two groups of specimens (n=30) were stored for 1 week and 13 weeks at 37±1 ºC prior to testing. The dry control and stacked specimens were stored in a polystyrene cylindrical 30 ml container (Sterilin Ltd, Aberbargoed, UK) whereas upright and upper surface exposed specimens were aligned in a standard 90 mm Petri dish (Sterilin Ltd, Aberbargoed, UK) containing putty material (Figure 6.1).

The BFS was determined at cross-head speed of 1.0 mm/min in a ball-on-ring configuration using a universal testing machine (UTM) (Model 5544, Instron Ltd, High Wycombe, Bucks, England). A 3 mm ball-indenter was used to centrally load the disc-shaped specimens supported on a 10 mm diameter knife-edge support. The

irradiated surface of specimen was placed uppermost, with the non-irradiated surface under tension. The load (N) at failure was recorded. The mean specimen thickness was measured at the point of fracture of each fragment with a screw-gauge micrometer (Moore and Wright, Sheffield, UK) accurate to 10 μm. The BFS was calculated according to Equation 6.1.

$$\sigma_{\max} = \frac{P}{h^2}\left\{(1+\nu)\left[0.485 \times \ln\left(\frac{a}{h}\right) + 0.52\right] + 0.48\right\} \qquad \text{Equation 6.1}$$

where σ_{max} was the maximum tensile stress (MPa), P the measured load of fracture (N), a the radius of knife-edge support (mm), h the sample thickness (mm) and ν Poisson's ratio for the material. A Poisson's ratio value of 0.25 was utilized in current study (Section 3.2.3).

6.2.3 Surface Hardness

Resin composite specimens were prepared according to the method outlined above. Initially, the surface hardness of nine specimens were tested dry and subsequently stored in a stacked, upright and upper surface exposed alignment (n=3) as described previously. The hardness of each specimen was measured following 1 week and 13 weeks wet storage regimes. Specimens were indented at a load of 1.96 N for 10 s using a surface hardness tester (Struers, Glasgow, UK) with a Vickers diamond pyramid head. Eleven equidistant indentations were performed at 1 mm intervals in a north to south direction relative to the light curing tip position on the upper and lower surface of each specimen.

6.2.4 Statistical Analysis

A one-way ANOVA and post hoc Tukey multiple comparison tests were performed on the BFS data (P=0.05) to highlight any differences between dry storage and wet specimen alignments. The surface hardness data were evaluated using repeated measures and one-way ANOVA (P=0.05).

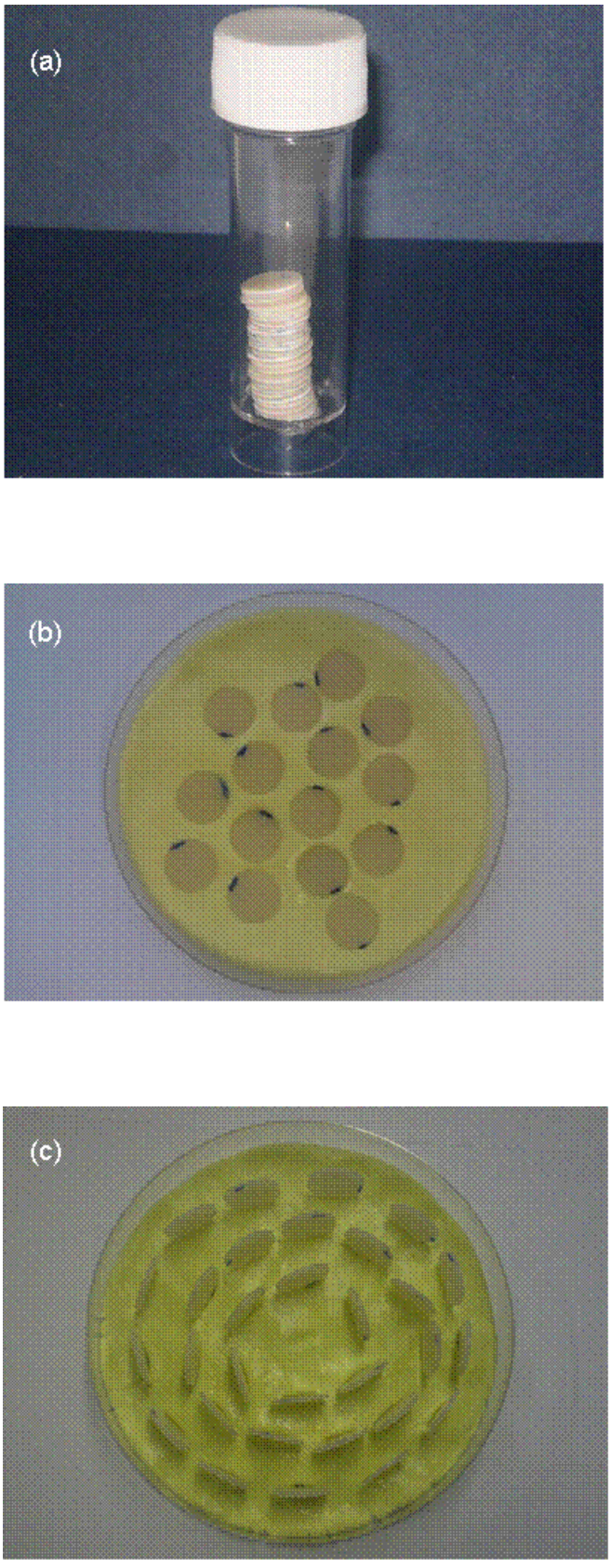

Figure 6.1. Images of (a) stacked (b) upper surface exposed (c) upright specimen alignments.

6.3 Results

6.3.1 Bi-axial flexure strength

Following 1 week storage, the BFS of the dry control group exhibited a significantly higher BFS (174 MPa) compared with all 3 wet alignments (stacked= 138 MPa, upper surface exposed=125 MPa, upright=111 MPa) ($P<0.001$), whereas no significant difference in BFS was observed between stacked and upper surface exposed ($P>0.001$) and upper surface exposed and upright alignments ($P>0.001$) respectively. The BFS of upright specimens highlighted a significant decrease in BFS compared with stacked specimens ($P<0.001$) (Table 6.1). Following 13 weeks storage, the dry control group also revealed a significantly higher BFS (163 MPa) in contrast to three wet alignments (stacked=150 MPa, upper surface exposed=91 MPa, upright=82 MPa) ($P<0.001$) and stacked alignment highlighted a significantly higher BFS compared with upper surface exposed and upright alignments ($P<0.001$). No significant difference was identified between BFS of 1 week and 13 weeks dry control groups ($P=0.091$). BFS of stacked alignment group increased following 13 weeks storage compared with 1 week stacked alignment ($P<0.05$) whereas a significant decline in BFS of upright and upper surface exposed alignments was identified following 13 weeks storage compared with 1 week dry storage ($P<0.001$) (Table 6.1).

Table 6.1. The mean BFS and associated standard deviations of resin composite at different specimen alignments following 1 week and 13 weeks storage regimes.

Specimen Alignment	Mean BFS (MPa) 1 week	Mean BFS (MPa) 13 weeks
Dry Control	174(30)[1a]	163(22)[1a]
Wet Stacked	138(22)[2b]	150(23)[2a]
Wet Upper surface exposed	125(17)[23a]	91(17)[3b]
Wet Upright	111(19)[3a]	82(14)[3b]

Superscript with similar numbers down columns and similar letters across rows indicate no statistically significant difference (P>0.05).

6.3.2 Surface hardness

The repeated measures analysis of combined surface hardness data highlighted no significant difference between upper and lower surface hardness (P=0.190), however, specimen alignment method and storage time significantly affected the surface hardness (P<0.001) (Figure 6.2).

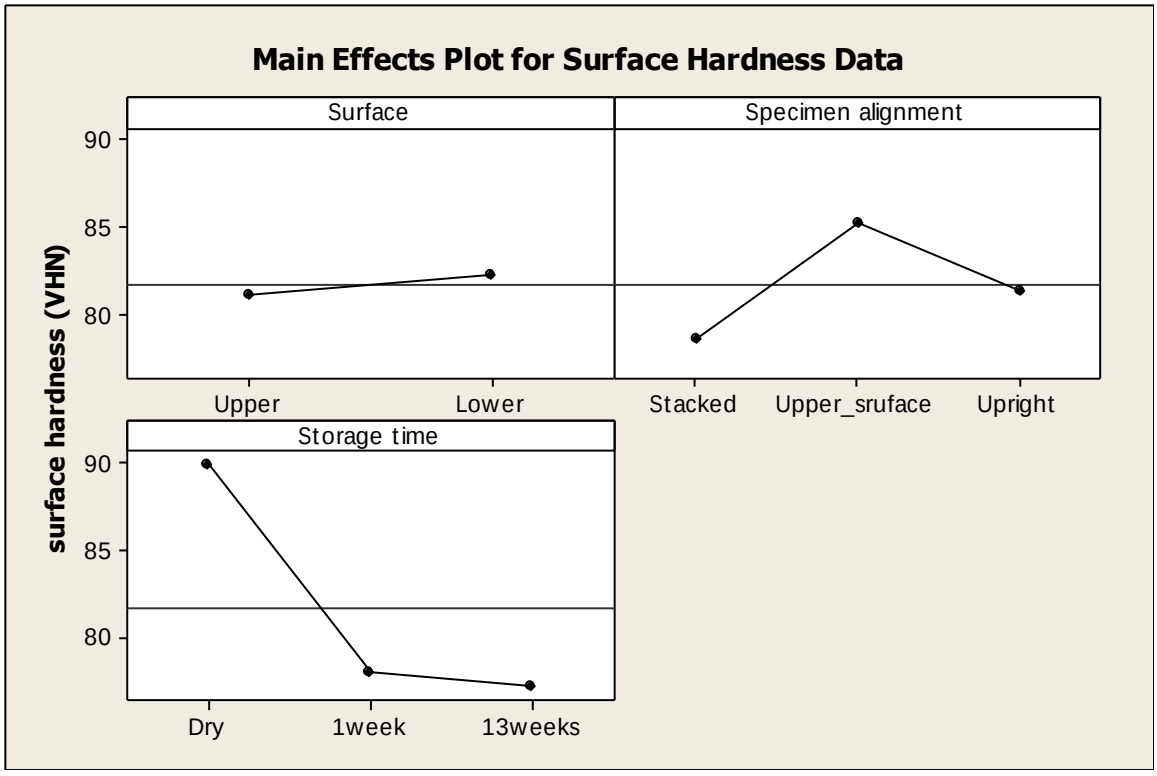

Figure 6.2. The main effects plot of the surface hardness data highlighting the significant effect of specimen alignment and storage time. The stacked specimens exhibit lower surface hardness compared with upright and upper surface exposed. The storage time demonstrates a decline in surface hardness following wet storage.

The additional repeated measures analysis of individual alignment revealed a significant effect of position (hardness values at 1 mm interval across the specimen width from north to south direction) ($P<0.001$) and storage time ($P<0.001$), however, effect of surface varied between specimen alignments. No significant difference between upper and lower surface hardness of stacked ($P=0.709$) and upright specimen ($P=0.168$) alignments was observed, however, lower surface of upper surface exposed alignment exhibited a significantly greater surface hardness compared with upper surface ($P<0.001$) (Figure 6.3). All specimen alignments highlighted a significantly lower combined surface hardness following wet storage compared with dry storage ($P<0.001$), whereas no significant difference between 1 week wet and 13 weeks wet storage was identified ($P>0.001$) (Figure 6.3). The upper and lower surface hardness

at positions from north to south direction for stacked, upper surface exposed and upright alignments following dry, 1 week wet and 13 weeks wet storage are shown in Figure 6.4.

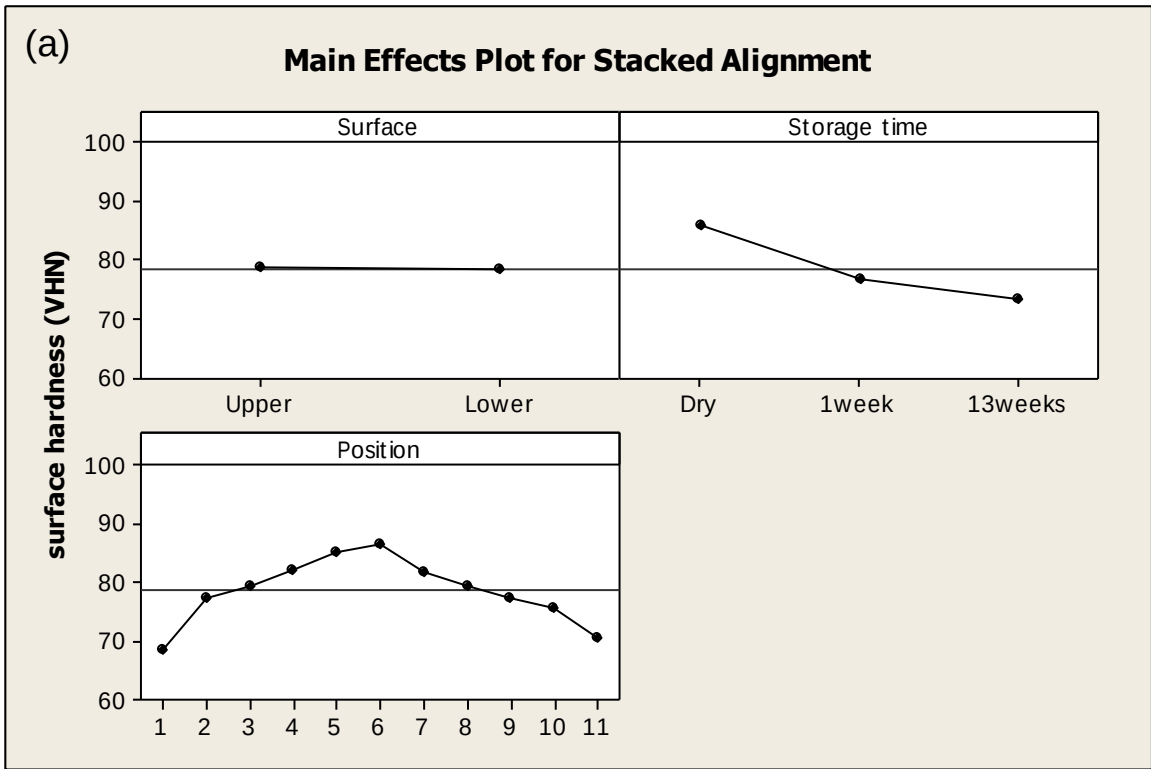

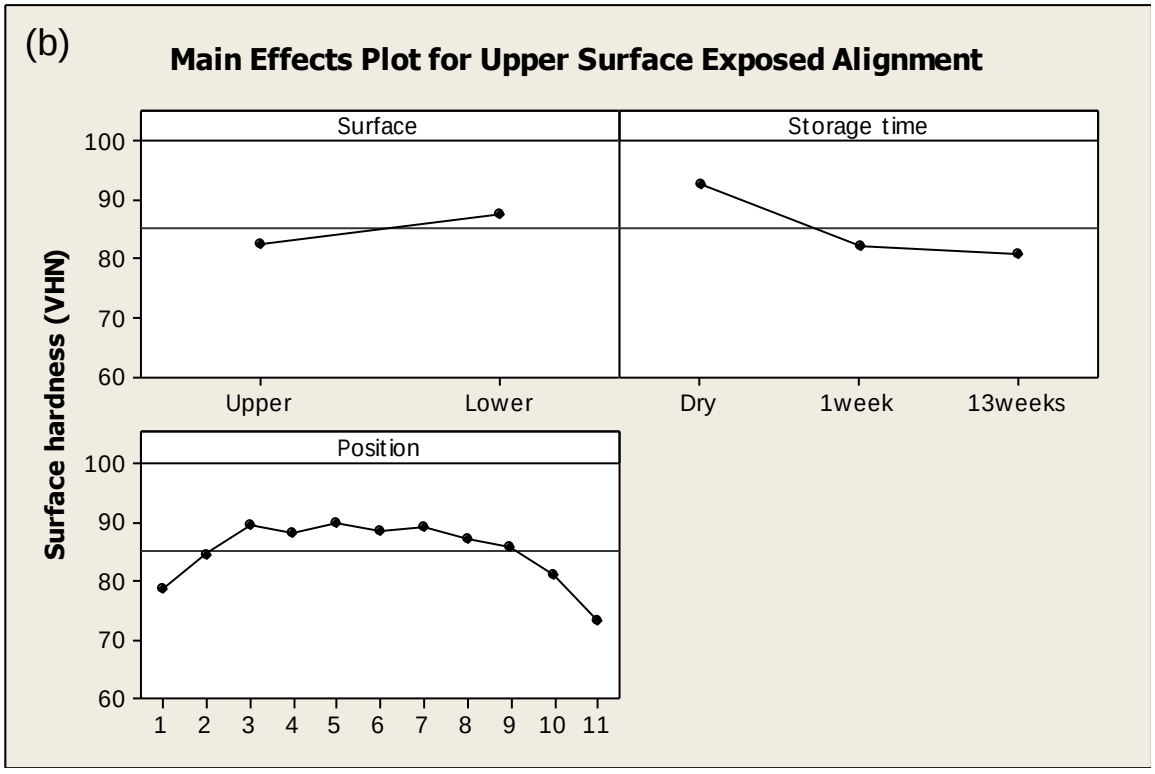

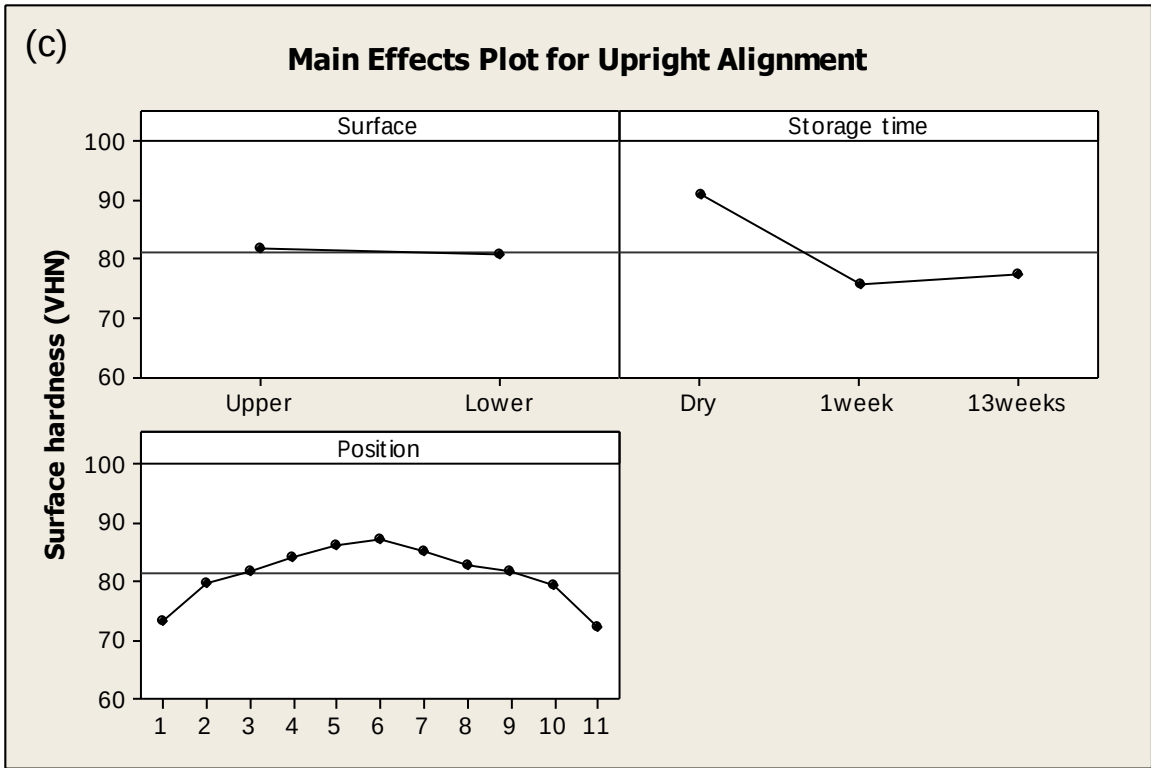

Figure 6.3. The main effects plots of surface hardness data of (a) stacked, (b) upper surface exposed and (c) upright specimen alignments. All alignments highlight a decrease in surface hardness following wet storage. In addition, reduction in hardness from centre-to-edge of specimens is also clear. The stacked and upright specimens indicate no significant difference between upper and lower surface hardness.

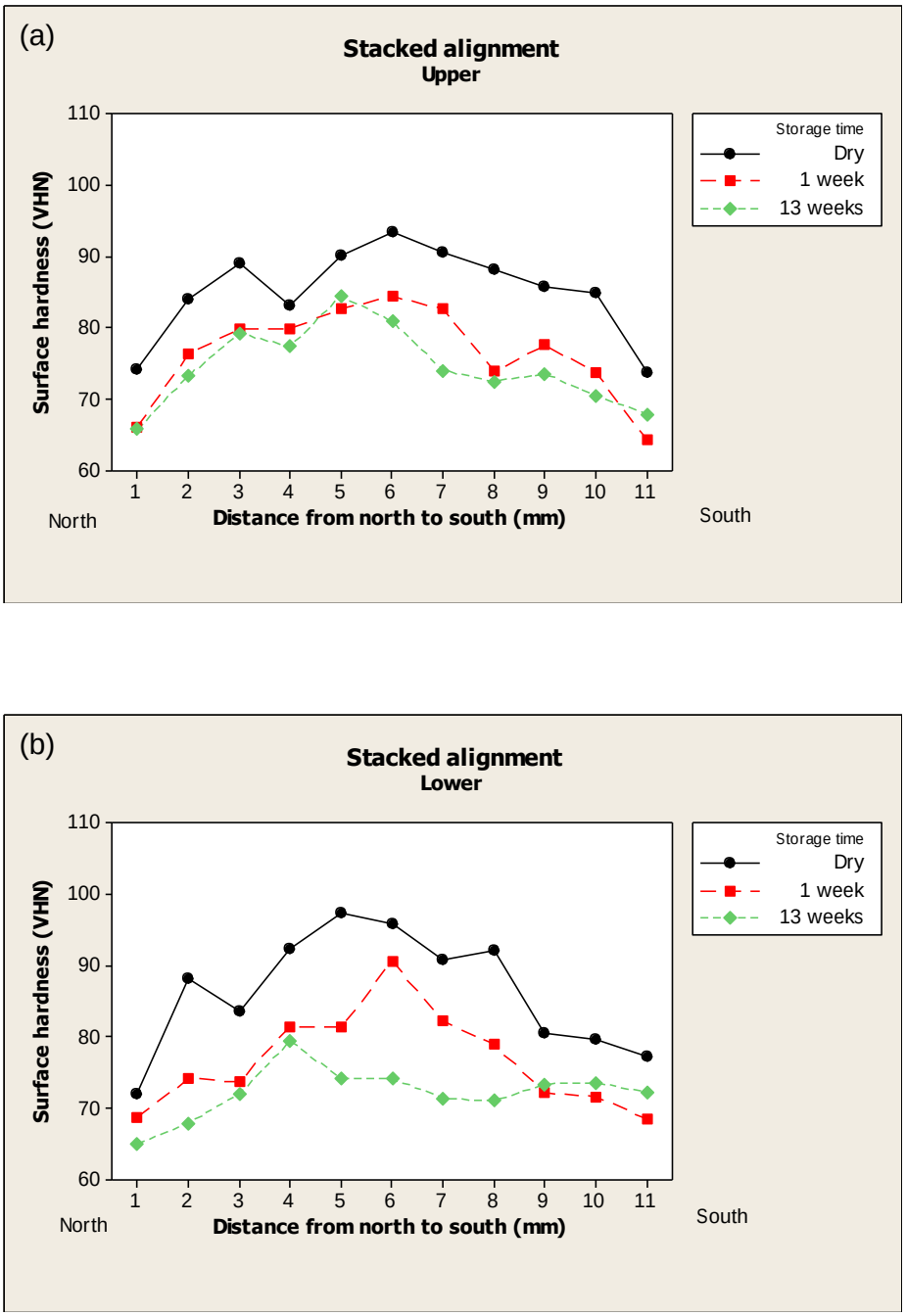

Figure 6.4. Plots highlighting the (a) upper and (b) lower surface hardness of stacked alignment from north to south direction following dry control, 1 week and 13 weeks wet storage regimes.

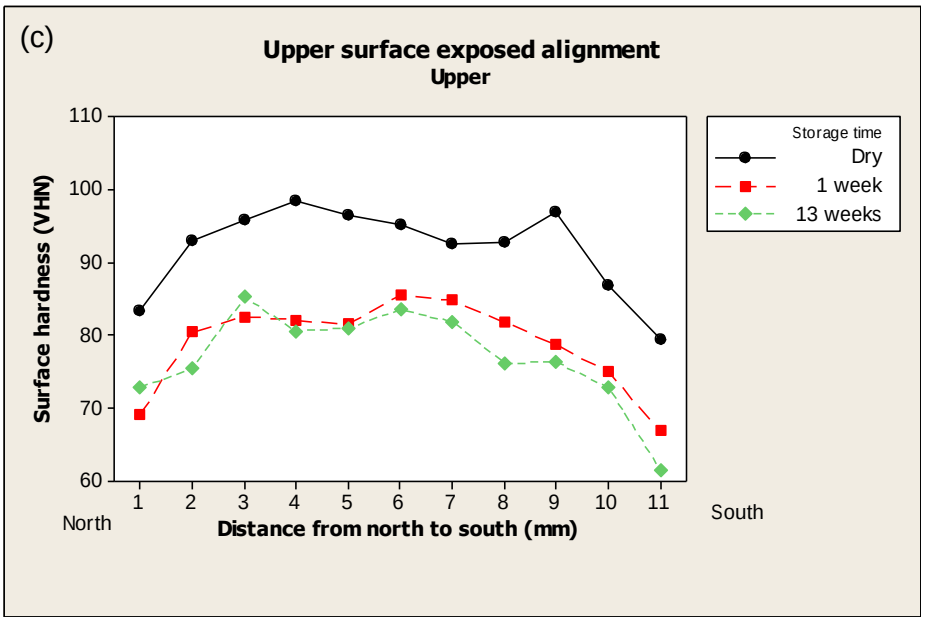

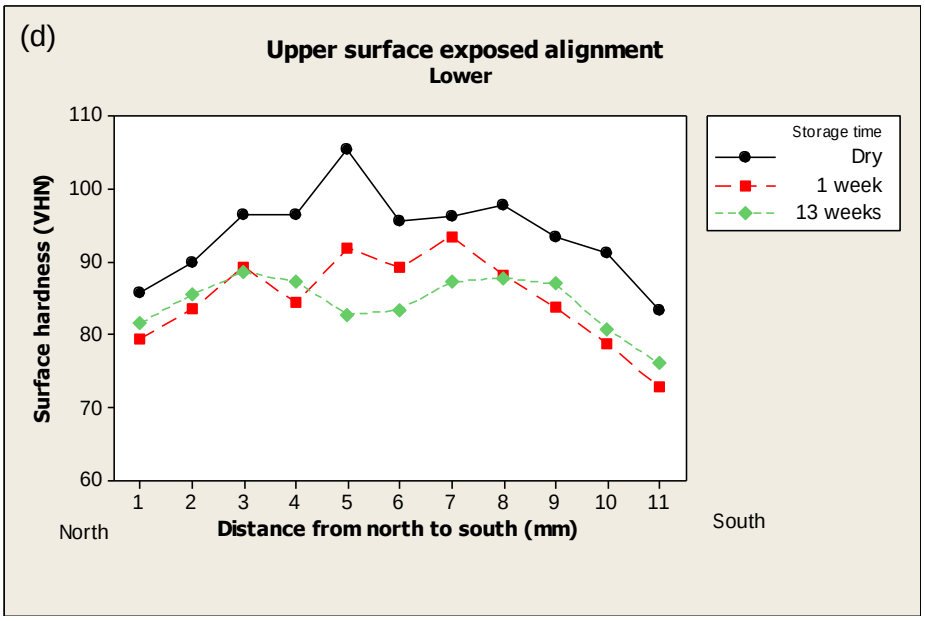

Figure 6.4 (continued). Plots highlighting the (c) upper and (d) lower surface hardness of upper surface exposed alignment from north to south direction following dry control, 1 week and 13 weeks wet storage regimes.

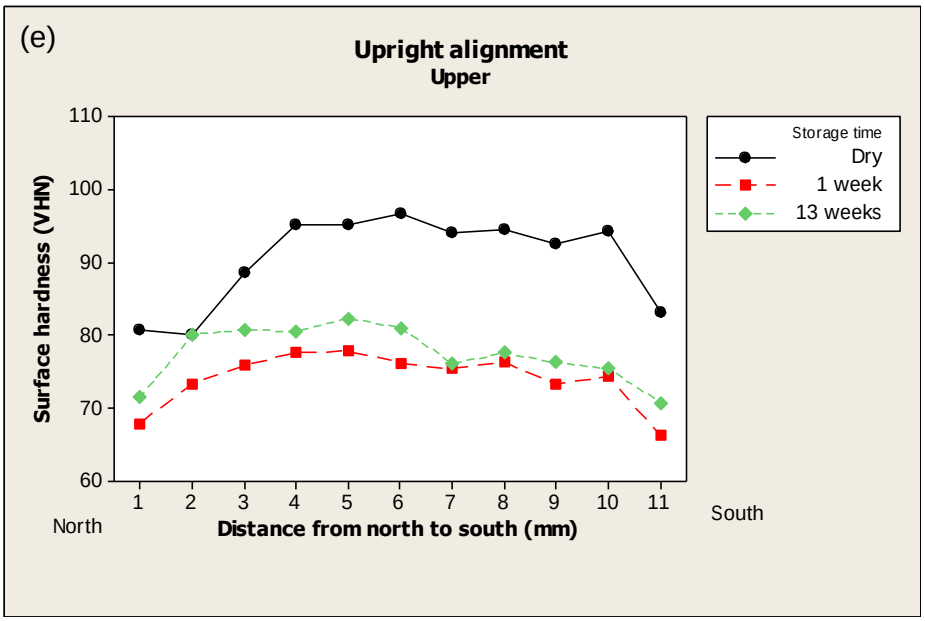

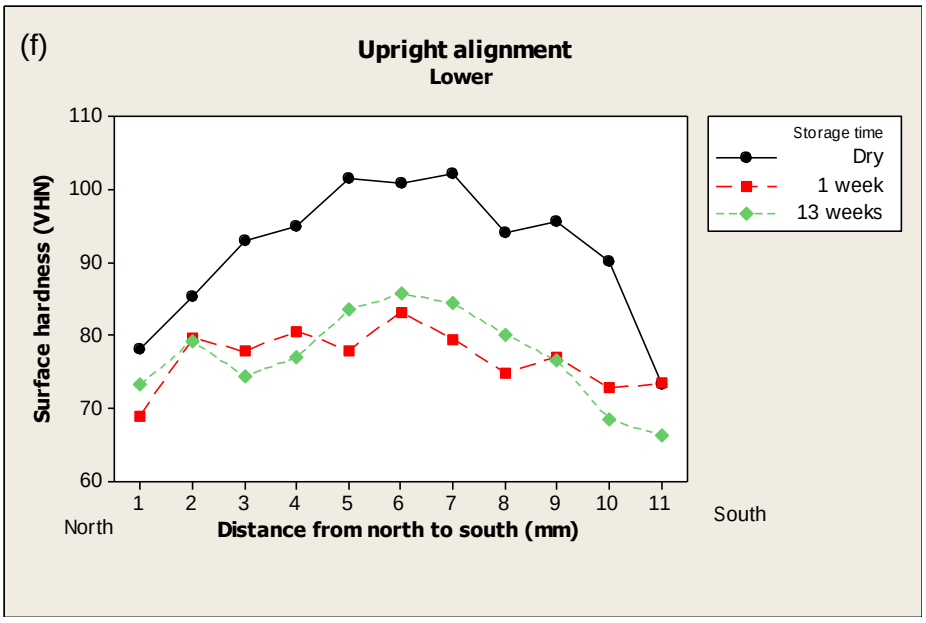

Figure 6.4 (continued). Plots highlighting the (e) upper and (f) lower surface hardness of upright alignment from north to south direction following dry control, 1 week and 13 weeks wet storage regimes.

6.4 Discussion

A significant reduction in BFS of the resin composite following each storage alignment compared with corresponding dry control group was identified (Table 6.1). The degradation of mechanical properties of RBCs after immersion in various storage media has been explained by two means. First, water sorption causes a softening and swelling of the polymer resin component and subsequently reduces the frictional forces between polymer chains (Ferracane et al., 1998) and leads to monomer leaching (Bastioli et al., 1990; Santerre et al., 2001). Second, mechanical properties of RBC may be compromised by failure of silane bond between resins and fillers (Soderholm and Roberts, 1990; Soderholm et al., 1984). However, in the current study, three distinct wet immersion protocols exhibited a reduction in BFS to different extents which may be attributed to a variation in diffusion coefficient as a result of varying specimen alignment.

The greater reduction in BFS of upright specimens compared with stacked specimen following 1 week storage (Table 6.1) may be ascribed to an increased uptake of water. As upright specimens are held on their diametral axis, a larger exposed surface area is likely to allow a greater diffusion of water compared with either upper surface exposed or stacked specimens. The further degradation of BFS in the upright and upper surface exposed specimens following 13 weeks (Table 6.1) is also likely to be a result of an increase in water sorption and associated diffusion. Previous studies also highlighted a decline in BFS of the same resin composite over 6 (Palin et al., 2005) and 12 months (Curtis et al., 2008) associated with an increase in water sorption. Conversely, an increased BFS of stacked specimens following 13 weeks compared with the corresponding 1 week alignment was observed. It is assumed that the main route of water ingress is from exposed edges of specimens in a

stacked alignment, however, the degree of water uptake at the centre point of the disc after 13 weeks will be lower. During BFS testing the area of the specimen in contact with the support ring is more likely to be saturated at 13 weeks compared with that at 1 week. Consequently, increased water sorption towards the outer diameter of the specimen may modify the stress distribution in the support ring contact region and thus exaggerate the measured BFS.

Surface hardness was evaluated in an attempt to highlight the degradative effect of water diffusion across the specimen width. However, it is difficult to differentiate the surface hardness findings between different specimen alignments since hardness trends generally appeared to be comparable from north to south direction across the specimen width (Figure 6.4). A general reduction in the surface hardness from centre-to-edge of specimens following all storage regimes was a result of reduction in light intensity towards the edge of the light-curing tip (Figure 6.3-6.4) (Palin et al., 2008). The significant reduction in surface hardness following wet storage regimes compared with dry surface hardness may be explained by hydrolytic effect described previously. However, no significant difference between 1 week and 13 weeks surface hardness (Figure 6.3) is likely to be a result of saturation of the resin polymer network following 1 week storage regime. The negligible effect of water on surface hardness of several commercial and experimental RBCs has previously been reported by many investigators (Chadwick et al., 1990; Ferracane et al., 1998; Fischer et al., 2010). Ferracane et al. (1998) attributed the limited effect of water on the surface hardness of resin composites to highly cross-linked nature of the polymer network. The authors suggested that a highly cross-linked network is less likely to swell further following intermediate or long storage regimes thus may not allow entry of water molecules and cause any reduction in surface hardness. A greater decrease in

surface hardness of the upright specimens from dry to 1 week and 13 weeks compared with stacked and upper surface exposed specimens suggests an increased diffusion of water in former and also supports the decreased BFS of upright specimens. However, the overall surface hardness of stacked specimens was lower in contrast to upper surface exposed and upright specimens (Figure 6.2) which may have resulted due to variation in specimen quality. No significant difference between upper and lower surface hardness of specimens except the one week and 13 weeks upper surface exposed specimens (Figure 6.3) may be due to their thickness resulting in an equivalent degree of cure on the lower surface of the resin composite. It has been suggested that the irradiance of light decreases as the result of light attenuation over the depth of specimen which may consequently result in the incomplete cure on the lower surface of resin composite (Bhamra et al., 2010). However, 1 mm thick specimens used in current study might reduce such effect of light attenuation and lead to an adequate cure throughout the specimen thickness. The lower surface of upper surface exposed alignment specimens exhibited greater surface hardness compared with the upper surface which was anticipated as the lower surface was not exposed to water.

In the current study, the experiments were conducted up to 13 weeks immersion of resin composite and considerable specimen alignment effects on BFS were observed, however, greater differences may be expected following longer storage periods. Moreover, only one resin composite was tested although RBCs with different resin chemistries and different filler content may also lead to variation in specimen alignment effects in terms of BFS and surface hardness. Nevertheless, the implications of the present investigation are significant to BFS testing.

The findings of current study reject the null hypothesis. The significant differences in BFS and surface hardness values following distinct specimen alignments warrant standardisation of experimental methodologies among scientists and research laboratories. The upper surface exposed specimen alignment may be considered most relevant as it more readily represents that associated with clinical dental restorations.

6.5 Conclusion

This study suggests that specimen alignment has a considerable effect on the BFS of RBCs which may lead to difficulty in interpretation of data among different researchers. Therefore, to ensure improved reliability and accurate assessment of RBCs strength among researchers and different test centres, it is important to standardise specimen alignment throughout storage regimes.

References

Bastioli C, Romano G, Migliaresi C. Water sorption and mechanical properties of dental composites. Biomaterials, 1990; 11: 219-223.

Bhamra GS, Fleming GJP, Darvell BW. Influence of LED irradiance on flexural properties and Vickers hardness of resin-based composite materials. Dental Materials, 2010; 26: 148-155.

Calais JG, Söderholm KJM. Influence of filler type and water exposure on flexural strength of experimental composite resin. Journal of Dental Research, 1988; 67:836-840.

Chadwick RG, McCabe JF, Walls AWG, Storer R. The effect of storage media upon the surface microhardness and abrasion resistance of three composites. Dental Materials, 1990; 6: 123.128.

Curtis AR, Shortall AC, Marquis PM, Palin WM. Water uptake and strength charactersistics of nanofilled resin-based composites. Journal of Dentistry, 2008; 36:186-193.

Deepa CS, Krishnan VK. Effect of resin matrix ratio, storage medium and time upon the physical properties of a radiopaque dental composite. Journal of Biomaterials applications, 2000; 14: 296-315.

Ferracane JL, Berge HX. Fracture toughness of experimental dental composites aged in ethanol. Journal of Dental Research, 1995; 74: 1418-1423.

Ferracane JL, Berge HX, Condon JR. In vitro aging of dental composites in water-Effect of degree of conversion, filler volume, and filler/matrix coupling. Journal of Biomedical Material Research, 1998; 42: 465-472.

Fischer J, Roeske S, Stawarczyk B, Hammerle CHF. Investigations in the correlation between martens hardness and flexural strength of composite resin restorative materials. Dental Materials Journal, 2010; 29: 188-192.

Musanje L, Darvell BW. Aspects of water sorption from the air, water and artificial saliva in resin composite restorative materials. Dental Materials, 2003; 19: 414-422.

Ortengren U, Andersson F, Elgh U. Influence of pH and storage time on sorption and solubility behaviour of three composite resin materials. Journal of Dentistry, 2001; 29:35-41.

Palin WM, Fleming GJP, Burke FJT, Marquis PM, Randall RC. The influence of short and medium-term immersion on hydrolytic stability of novel low-shrink dental composites. Dental Materials, 2005; 21:852-863.

Palin WM, Senyilmaz DP, Marquis PM, Shortall AC. Cure width potential for MOD resin composite molar restorations. Dental Materials, 2008; 24: 1083-1094.

Prakki A, Cilli R, Mondelli RFL. Influence of pH on polymer based dental material properties. Journal of Dentistry, 2005; 33: 91-98.

Santerre JP, Shajii L, Leung BW. Relation of dental composite formulation to their degradation and the release of hydrolyzed polymeric-resin-derived products. Critical Reviews in Oral Biology and Medicine. 2001; 12: 136-151.

Södeholm KJ, Zigan M, Ragan M. Hydrolytic degradation of dental composites. Journal of Dental Research, 1984, 63:1248-1254.

Södeholm KJM, Roberts MJ. Influence of water exposure on the tensile strength of dental composites. Journal of Dental Research, 1990; 69:1812-1816.

Södeholm KJM, Mukherjee R, Longmate J. Filler leachability of composites stored in distilled water or artificial saliva. Journal of Dental Research, 1996; 75: 1692-1699.

Shawkat ES, Shortall AC, Addison O, Palin WM. Oxygen inhibition and incremental layer bond strengths of resin composites. Dental Materials, 2009; 25: 1338-1346.

Watts DC, Amer OM, Combe EC. Surface hardness development in light-cured composites. Dental Material, 1987; 3: 265-269.

Zhang Y, Xu J. Effect of immersion in various media on the sorption, solubility, elution of unreacted monomers, and flexural properties of two model dental composite compositions. Journal of Materials Science: Materials in Medicine, 2008; 19: 2477-2483.

Chapter 7 Executive Summary

Resin-based composites are being increasingly used for the restoration of load-bearing posterior dentition and their adequate longevity comparable with dental amalgam has been reported (Opdam et al., 2007; Opdam et al., 2010). Currently, a lack of consensus exists among researchers regarding the classification of RBCs as a result of slight variations in filler size and associated interchangeable mechanical properties of "microhybrid", "nanohybrid" and "nanofilled" RBCs (Ilie and Hickel, 2009a). These differences in the data may be attributed in-part to variability in testing methods between investigators and the effect of confounding variables such as resin and photo-initiator chemistry in commercial RBC formulations.

One reason for in vitro mechanical characterisation of dental restorative materials is to predict their in vivo performance. However, the resultant in vitro data may only be meaningful when relevant and reproducible laboratory techniques and appropriate data analysis methods are employed. The inconsistency in mechanical property testing of RBCs is evident amongst researchers. Consequently, in the current investigation, variability in experimental and statistical testing methodologies was explored. The resultant data provided significant findings (summarised below), which may aid the understanding and development of improved materials.

7.1 Clinical relevance

It is well known that the nature of masticatory forces vary from patient to patient (Yamashita et al., 1999; Koolstra, 2002). Therefore, the determination of mechanical properties of RBCs at a single crosshead speed may be questioned. In the current investigation, bi-axial flexure strength (BFS) of commercial and experimental

RBCs was determined at varying deformation rates (Chapter 4, 5). Generally, all commercial RBCs exhibited deformation rate dependence to different extents. However, the sensitivity of the recorded BFS to deformation rate was extremely complex for the commercial materials and no obvious effect of resin and filler constituents was identified. The wide variation in the behaviour of materials was attributed to differences in their formulations. Consequently, in an attempt to understand the mechanistic pathways, experimental unfilled resins and RBCs with systematic formulations were investigated. Experimental unfilled resins revealed deformation rate dependence in BFS following one week 'dry', one and 13 weeks 'wet' storage regimes, whereas the addition of fillers modified the deformation rate dependence following 13 weeks 'wet' storage and resulted in the BFS of filled resin composites being independent of testing speed. These findings suggested the need for the development of RBCs with appropriate formulations for clinical situations where variable strain rates may occur. For example, in bruxism, RBC restorations may be subjected to sustained forces (Ruyter and Øysæd, 1982) for extended periods at low deformation rates in contrast to the much more transient loading forces in normal mastication (Glaros and Rao, 1977). The various combination of filler particle size and nanoparticle addition did not highlight any effect on the deformation rate dependence of RBCs, which suggested a dominating behaviour of the resin matrix.

7.2 Inconsistency among investigators

Mixing of model RBC formulations, specimen preparation and subsequent storage in media and mechanical testing of RBCs at a single crosshead speed are common laboratory procedures and in accordance with ISO 4049. Any inconsistency

with respect to these basic steps among investigators may cause a variation in the resultant data and lead to difficulty in interpretation.

Commonly, the majority of researchers mix RBC formulations using hand-spatulation (Venhoven et al., 1994; Lim et al., 2002; Atai et al., 2004; Skrtic and Antonucci, 2007; O'Donnell et al., 2008) and report the significant findings in their research. However, the reliability of the results is questionable as a result of incorporation of air during mixing which may lead to an inhomogeneous mix (Appendix). Moreover, during hand-spatulation of RBCs, mixing speed, pressure and time are not controlled which may also cause variations in resultant RBC batches and thus lead to variation in data among investigators. In the current investigation, lower BFS, Weibull modulus and increased porosity of hand-spatulated RBCs compared with mechanically-mixed RBCs suggested an incorporation of air and inhomogeneous mix in the hand-spatulated RBCs (Appendix). Thus, the research work based on hand-spatulation of model RBC formulations may not be reliable and may affect the development of materials. The mechanically-mixed and commercial RBCs showed no significant difference between their Weibull moduli, which highlighted the reliability of both materials. Consequently, model RBC formulations based on mechanical-mixing may be considered more homogenous and reproducible compared with hand-spatulation.

In the current deformation rate related experiments, each specimen set (n=30) was stored in a cylindrical container containing distilled water and specimens stacked directly on the top of each other (Chapter 4). The resulting BFS values of commercial RBCs were significantly greater than a previous study (Curtis, 2009), which investigated similar materials and used similar specimen geometries and light curing protocols at 1.0 mm/min cross-head speed. The differences were attributed to a

variation in diffusion of water as the result of the difference in exposed surface areas of the specimen compared with the previous study, which stored specimens on their diametral axis (Curtis, 2009). To confirm these findings, the BFS and surface hardness of one RBC was evaluated following stacked, upper surface exposed and upright specimen alignments (Chapter 6). The wet upright specimens exhibited a greater decrease in both properties compared with either stacked or upper surface exposed alignments and supported the assumption that variation in specimen alignment may lead to different findings and associated interpretation between investigators.

The variation in the pattern of BFS between commercial RBCs with respect to deformation rate significantly affected the interpretation of the BFS data (Chapter 4). This suggested that evaluation of mechanical properties of identical material and test specimen at different deformation rates between researchers may affect the interpretation of data and associated research and development of RBCs. Indeed, the variation in selection of cross-head speed is very common among researchers (Table 2.2, Page 48).

7.3 Statistical relevance

Several investigators have employed Weibull statistics for the analysis of RBCs strength data (Palin et al., 2003; Palin et al., 2005; Rodrigues Junior et al., 2008; Curtis et al., 2009; Ilie and Hickel, 2009b) and have reported major findings on the basis of associated Weibull modulus. However, RBCs are viscoelastic and less brittle materials compared with ceramic-based materials, for which Weibull statistics are well established (Cattell et al., 1997; Bhamra et al., 2002; Lohbauer et al., 2002; Bona et al., 2003; Addison et al., 2007ab). Therefore, the applicability of Weibull

statistics might be questioned for RBCs. In the current study (Chapter 3), the BFS of glass cover slips highlighted a similar Weibull distribution and an overlap in 95 % confidence intervals between ball-on-ring and ring-on-ring configurations, which supported the applicability of Weibull statistics, as expected. On the contrary, the porcelain specimens exhibited a reduced Weibull modulus following ring-on-ring compared with the ball-on-ring test, which was not expected as ceramics are often assumed to follow Weibull theory. It was suggested that transient and residual stresses are likely to happen in porcelain specimen during sintering and cooling. Since, ring-on-ring testing stresses a larger area radial to the centre point of the disc specimen compared with ball-on-ring, it is likely that different defects or defects subjected to differing residual stress states may be encountered leading to the observed decrease in the Weibull modulus. The microhybrid and nanofilled RBCs also followed similar pattern as the glass cover slips, which confirmed the applicability of Weibull statistics for both materials. Conversely, a lower Weibull modulus was identified for the flowable RBC following the ring-on-ring test compared with ball-on-ring test, which suggested that RBCs with greater resin content are likely to exhibit more viscous deformation, and therefore may affect the existence of Weibull distributions. It was demonstrated that Weibull statistics may not necessarily be applicable to all RBCs.

An understanding of the interaction between microstructure and property of materials, and monitoring of the effects of changes in the composition or processing on the properties of material in vitro are the important initial steps in the development of new materials. Therefore, any variability in the laboratory testing methods among investigators is likely to affect the development of RBCs. The findings of the current study with regard to deformation rate (cross-head speed), specimen alignment and

mixing regimes clearly indicate the need for the standardisation of the testing methods of RBCs. Moreover, deformation rate dependence of RBCs suggests the need for the development of RBCs with appropriate formulations for clinical situations where variable strain rates may occur.

References

Addison O, Marquis PM, Fleming GJP. The impact of hydrofluoric acid surface treatments on the performance of a porcelain laminate restorative material. Dental Materials, 2007a; 23: 461-468.

Addison O, Marquis PM, Fleming GJP. The impact of modifying alumina air abrasion parameters on the fracture strength of a porcelain laminate restorative material. Dental Materials, 2007b; 23: 1332-1341.

Atai M, Nekoomanesh M, Hashemi SA, Amani S. Physical and mechanical properties of an experimental dental composite based on a new monomer. Dental Materials, 2004; 20: 663-668.

Bhamra G, Palin WM, Fleming GJP. The effect of surface roughness on the flexure strength of an alumina reinforced all-ceramic crown material. Journal of Dentistry, 2002; 30: 153-160.

Bona AD, Anusavice KJ, DeHoff PH. Weibull analysis and flexural strength of hot-pressed core and veneered ceramic structures. Dental Materials, 2003; 19: 662-669.

Cattell MJ, Clarke RL, Lynch EJR. The biaxial flexural strength and reliability of four dental ceramics- part II. Journal of Dentistry, 1997; 25: 409-414.

Curtis AR. The influence of 'nanocluster' reinforcement on the mechanical properties of a resin-based composite material. PhD Thesis, University of Birmingham, 2008; Page.76.

Curtis AR, Palin WM, Fleming GJP, Shortall ACC, Marquis PM. The mechanical properties of nanofilled rein-based composites: The impact of dry and wet cyclic pre-loading on bi-axial flexure strength. Dental Materials, 2009; 25:188-197.

Glaros AG, Rao SM. Effects of bruxism: A review of the literature. Journal of Prosthetic Dentistry, 1977; 38: 149-157.

Ilie N, Hickel R. Investigations on mechanical behaviour of dental composites. Clinical Oral Investigations, 2009a; 13: 427-438.

Ilie N, Hickel R. Macro-, micro- and nano-mechanical investigations on silorane and methacrylate-based composites. Dental Materials, 2009b; 25: 810-819.

Koolstra JH. Dynamics of the human masticatory system. Critical Reviews in Oral Biology & Medicine, 2002; 13: 366-376.

Lim BS, Ferracane JL, Condon JR, Adey JD. Effect of filler fraction and filler surface treatment on wear of microfilled composites. Dental Materials, 2002; 18: 1-11.

Lohbauer U, Petschelt A, Greil P. Life time prediction of CAD/CAM dental ceramics. Journal of Biomedical Materials Research (Applied Biomaterials), 2002; 63: 780-785.

O'Donnell JNR, Langhorst SE, Fow MD, Skrtic D, Antonucci JM. Light-cured dimethacrylate-based resins and their composites: Comparative study of mechanical strength, water sorption, and ion release. Journal of Bioactive and Compatible Polymers, 2008; 23: 207-226.

Opdam NJM, Bronkhorst EM, Roeters JM, Loomans BAC. A retrospective clinical study on longevity of posterior composite and amalgam restorations Dental Materials, 2007; 23:2-8.

Opdam NJM, Bronkhorst EM, Loomans BAC, Huysmans MCDNJM. 12-year survival of composite vs. amalgam restorations. Journal of Dental Research, 2010; 89: 1063-1067.

Palin WM, Fleming GJP, Burke FJT, Marquis PM, Randall RC. The reliability in flexural strength testing of a novel dental composite. Journal of Dentistry, 2003; 31:549-557.

Palin WM, Fleming GJP, Marquis PM. The reliability of standardised flexural strength testing procedure for a light-activated resin-based composite. Dental Materials, 2005; 21: 911-919.

Rodrigues Junior SA, Ferracane JL, Bona AD. Flexural strength and Weibull analysis of a microhybrid and nanofill composite evaluated by 3- and 4-point bending tests. Dental Materials, 2008; 24:426-431.

Ruyter IE, Øysæd H. Compressive creep of light cured resin based restorative materials. Acta Odontologica Scandinavica, 1982; 40: 319-324.

Skrtic D, Antonucci JM. Dental composites based on amorphous calcium phosphate – Resin composition/physicochemical properties study. Journal of Biomaterials Applications, 2007; 21: 375-393.

Venhoven BAM, De Gee AJ, Werner A, Davidson CL. Silane treatment of filler and composite blending in a one-step procedure for dental restoratives. Biomaterials, 1994; 15: 1152-1156.

Yamashita S, Hatch JP, Rugh JD. Does chewing performance depend upon a specific masticatory pattern? Journal of Oral Rehabilitation, 1999; 26: 547-553.

Chapter 8 Recommendations for Further Work

The current investigation highlighted the applicability of using Weibull statistics for a nanofilled and one microhybrid resin-based composite (RBC) (Chapter 3). However, it was concluded that Weibull statistics were not applicable with the flowable RBC due to an increased plastic deformation as a result of higher resin content compared with both the nanofilled and microhybrid RBCs. Consequently, it is suggested that experimental RBC formulations with different resin/filler ratios should be used to investigate the appropriateness of using Weibull statistics to assess the reliability of strength data, which may advocate an approximate resin/filler ratio for a Weibull material. Also, finite element analysis (FEA) is considered as an effective approach for the analysis of stress distribution of structures. In a previous study, Pick et al. (2010) compared the experimental strength of bi-axial and uni-axial flexure tests with the corresponding analytical strength determined using FEA. The authors suggested the reliability of bi-axial testing compared with uni-axial testing as a result of close approximation between experimental and analytical strength for the former. In the similar manner, the reliability of ball-on-ring and ring-on-ring bi-axial flexure tests utilized in current study (Chapter 3) may also be determined with FEA in order to validate the data.

The various combinations of filler particle size and nanoparticle addition did not highlight any effect on the deformation rate dependence of bi-axial flexure strength (BFS) and flexural modulus of experimental RBCs, which was likely to be the result of a dominating behaviour of the resin matrix (Chapter 5). This suggests that an additional study with regard to different resin formulations should be conducted, which may aid the further understanding and also assist in the development of improved materials. In addition, a general decrease in the mechanical

properties of RBCs with an increased addition of nanoparticle was assumed as a result of agglomeration of nanoparticles (Chapter 5). It is therefore suggested that transmission electron microscopy should be performed in order to examine the distribution of nanoparticles.

Generally, all commercial and experimental RBCs highlighted viscoelastic behaviour by exhibiting deformation rate dependence. The evaluation of the same RBCs with traditional viscoelastic testing methods such as creep resistance or dynamic mechanical analysis may further enhance material property characterisation. Moreover, fractographic analysis of fractured RBC specimens following each deformation rate may be conducted to identify the failure mechanisms.

The unfilled resins exhibited a greater BFS compared with an experimental RBC. It was assumed that multiple factors, for example, inadequate silanisation of the filler, uneven distribution of filler particles or a decreased degree of cure as the result of light scattering may be responsible for the a significant reduction in BFS of RBCs (Chapter 5). Therefore, evaluation of the aforementioned variables, for example, using various filler loads to investigate degree of polymer conversion (measured by infra-red spectroscopy) may be carried out to highlight their effects on BFS of RBCs.

The variation in specimen alignment in wet storage significantly affected the BFS and surface hardness of the RBCs investigated in the current study (Chapter 6). However, only one RBC was tested, although RBCs with different resin chemistries and different filler content may lead to variation in specimen alignment effects in terms of BFS and surface hardness. Therefore, it is important to investigate the effect of specimen alignment on a wide range of RBC types.

The 12 mm disc specimens utilized in bi-axial flexure testing allow for “one-shot” curing and, as such are considered more clinically relevant. However, there is

likely to be inhomogeneous curing in an axial direction due to Gaussian distribution of light intensity across the face of a curing-tip, which was confirmed indirectly in the surface hardness data (Chapter 6). Consequently, inconsistency in bi-axial flexure data may be expected. In a previous study, 12 mm disc specimens of a commercial RBC were polymerised with either hand-held or oven light curing units and no significant difference between Weibull modulus of specimens irradiated with hand-held or oven light curing units was identified (Palin et al., 2005). However, such consistency may be questioned for other RBCs with different resin and photoinitiator chemistries. Therefore, it is suggested that BFS of different RBCs following irradiation with the hand-held and oven light curing units should be conducted in order to standardise the in vitro curing methods for future BFS testing.

References

Palin WM, Fleming GJP, Marquis PM. The reliability of standardised flexural strength testing procedure for a light-activated resin-based composite. Dental Materials, 2005; 21: 911-919.

Pick B, Meira JBC, Driemeier L, Braga RR. A critical view on biaxial and short-beam uniaxial flexural strength tests applied to resin composites using Weibull, fractographic and finite element analyses. Dental Materials, 2010; 26: 83-90.

Appendix 1: Standardisation of Mixing Method for Experimental Resin-Based Composite Research

Many research investigations employ commercial RBCs for comparative evaluation. Interpretation of significant findings from such studies is limited both by multiple differences in the formulations of commercial RBCs, and the fact that manufacturers are reluctant to reveal precise details of formulation differences in proprietary products. Consequently, it is difficult to identify the most specific component that causes a variation in material properties. The use of experimental RBCs with controlled formulations is important in that it allows systematic investigation of variables controlling RBC behaviour, thus allowing hypothesis testing of fundamental concepts.

During experimental RBC preparation, the incorporation of filler particles into a resin mixture is normally carried out by hand spatulation (Venhoven et al., 1994 Lim et al., 2002; Atai et al., 2004; Skrtic and Antonucci, 2007; O'Donnell et al., 2008) and therefore the incorporation of porosity may be anticipated which may affect the mechanical and physical properties of materials under investigation (Bassiouny and Grant, 1980; Ogden, 1985 ; McCabe and Ogden,1987; Kandil et al., 1989) and consequently decrease the reliability of data. Thus, a preliminary experiment was conducted to highlight the influence of hand-spatulated and mechanically-mixed model resin composite formulations on bi-axial flexure strength.

Experimental RBCs preparation

Two batches (10g) each of experimental resin composite paste were prepared by either hand-spatulation or mechanical-mixing. The resins (45 volume%) (Section 5.2.2.1) were mixed with 46 volume% silanised barium glass particles with an

average particle size of 0.7 µm (Schott AG, Hattenbergstrasse, Germany) and 9 volume% of fumed silica particles, approximately 14 nm diameter (Aerosil R 711, Evonik Industries, Germany).

Hand-spatulation was carried out for approximately 10 min in a glass beaker using a glass rod (7 mm diameter). A centrifugal mixing device (Speed-Mixer, DAC 150 FVZ-K, Hauschild Engineering, Germany) was used to mechanically incorporate the filler. For hand-spatulation, fumed silica was initially incorporated into the resin followed by the barium glass particles. For mechanical-mixing, resins were mixed with fumed silica at 2300 rpm and 3500 rpm each for 1 min and this regime was again repeated after addition of glass particles into the initial mix.

A commercially available microhybrid RBC (Z100 MP Restorative^{TM} batch 8YR; shade A3) (3M ESPE Dental Products, St. Paul, MN, USA) was evaluated as a control group.

Bi-axial flexure strength and scanning electron microscopy

Thirty disc specimens (12mm diameter, 1mm thickness) of each RBC were prepared as described in (Section 5.1.2.4) and bi-axial flexure strength (BFS) was determined as outlined in (Section 5.1.2.5). Scanning electron microscopy (SEM) of fractured surface of three disc specimens for each RBC was employed using a Jeol JSM-840A (Jeol LTD, Akishima, Tokyo, Japan) with an acceleration voltage of 5 kV.

Statistical analysis

A one-way ANOVA and post-hoc Tukey multiple comparison tests were performed on the BFS data (P=0.05) to highlight any difference between hand-spatulated, mechanically-mixed and commercial RBCs. Subsequently, BFS data were

submitted to Weibull statistics (Section 3.2.4) in order to assess the reliability of BFS between material groups and r^2-values were obtained using regression analysis of the Weibull data.

Results

A statistically significant difference between the mean BFS of mechanically-mixed (95±13 MPa) and hand-spatulated (83±15 MPa) RBCs was identified ($P<0.001$). The commercial RBC exhibited a significantly higher BFS (135±20 MPa) compared with both hand-spatulated and mechanically-mixed RBCs ($P<0.001$) (Table). The Weibull modulus of BFS data of hand-spatulated RBC was considered to be significantly decreased compared with the Weibull modulus of mechanically-mixed and commercial RBCs as the 95% confidence intervals did not overlap. The differences between Weibull modulus of mechanically-mixed and commercial RBCs were considered non-significant since the 95% confidence intervals overlapped. The r^2-values of 0.91, 0.96 and 0.93 were identified for the BFS of hand-spatualed, mechanically-mixed and commercial RBCs, respectively (Table). SEM highlighted consistently larger and more numerous microscopic defects in hand-spatulated RBC compared with mechanically-mixed and commercial RBCs (Figure).

Table. The mean BFS, Weibull modulus, 95% confidence intervals and r^2-values of hand-spatulated, mechanically-mixed and commercial RBCs.

Mixing regime	Mean BFS (MPa)	Weibull modulus	95% Confidence intervals	r^2-value
Hand-spatulated	83 (15)	5.0	4.4-5.6	0.91
Mechanically-mixed	95 (13)	8.0	7.3-8.6	0.96
Commercial (Control)	135(20)	7.4	6.6-8.2	0.93

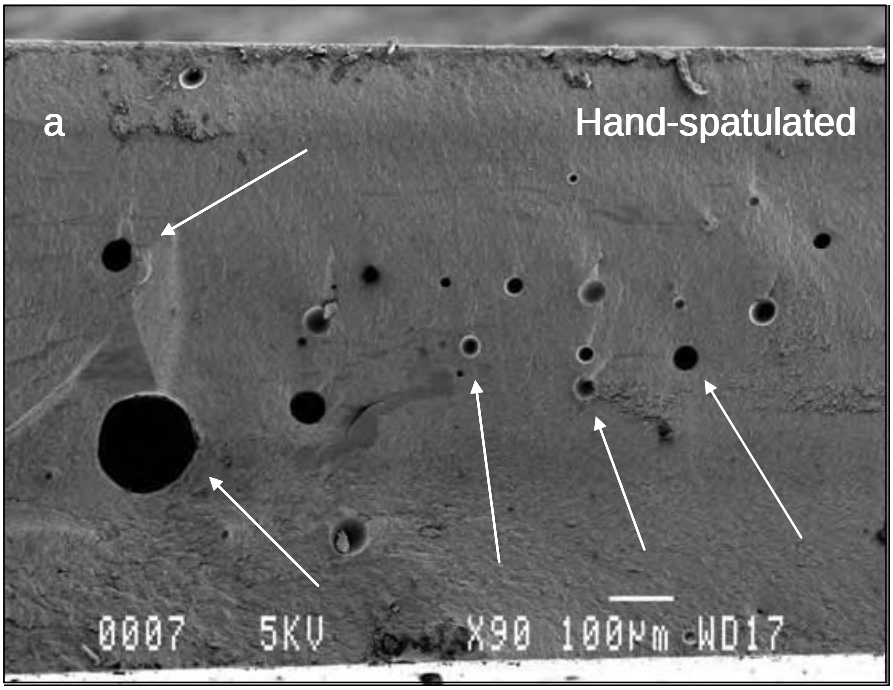
a
Hand-spatulated
0007 5KV X90 100µm WD17

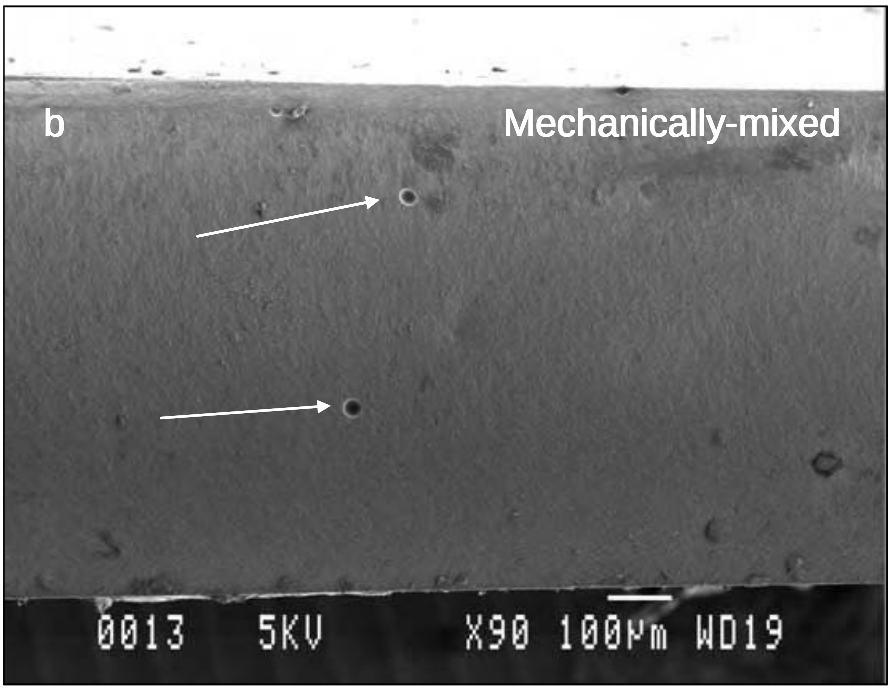
b
Mechanically-mixed
0013 5KV X90 100µm WD19

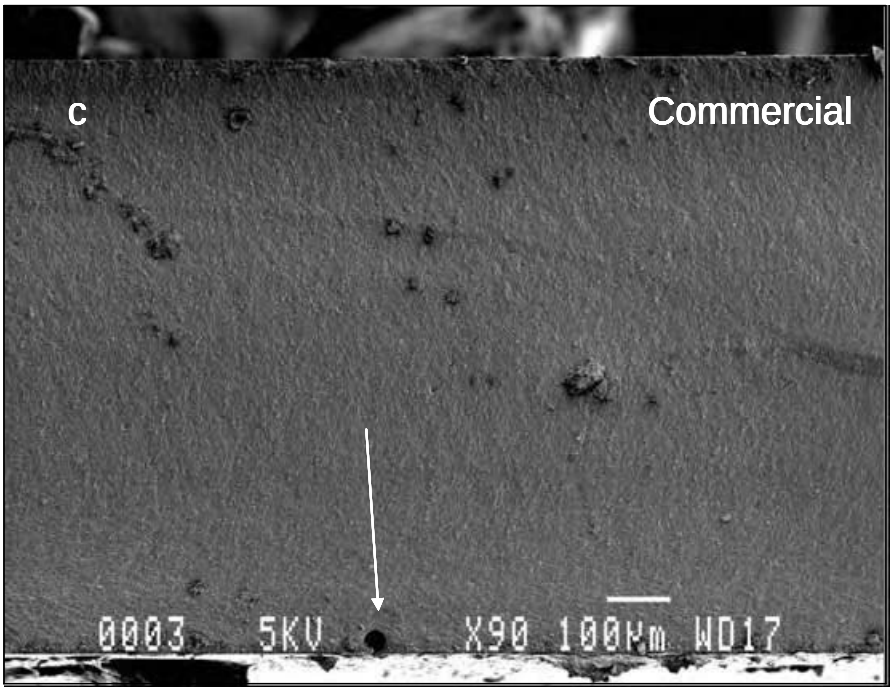

Figure. SEM of the fractured surface of (a) hand-spatulated (b) mechanically-mixed and (c) commercial RBC specimens illustrating porosity (arrows). It is apparent that hand-spatulated RBC showed greater porosity compared with mechanically-mixed and commercial RBCs.

Discussion

The significant decrease in BFS, associated Weibull modulus and r^2 values of hand-spatulated RBC compared with mechanically-mixed and commercial RBCs suggests a wider flaw distribution in the former, which was subsequently confirmed by SEM examination (Figure). The SEM of hand-spatulated RBC highlighted greater porosity, which is expected due to incorporation of air during mixing. In addition, the substantial reduction in BFS and reliability of the hand-spatulated RBC suggests the possibility of a deleterious effect of porosity on other mechanical and physical characteristics of RBCs. De Gee (1979) reported that vacuum mixing of a composite resin led to a 90% reduction in porosity and an associated 11.5% increase in diametral

tensile strength of the material. McCabe and Ogden (1987) found that 20 seconds spatulation in air of the single paste light-cured composite resin Prisma-Fil led to a mean porosity increase from 0.23% for minimally handled material to 1.53% for hand spatulated material. Diametral tensile strength was reduced by 21% and compressive fatigue strength by 14.6% following air introduction by spatulation. In addition to adversely affecting mechanical properties increased porosity levels in experimental samples will impact on physical and optical properties (Jörgensen and Hisamitsu, 1983; Ogden, 1985). The majority of investigators prepare model RBCs using hand-spatulation and report significant findings in their research. However, those conclusions may not necessarily be valid due non-homogenous mixing of RBCs. Thus the research work based on the hand-spatulation of RBCs may affect the development of improved materials. Finally, another drawback of hand-spatulation is that mixing speed, pressure and time are not controlled which may also cause variations in resultant RBC batches.

No significant difference between the Weibull modulus of the mechanically-mixed and the commercial RBCs (Table) signifies a narrow distribution of defects and an increased reliability of strength data of both materials. However, the significant difference in the mean BFS of these two materials may be attributed to compositional variations. It appears that model RBC formulation based on mechanical-mixing is more homogenous and reproducible compared with hand-spatulation. As a result, associated research would yield more consistent data patterns which should assist in the understanding and development of improved resin composite materials. Therefore, in order to accurately examine the data of experimental RBCs among researchers and different test centres, the standardisation and reproducibility of mixing method should be optimised to obtain consistently reliable results.

References

Atai M, Nekoomanesh M, Hashemi SA, Amani S. Physical and mechanical properties of an experimental dental composite based on a new monomer. Dental Materials, 2004; 20: 663-668.

Bassiouny MA, Grant AA. Physical properties of a visible-light-cured composite resin. Journal of Prosthetic Dentistry, 1980; 43: 536-541.

De Gee AJ. Some aspects of vacuum mixing of composites and its influence on porosity. Quintessence International, 1979; 10: 69-74.

Jörgensen KD, Hisamitsu H. Porosity in microfill restorative composites cured by visible light. Scandinavian Journal of Dental Research, 1983 ; 91 : 396-405.

Kandil SH, Kamar AA, Shaaban SA, Taymour NM, Morsi SE. Effect of temperature and aging on the mechanical properties of dental polymeric composite materials. Biomaterials, 1989; 10: 540-544.

Leinfelder KF, Bayne SC, Swift Jr EJ. Packable composites: Overview and technical considerations. Journal of Esthetic Dentistry, 1999; 11: 234-249.

Lim BS, Ferracane JL, Condon JR, Adey JD. Effect of filler fraction and filler surface treatment on wear of microfilled composites. Dental Materials, 2002; 18: 1-11.

Mackert Jr JR, Wahl MJ. Are there acceptable alternatives to amalgam? Journal of California Dental Association, 2004; 32: 601-610.

McCabe JF, Ogden AR. The relationship between porosity, compressive fatigue limit and wear in composite resin restorative materials. Dental Materials, 1987; 3: 9-12.

O'Donnell JNR, Langhorst SE, Fow MD, Skrtic D, Antonucci JM. Light-cured dimethacrylate-based resins and their composites: Comparative study of mechanical strength, water sorption, and ion release. Journal of Bioactive and Compatible Polymers, 2008; 23: 207-226.

Ogden AR. Porosity in composite resins-an Achilles' heel? Journal of Dentistry, 1985; 13: 331-340.

Opdam NJM, Bronkhorst EM, Loomans BAC, Huysmans MCDNJM. 12-year survival of composite vs. amalgam restorations. Journal of Dental Research, 2010; 89: 1063-1067.

Skrtic D, Antonucci JM. Dental composites based on amorphous calcium phosphate – Resin composition/physicochemical properties study. Journal of Biomaterials Applications, 2007; 21: 375-393.

Venhoven BAM, De Gee AJ, Werner A, Davidson CL. Silane treatment of filler and composite blending in a one-step procedure for dental restoratives. Biomaterials, 1994; 15: 1152-1156.

Appendix 2: Water Sorption and Solubility of Dental Resin-Based Composites

Four commercial RBCs, Z100 MP Restorative™ (Z100; batch 8YR; shade A3), Filtek™ Z250 (Z250; batch 8MA; shade A3) and Filtek™ Supreme XT 'body' (FSB; batch 8NU; shade A3) and 'translucent' shades (FST; batch 6C; shade YT) (3M ESPE Dental Products, St. Paul, MN, USA) were investigated in the current investigation. Twenty disc-shaped specimens (12 mm diameter, 1 mm thickness) of each RBC were fabricated as described in section 4.2.2 and water sorption (sp) and solubility (sl) were evaluated following 1 and 13 weeks storage regimes (n=5). Specimens were initially placed in a dessicator containing dehydrated silica gel (Fisher Scientific, Leicester, UK) at 37±1 ºC for 22 h. Subsequently, specimens were removed and stored at 23±1 ºC for 2 h in the second dessicator. Specimens were then weighed to an accuracy of ±0.1 mg and this cycle was repeated until a constant mass (m_1) achieved. After drying, the diameter and thickness of each specimen was measured with a micrometer screw gauge (Moore and Wright, Sheffield, England) accurate to 10 μm in order to calculate specimen volume in cubic millimeters. The specimens were stored in distilled water at 37±1 ºC for 1 and 13 weeks storage regimes. Following storage, the excess water of each specimen was removed using absorbent tissue and the specimen waved in the air and reweighed (m_2). The specimens were again reconditioned to a constant mass (m_3) in the desiccators using the cycle described above. The mean water sorption and water solubility of each specimen were calculated using the Equations A2.1 and A2.2 and results of all RBCs are shown in Table A2.1-A2.2 and Figure A2.1-A2.2.

$$sp = \frac{m_2 - m_3}{v} \qquad \text{Equation A2.1}$$

$$sl = \frac{m_1 - m_3}{v} \qquad \text{Equation A2.2}$$

Table A2.1. The mean water sorption ((μg/mm^3) of Z100, Z250, FSB and FST RBCs following 1 and 13 weeks storage regimes.

Storage regime	Z100	Z250	FSB	FST
1 week	21.9 (1.1)^{b2}	17.3 (1.3)^{c2}	23.6 (0.7)^{a2}	18.7 (0.6)^{c2}
13 weeks	27.4 (1.6)^{a1}	23.5 (0.6)^{b1}	27.4 (1.3)^{a1}	24.9 (1.0)^{b1}

Superscript notation with dissimilar letters across rows and dissimilar numbers down columns indicate statistically significant difference (P<0.05).

Table A2.2. The mean water solubility ((μg/mm^3) of Z100, Z250, FSB and FST RBCs following 1 and 13 weeks storage regimes.

Storage regime	Z100	Z250	FSB	FST
1 week	3.8 (1.8)^{a1}	1.5 (0.9)^{b1}	2.3 (0.8)^{ab2}	1.1 (0.5)^{b1}
13 weeks	4.6 (1.2)^{a1}	1.1 (0.4)^{b1}	3.6 (0.7)^{a1}	1.0 (0.4)^{b1}

Superscript notation with dissimilar letters across rows and dissimilar numbers down columns indicate statistically significant difference (P<0.05).

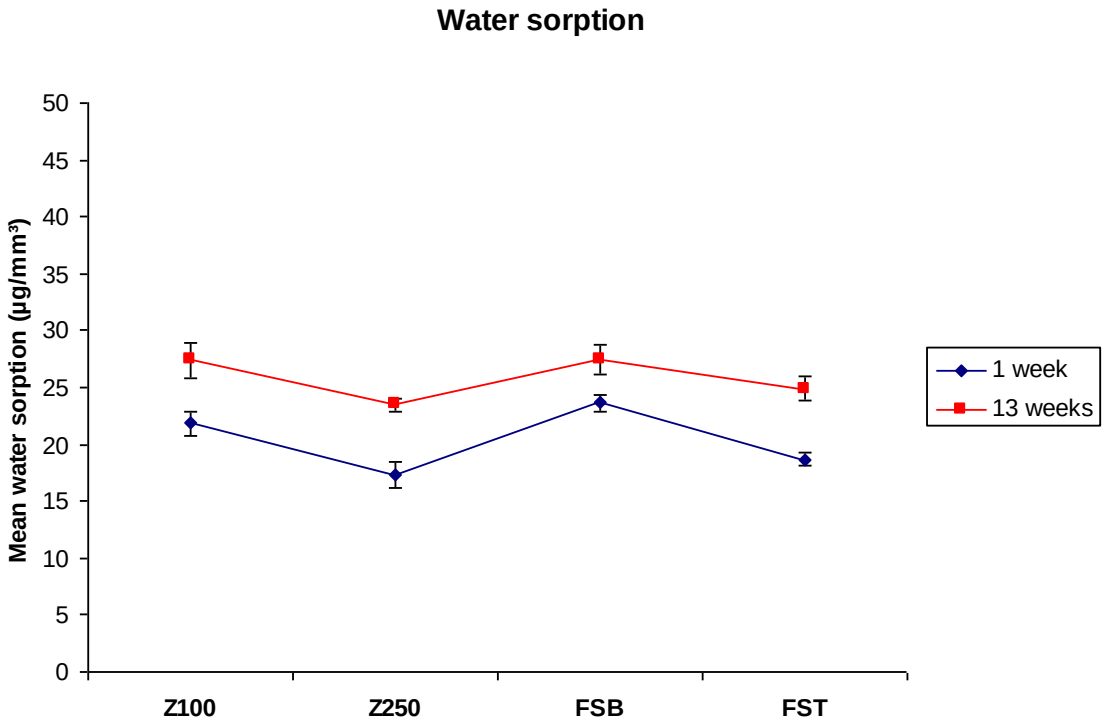

Figure A2.1. Plot illustrating the mean water sorption (and associated standard deviations) of Z100, Z250, FSB and FST following 1 and 13 weeks storage regimes.

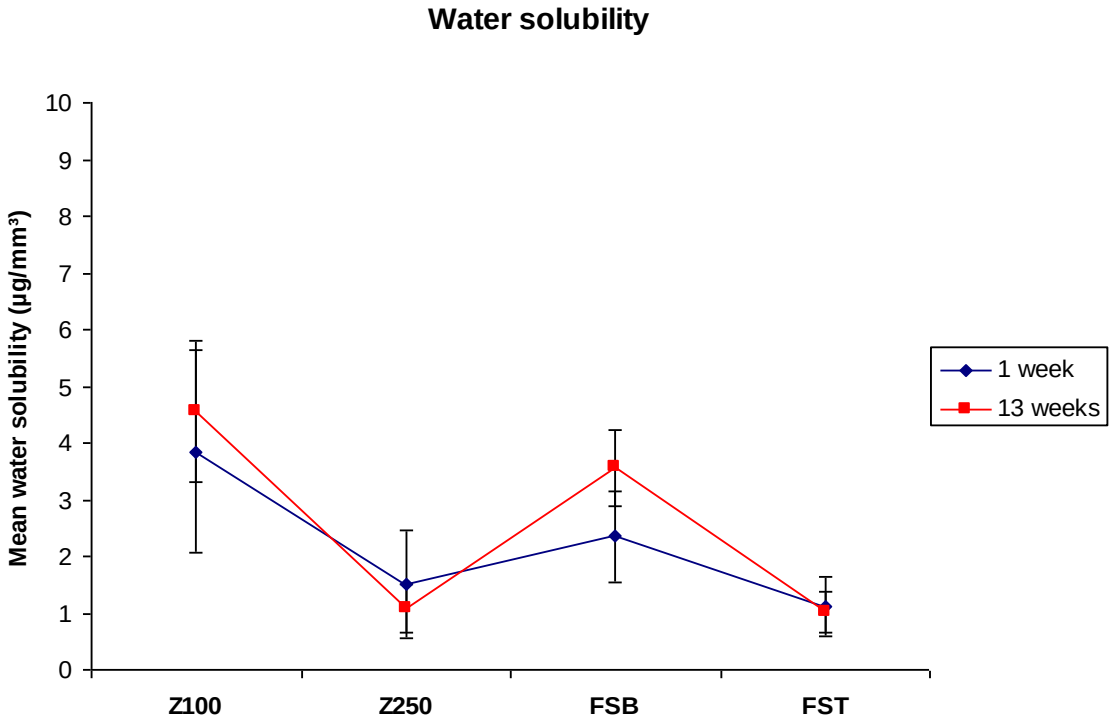

Figure A2.2. Plot illustrating the mean water solubility (and associated standard deviations) of Z100, Z250, FSB and FST following 1 and 13 weeks storage regimes.